

UNIVERSIDADE TÉCNICA DO ATLÂNTICO
INSTITUTO DE ENGENHARIA E CIÊNCIAS DO MAR

WEST AFRICAN SCIENCE SERVICE CENTRE ON CLIMATE CHANGE
AND ADAPTED LAND USE

Master Thesis

**ASSESSMENT OF DRY AND WET EVENTS IN
TOGO (2001-2019) USING THE STANDARD
PRECIPITATION INDEX AND THEIR
RELATIONSHIP WITH OCEAN-ATMOSPHERE
CLIMATE VARIABILITY MODES**

Agnessa TADOUNA

Master Research Program on Climate Change and Marine Sciences

São Vicente
2021

UNIVERSIDADE TÉCNICA DO ATLÂNTICO
INSTITUTO DE ENGENHARIA E CIÊNCIAS DO MAR
WEST AFRICAN SCIENCE SERVICE CENTRE ON CLIMATE CHANGE
AND ADAPTED LAND USE

Master Thesis

**ASSESSMENT OF DRY AND WET EVENTS IN
TOGO (2001-2019) USING THE STANDARD
PRECIPITATION INDEX AND THEIR
RELATIONSHIP WITH OCEAN-ATMOSPHERE
CLIMATE VARIABILITY MODES**

Agnessa TADOUNA

Master Research Program on Climate Change and Marine Sciences

Supervisor | Prof. Dr. Nilton Évora do Rosário

São Vicente
2021

UNIVERSIDADE TÉCNICA DO ATLÂNTICO
INSTITUTO DE ENGENHARIA E CIÊNCIAS DO MAR
WEST AFRICAN SCIENCE SERVICE CENTRE ON CLIMATE CHANGE
AND ADAPTED LAND USE

Assessment of dry and wet events in Togo (2001-2019) using the Standard Precipitation Index and their relationship with Ocean-Atmosphere climate variability modes

Agnessa TADOUNA

Master's thesis presented to obtain the master's degree in Climate Change and Marine Sciences by the Institute of Engineering and Marine Sciences, Atlantic Technical University in the framework of the West African Science Service Centre on Climate Change and Adapted Land Use

Supervisor

Prof. Dr. Nilton Évora do Rosário

Environmental Sciences Department
Federal University of Sao Paulo - Brazil

São Vicente
2021

**UNIVERSIDADE TÉCNICA DO ATLÂNTICO
INSTITUTO DE ENGENHARIA E CIÊNCIAS DO MAR
WEST AFRICAN SCIENCE SERVICE CENTRE ON CLIMATE CHANGE
AND ADAPTED LAND USE**

Assessment of dry and wet events in Togo (2001-2019) using the Standard Precipitation Index and their relationship with Ocean-Atmosphere climate variability modes

Agnessa TADOUNA

Panel defense

President

Examiner 1

Examiner 2

São Vicente
2021



SPONSORED BY THE



Federal Ministry
of Education
and Research

Financial support

The German Federal Ministry of Education and Research (BMBF) in the framework of the West African Science Service Centre on Climate Change and Adapted Land Use (WASCAL) through WASCAL Graduate Studies Programme in Climate Change and Marine Sciences at the Institute for Engineering and Marine Sciences, Atlantic Technical University, Cabo Verde.

Dedication

I dedicated this thesis to my father, Joachim Bakétoua TADOUNA, and my mother, Sidé SAGO, who have consistently supported me throughout my training by prayer.

Acknowledgments

First and foremost, I would like to thank Almighty GOD for His unconditional blessings, without whom this would not have been a reality today.

I want to express my deepest appreciation to my supervisor Prof. Dr. Nilton Évora do Rosário, for his guidance and for being an inexhaustible source of motivation, inspiration, and a great good mood. Working with him always motivated me to work hard, be diligent and do better.

I am equally thankful to the Director of WASCAL Cabo Verde, Dr. Corrine Almeida, the Deputy Director, Dr. António Pinto Almeida, and to the Scientific coordinator Dr. Estanislau Baptista Lima, for all their support and constructive criticism during different stages of my studies.

I would like to acknowledge the Federal Ministry of Education and Research (BMBF) that funded the West Africa Science Service Center on Climate Change and Adapted Land Use (WASCAL) which offered me the Master Research Program in Climate change and Marine Sciences fellowship.

I also express my heartfelt gratitude to all the staff of WASCAL Cabo Verde and the Institute of Engineering and Marine Sciences (ISECMAR) of the Atlantic Technical University and more so to all my lecturers for all forms of guidance they offered during my studies period.

"Life is a combination of joy and sorrow that which one you will face depends on your attitude to life and your internal peace." (Aysim Damla Atalay). Thus, this Master's Programme helped me a lot to improve my attitude towards life in various ways, and I am thankful for this experience.

Resumo

A economia do Togo é fortemente baseada na agricultura, que representa 40% do PIB do país. Por conseguinte, Togo, como a maioria dos países da África Ocidental, é altamente vulnerável a eventos climáticos extremos, em particular os relacionados com a variabilidade da pluviosidade. Neste estudo, eventos secos e húmidos ocorridos durante as últimas décadas (2001-2019) no país foram identificados e analisados a partir do Índice de Precipitação Padrão (SPI). Para este fim, foram utilizados as estimativas mensais de chuva do IMERG e medições de 9 pluviómetros da rede de estações meteorológicas em Togo. Préviamente, foi realizado um estudo comparativo entre a pluviosidade mensal derivada dos dados de pluviómetros e a estimativa do IMERG. Além disso, com base em análises de correlação, a relação entre SPI e os índices climáticos Nino 3.4 e SAODI foi investigada a fim de avaliar a influência do ENSO e do SAOD na variabilidade da precipitação em Togo. Os resultados indicaram que a precipitação do IMERG é capaz de reproduzir as principais características temporais e espaciais da precipitação em Togo. Por exemplo, no geral, a distribuição sazonal e as anomalias interanuais da precipitação foram bem representadas pelo IMERG. No entanto, no que diz respeito à variabilidade sazonal, foram identificadas diferenças importantes entre o IMERG e o pluviómetro na zona costeira, em Lomé, e subestimação da chuva nas zonas de maior altitude, em Kouma Konda. A análise conjunta do SPI utilizando dados de pluviómetros e do IMERG também mostrou que o IMERG é capaz de identificar a ocorrência dos principais períodos húmidos e secos. A partir das análises do SPI, foi possível identificar dois períodos de destaque para Togo, um marcado por eventos muito úmidos, entre 2008 e 2010, e outro dominado por secas severas, entre 2013 e 2015. Finalmente, com as análises de correlação entre os SPIs regionais e os índices Nino 3.4 e SAODI foram encontrados: **a)** correlações positivas baixa (regiões a norte de Togo) a moderada (regiões marítimas e planálticas) com o SAODI; **b)** as correlações aumentam durante a época das monções da África Ocidental; **c)** As fases do SAODI foram consistentes com a falta de precipitação (fase negativa) entre os anos de 2013 e 2015, e com a maior quantidade de precipitação (fase positiva) observada em 2007 e 2009, durante a qual o Togo sofreu os mais recentes eventos de cheias graves; **d)** uma correlação fraca, negativa e não estatisticamente significativa entre o índice Nino 3.4 e os SPIs regionais. Em conclusão, IMERG reproduziu consistentemente as principais características da variação sazonal e espacial da precipitação e também foi capaz de captar os eventos secos e húmidos das majors sobre o Togo para o período de estudo.

Palavras-chave: Togo, IMERG, Precipitação, SPI, Eventos extremos, Secas, SAOD, ENSO

Abstract

Togo's economy is based mainly on agriculture, which represents 40% of the country's GDP. Therefore, like most West African countries, Togo is highly vulnerable to extreme climate events, remarkably rainfall variability. In this study, dry and wet events in Togo at local and regional scales during the period 2001-2019, were assessed using the Standard Precipitation Index (SPI). Monthly rainfall dataset from the Integrated Multi-satellitE Retrievals for GPM (IMERG) rainfall estimation and rain-gauge measurement from 9 meteorological stations across Togo were used for this purpose. Previously, an intercomparison study between rain gauge monthly rainfall and IMERG estimation was performed. Furthermore, based on correlation analysis, the SPI relationship with the climate indices Nino 3.4 and SAODI was investigated in order to explore, respectively, the influence of ENSO and SAOD on Togo rainfall. The results demonstrated that IMERG rainfall could reproduce the main temporal and spatial features of precipitation across Togo. For instance, the seasonal precipitation distribution and also the interannual anomalies. Nevertheless, regarding the seasonal variability, essential deviations from rain gauge occurred in the coastal area, specifically at Lomé, and underestimation in the high elevation areas, especially at Kouma Konda. The SPI analysis using rain gauge measurement and IMERG rainfall at a local scale also showed that IMERG could capture the occurrence of significant wet and dry periods in Togo. Based on the SPI results, two major climate periods were identified, one dominated by wet events from 2008 to 2010 and a second marked by severe and extreme dry events from 2013 to 2015. Finally, based on the correlation analysis between regional SPI and Nino 3.4 and SAODI, the results showed : **a)** low to moderate positive correlation with SAODI across Togo regions, with the highest correlation for Maritime and Plateaux regions; **b)** those correlations are stronger during the West Africa Monsoon season; **c)** that the signature of SAODI was consistent with the severe lack of precipitation (negative phase) during the 2013, 2014 and 2015 years, and also with a large amount of precipitation (positive phase) observed in 2007, 2008 and 2009, during which Togo experienced the most recent severe flooding events; **d)** weak, negative and not statistically significant correlation between Nino 3.4 index and SPI for all Togo regions. In conclusion, IMERG reproduced consistently the main features of seasonal and spatial variation of rainfall and also was able to capture the majors dry and wet events over Togo for the study period.

Keywords: Togo, IMERG, Rainfall, SPI, Extreme events, Droughts, SAOD, ENSO

Abbreviations and acronyms

DM	Deciles Method
DM	Drought Magnitude
DMI	Dipole Mode Index
ENSO	El Niño Southern Oscillation
ERSST	Extended Reconstructed Sea Surface Temperature
GOG	Gulf of Guinea
JJAS	June – July – August – September
GCMs	General Circulation Models
GDP	Gross Domestic Product
GPCC	Global Precipitation Climatology Centre
GPM	Global Precipitation Measurement
HadISST2	Hadley Center Ice-SST version 2
ICOADS	International Comprehensive Ocean-Atmosphere Dataset
IMERG	Integrated Multi-SatellitE Retrievals for GPM
IMERG-F	Integrated Multi-SatellitE Retrievals for GPM Final-run
IMERG-L	Integrated Multi-SatellitE Retrievals for GPM Late-run
IMERG-E	Integrated Multi-SatellitE Retrievals for GPM-Early-run
IPCC	Intergovernmental Panel on Climate Change
ITCZ	Intertropical Convergence Zone
ITD	Intertropical Discontinuity
MAE	Mean Absolute Error
MASL	Meters above Sea Level
NAO	North Atlantic Oscillation
NASA	National Aeronautics and Space Administration

NOAA	National Oceanic and Atmospheric administration
NEP	North East Pole
ONI	Oceanic Niño Index
PDO	Pacific Decadal Oscillation
PDSI	Palmer Drought Severity Index
PI	Peak Intensity
RMSE	Root Mean Square Error
SAOD	South Atlantic Ocean Dipole
SAODI	South Atlantic Ocean Dipole Index
SDAT	Standardized Drought Analysis Toolbox
SPEI	Standardized Precipitation Evapotranspiration Index
SPI	Standard Precipitation Index
SST	Sea Surface Temperature
SWP	South West Pole
TSA	Tropical Southern Atlantic
UNIFEI	Universidade Federal de Itajubá
WAM	West African Monsoon
WRF	Weather Research and Forecasting
WMO	World Meteorological Organization
4 ^{em} RGPH	Quatrieme Recensement Genral de la Population et de l’Habitat

General index

Financial support	i
Dedication	ii
Acknowledgements	iii
Resumo	iv
Abstract	v
Abbreviations and acronyms	vi
General index	viii
Figure index.....	x
Table index.....	xii
1. INTRODUCTION.....	1
1.1. Background and Problem Statement	1
1.2. Research Questions	4
1.3. Relevance and importance of this research	5
1.4. Objectives of the work	5
1.5. Structure of the work.....	5
2. CONCEPTUAL FRAMEWORK AND LITERATURE REVIEW	6
2.1. Conceptual framework	6
2.1.1. Sea Surface Temperature and rainfall variability.....	6
2.1.2. West Africa Monsoon (WAM)	7
2.1.3. Intertropical Convergence Zone (ITCZ)	8
2.1.4. Global Warming	9
2.2. Literature review	10
3. STUDY AREA, MATERIALS AND METHODS.....	14
3.1. Study area.....	14
3.2. Rainfall dataset.....	18
3.2.1. Togo synoptic weather stations network rainfall data.....	18
3.2.2. IMERG rainfall data.....	19
3.3. Ocean-Atmosphere climate modes variability	20
3.3.1. Niño3.4 index	20
3.3.2. South Atlantic Ocean Dipole Index (SAODI).....	21
3.3.3. Extended Reconstructed Sea Surface Temperature (ERSST) dataset.....	22
3.4. Methods.....	23
3.4.1. Inter-comparison between rain gauge data and IMERG rainfall product	23

3.4.2. Dry and Wet events characterization: Standard Precipitation Index (SPI)	24
3.4.3. Correlation analysis between regional SPI and Nino 3.4 index, SAODI and South Atlantic SST anomaly.	25
4. RESULTS AND DISCUSSION	27
4.1. Spatial and time variability of monthly precipitation over Togo: Comparison of gauge measurements with Integrated Multi-Satellite Retrievals for GPM (IMERG) estimates.	27
4.1.1. Spatial and mean precipitation variability based on IMERG.....	27
4.1.2. Comparative evaluation at seasonal scale between rain gauge and IMERG rainfall.	30
4.1.3. Interannual rainfall variability over Togo meteorological stations: IMERG versus Rain Gauge	31
4.1.4. Statistical comparison between rain gauge rainfall and IMERG rainfall at monthly scale.....	38
4.2. Characterization of dry and wet events in Togo using SPI at different time and spatial scales	43
4.2.1. SPI analysis at local scale: Rain gauges measurements against IMERG's precipitation estimations at rain gauges coordinates.....	44
4.2.1.1. SPI from rain gauge and IMERG at Dapaong and Mango (Savanes region)	44
4.2.1.2. SPI characterization from rain gauge and IMERG at Niamtougou and Kara (Kara region)	48
4.2.1.3. SPI Characterization from rain gauge and IMERG at Sokodé (Centrale region)	52
4.2.1.4. SPI Characterization from rain gauge and IMERG at Atakpamé and Kouma Konda (Plateaux region).....	54
4.2.1.5. SPI Characterization from rain gauge and IMERG at Tabligbo and Lomé (Maritime region)	57
4.2.2. Medium and long term dry and wet events across Togo administrative regions ...	63
4.3. Dry and wet events in Togo and their relationships with the El Niño-Southern Oscillation (ENSO) and South Atlantic Ocean Dipole	69
4.3.1. Description of SAOD and ENSO indices features during the study period.....	69
4.3.2. Relationship between ENSO and SAOD indices and SPI across Togo regions	71
4.3.3. Correlation analysis between SPI 1-month and spatial SST anomalies in the South Atlantic	75
5. CONCLUSIONS AND RECOMMENDATIONS	80
5.1. Conclusion.....	80
5.2. Recommendations	82
6. REFERENCES	84

Figure index

Figure 1: Surface wind patterns, ITCZ position, and precipitation features over Africa during: (left) northern hemisphere summer period (June-September), during the West Africa Monsoon; (right) northern winter period (Jan-March), when the region is not experiencing the monsoon regime. (Source: Encyclopædia Britannica, 2008).....	8
Figure 2: Study area with the 5 administrative regions and the locations of the synoptic weather stations used in this study (Source: JICA data, DGC, TOGO ASTER GDEM 2 Data).	17
Figure 3: Geographical location of Nino 3.4 region (Source: NOAA, 2015).....	21
Figure 4: Geographic location of the North East Pole (NEP, 10°E–20°W, 0°S–15°S) and South-West Pole (SWP, 10°W–40°W, 25°S–40°S) used to calculate the SAODI. (Source: Nnamchi et al., 2011).....	22
Figure 5: Spatial distribution of monthly mean precipitation across Togo from 2001 to 2019. The named sites correspond to the location of the rain gauge stations used in this study, and the division of the country to the sub-regions, from north to south, Savanes, Kara, Centrale, Plateaux, Maritime.	29
Figure 6: Mean seasonal variability of rainfall (2001-2019) at Togo meteorological stations location as estimate by IMERG rainfall product and obtained from the rain gauge.....	31
Figure 7: Interannual variability of the total precipitation (right) and precipitation anomaly (left) from rain-gauge data and IMERG rainfall estimates data for Dapaong and Mango meteorological stations.....	33
Figure 8: Interannual variability of the total precipitation (right) and precipitation anomaly (left) from rain-gauge data and IMERG rainfall estimates data for Kara and Niamtougou meteorological stations.....	34
Figure 9: Interannual variability of the total precipitation (right) and precipitation anomaly (left) from rain-gauge data and IMERG rainfall estimates data for Sokodé meteorological station.	35
Figure 10: Interannual variability of the total precipitation (right) and precipitation anomaly (left) from rain-gauge data and IMERG rainfall estimates data for Atakpamé and Kouma Konda meteorological stations.....	36
Figure 11: Interannual variability of the total precipitation (right) and precipitation anomaly (left) from rain-gauge data and IMERG rainfall estimates data for Lomé and Tabligbo meteorological stations.....	37
Figure 12: Scatter plots of monthly accumulated rainfall from rain-gauge stations versus IMERG rainfall estimate at rain-gauge coordinates considering all months of the year.	39
Figure 13: Standard Precipitation Index calculated for Dapaong (top figures) and for Mango (down figures) sites using IMERG rainfall dataset (right figure) and rain gauge rainfall dataset (left figure). The vertical cyan colors indicate the monsoon season period, and the horizontal dot pink line indicates the separation of the near and normal conditions (values between -1 and 1) from the very, moderately, and extremely scenarios (≤ -1 and $\geq +1$).....	46
Figure 14: Standard Precipitation Index calculated for Niamtougou (top figures) and for Kara (down figures) sites using IMERG rainfall dataset (right figure) and rain gauge rainfall dataset	

(left figure). The vertical cyan colors indicate the monsoon season period, and the horizontal dot pink line indicates the separation of the near and normal conditions (values between -1 and 1) from the very, moderately, and extremely scenarios (≤ -1 and $\geq +1$)..... 52

Figure 15: Standard Precipitation Index calculated for Sokodé sites using IMERG rainfall dataset (right figure) and rain gauge rainfall dataset (left figure). The vertical cyan colors indicate the monsoon season period, and the horizontal dot pink line indicates the separation of the near and normal conditions (values between -1 and 1) from the very, moderately, and extremely scenarios (≤ -1 and $\geq +1$)..... 54

Figure 16: Standard Precipitation Index calculated for Atakpamé (top figures) and for Kouma Konda (down figures) sites using IMERG rainfall dataset (right figure) and rain gauge rainfall dataset (left figure). The vertical cyan colors indicate the monsoon season period, and the horizontal dot pink line indicates the separation of the near and normal conditions (values between -1 and 1) from the very, moderately, and extremely scenarios (≤ -1 and $\geq +1$) 57

Figure 17: Standard Precipitation Index calculated for Tabligbo (top figures) and for Lomé (down figures) sites using IMERG rainfall dataset (right figure) and rain gauge rainfall dataset (left figure). The vertical cyan colors indicate the monsoon season period, and the horizontal dot pink line indicates the separation of the near and normal conditions (values between -1 and 1) from the very, moderately, and extremely scenarios (≤ -1 and $\geq +1$)..... 60

Figure 18: 12-months SPI at the end of each year for the entire study period over Togo. From north to south, the five administrative divisions are displayed: Savanes, Kara, Centrale, Plateaux, and Maritime. The black dots represent the rain gauge stations used in the present study: Dapaong (Da), Mango (Ma), Niamtougou (Ni), Kara (Ka), Sokodé (So), Atakpamé (At), Kouma-Konda (Ko), Tabligbo(Ta) and Lomé (Lo). 62

Figure 19: SPI-6 (left figures) and SPI-12 (right figures) time series for each Togo administrative region..... 64

Figure 20: Time series plot of SAOD indices for the study period (2001 to 2019) based on the extended reconstruction of sea surface temperature to a base climatology from 1979 – 2020; using data from ERSST V5..... 70

Figure 21: Time series plot of Nino 3.4 indices for the study period (2001 – 2019) base on SST data from ISST V2 to a base climatology from 1979 – 2020. 71

Figure 22: Correlation map between SST anomalies and SPI 1-month for in all the Togo regions considering all months..... 76

Figure 23: Correlation map between SST anomalies and SPI 1-month for each Togo region for the West Africa Monsoon months..... 77

Table index

Table 1: Togo weather stations used in the present study and their location details. 19

Table 2: Categories and scale of SPI index adapted from (McKee et al.,1993) 25

Table 3: Statistics indicators obtained from the intercomparison between IMERG monthly rainfall estimate and rain gauge measurements considering the entire year. 40

Table 4: Statistics indicators obtained from intercomparison between IMERG monthly rainfall estimate and rain gauge measurements during the period out of West Africa Monsoon season 41

Table 5: Statistics indicators obtained from intercomparison between IMERG monthly rainfall estimate and rain gauge measurements for the meteorological stations during the West Africa Monsoon season (JJAS) 42

Table 6: Number of dry events per category in different regions for medium (SPI-6) and long-term (SPI-12). 66

Table 7: Number of wet events per category in different regions for medium (SPI-6) and long-term (SPI-12). 66

Table 8: La Niña and El Niño events occurred during this study period (2001 to 2019). 71

Table 9: Correlation coefficient and significance level between SPI 1-month for each Togo administrative region and Niño 3.4 index considering all months of the year and for WAM season only. 73

Table 10: Correlation coefficient and significance level between SPI 1-month for each Togo administrative and SAODI for all months of the year and for WAM season. 74

1. INTRODUCTION

1.1. Background and Problem Statement

The inhabitants of West Africa are highly dependent on rain for their sustenance. About 95% of the land in the region is used for agriculture, the main regional occupation (Aondove, Zakar, Saley-Bana, 2009). Enhancement of precipitation intensity and variability is projected to increase the risks of flooding and drought and thus affect agricultural production and water security, leading to severe socio-economic disruption (FAO, 2016; IPCC, 2021). That has been the case in the past and, under the ongoing global climate change process, precipitation extreme events frequency is predicted to increase in the future (IPCC, 2013). Therefore, understanding extreme events (droughts and floods) scenarios and studying their temporal and spatial variabilities is fundamental for countries in the region to build the needed knowledge to assess their vulnerability and develop monitoring and forecast tools to mitigate and adapt. According to the Intergovernmental Panel on Climate Change (IPCC, 2014), Africa is one of the most vulnerable continents to climate change impacts due to its high exposure and low adaptive capacity.

According to IPCC Panel (2014), from 1900 to 2005, trends have been observed in rainfall amounts in many regions, including an important interannual variability of rainfall observed in Africa (Laban, 2009, IPCC, 2014). Increased variability of rainfall, combined with the prediction of higher temperatures and increasing amounts of evapotranspiration, is expected to significantly impact the economic and social characteristics worldwide (Xu et al., 2019).

Rainfall is one of the most usable weather parameters to determine climate variability, particularly in West Africa (Kouadio et al., 2003). Its measurement is a great concern in the region as it plays a significant role in hydrological and climate studies. Furthermore, West African countries' social and economic development is strongly linked to agricultural and water resources (Molua, 2012). In the last decades, alternating periods with extreme rainfall events with dry conditions has led to a succession of flood events and drought years in the region (Mouhamed et al., 2013). Climate extreme events, and their frequency increase, constitute the most challenging impact of climate change on society compared to long-term changes in mean climate conditions (Brown, 1992).

Droughts and flooding triggers aspects are not fully understood because the processes that drive their onset, duration are diverse, while recovery occurs at multiple temporal (seasonal, annual, and decade) and spatial (local, regional, and continental) scales (Kao & Govindaraju, 2010; Aghakouchak et al., 2015; Dai, 2013). Drought and flood events are

ordinarily forced by extremes in climatic scenarios, which in turn are usually related to the interactions between the atmosphere, oceans, and land surface (McCabe et al., 2004; Seager et al., 2013).

The distribution of rainfall events spatially and temporally is not homogenous across the West Africa region. This inhomogeneous rainfall distribution can cause flooding or drought with significant negative socio-economic and environmental impacts. For example, the deficit and rainfall irregularity can lead to persistent drought. That was the case in the early 1970s, during which the Sahel region experienced a severe drought and devastating famine (Lhomme, 1982). On the other hand, flood periods can also have disastrous consequences in West African countries. In 2020, flooding affected 2.7 million people in 18 West and Central Africa countries, with many regions recording excess rainfalls (OCHA, 2020).

In Togo, as in many others countries of west Africa, rainfed agriculture is the backbone of the economy, and it contributes to approximately 45% of the country's Gross Domestic Product (GDP) (Batebana et al., 2015). In addition to direct environmental impacts, such as soil degradation and loss of biodiversity, the socio-economic consequences of extreme precipitation events, especially those related to drought, include a reduction in agricultural yields, death of livestock, reduction in agricultural revenue, an increase in rural to urban migration, exacerbation of famine, and an upsurge in water and vector-borne diseases. Several studies have revealed a persistent rainfall deficit in Togo since 1970 (Adewi et al., 2010; Adewi, 2009; Badameli, K.S.M., 1996). Sogbedji (1999) found that the decrease in seasonal rainfall represents a serious threat to maize growth during the second growing season. Djaman and Komla (2015) used reference evapotranspiration (ET_o) and aridity index from 1961 to 2011 and found a declining trend in the ratio of precipitation/ET_o, which adversely implies an increase in the severity of the aridity in Lomé, Tabligbo, and Sokodé.

Rainfall distribution over Togo and West Africa as a whole, in seasonal and interannual scales, is mainly associated with the West African Monsoon (WAM) and its variability (Batebana et al., 2015). The spatial dimension, intensity, and timing of WAM play a significant role in regional agriculture and water resources (Hall & Peyrillé, 2006). Numerous studies have identified that Sea Surface Temperature (SST) conditions in both Atlantic and Pacific Oceans play a role in controlling the WAM variability (e.g., Me et al., 1998; Joly and Voltaire, 2010). Deser et al. (2010) noted the relationship between Pacific, Atlantic, and Indian oceans SSTs and atmosphere through the exchange of surface fluxes. Over the oceans in the tropics overall, it is well understood that higher sea surface temperatures (SSTs) are accompanied by increased convection (Trenberth & Shea, 2005).

In addition, previous studies indicated that precipitation tends to increase over West Africa region linearly with increasing SST over tropical basins such as (West Africa) monsoon basins, suggesting a noticeable impact of SST on tropical precipitation (Roxy, 2014). According to Joly and Voldoire (2010), a significant part of the WAM variability at interannual scale can be explained by the remote influence of El Niño–Southern Oscillation (ENSO), and that the WAM is influenced either during the developing phase of ENSO or during the decay of some long-lasting La Niña events.

Rainfall variability in the WAM region, arising from the interaction of the regional climate with large-scale atmospheric and oceans conditions, may result in extreme events such as drought and flooding (Nmanchi et al., 2013; Ta et al., 2016). These events' predictions remain a major challenge, even for the state-of-the-art coupled climate models (Joly & Voldoire, 2010), and so are their impacts, especially for agricultural production and, therefore, for food security in West African countries. Coupled climate model's difficulty in simulating rainfall variability accurately in the WAM region makes West Africa a region where the precipitation response to anthropogenic climate change is the most uncertain (Douveille et al., 2007). This might be the consequence of the complex interactions that control the observed WAM climate, including both regional processes, such as a strong atmosphere - land surface coupling (Koster et al., 2014), and remote effects, such as a strong sensitivity to tropical SSTs variability (Giannini & Chang, 2005). Therefore, continuous monitoring and a better understanding of extreme precipitation events scenarios are crucial to develop a warning system able to allow, as early as possible, adaptation plans and to mitigate their socio-economic impacts, especially for long-lasting drought events. On this regard, while rain gauges ability to represent valuable and accurate information for local, country level and regional monitoring effort is well established, West Africa countries sparsely rain gauge networks has been a long-term challenge (Winifred Ayinpogbilla Atiah et al., 2020). On the other hand, in addition to the regional perspective, the new high spatial resolution spaceborne rainfall products have the potential to provide local and national level monitoring, which added to the limited rain gauges network can contribute to support the development of a more robust and comprehensive national warning system.

For all that has been described above in the context of West Africa, and targeting a country-level analysis; in the present study, Togo was selected as the geographical domain to focus on and to perform an investigation on the precipitation variability and the occurrence of dry and wet events across the country administrative regions during almost the last two decades (2001 to 2019). Subsequently, the role of the Tropical Pacific and South Atlantic ocean's most important SST variability modes to the precipitation in Gulf of Guinea countries on the dry and

wet events over Togo is explored. The pursuit of these goals was carried by combining the Togo national rain gauge network and IMERG rainfall datasets aiming to evaluate the application of the satellite-based product to monitor dry and wet events.

Togo, as part of the West Africa region, is probably among the most vulnerable countries in the world, as far as water resources and food production are concerned (WBG, 2021). Droughts and floods are recurring extreme events in the country that poses a significant threat, which cannot be eradicated but managed. Monitoring of flood and drought scenarios over Togo are essential to support public policies, mainly those focused on water, food, and energy security.

A few studies have explored the influence of SST variability on the rainfall distribution over Togo. Batebana et al. (2015) investigated the spatiotemporal changes in extreme rainfall over Togo and their relationship with atmospheric circulation anomalies and sea surface temperature variations in the Southern Atlantic. The study pointed out statistically significant correlations between oceanic climate indices (e.g., Oceanic Nino Index (ONI); South Atlantic Ocean Dipole Index (SAODI); Dipole Mode Index (DMI)) and rainfall variability in Togo, but the study did not analyze focus on the relationship between these oceanic indices and the occurrence of wet and dry extreme conditions over Togo. Koudahe et al. (2017) used the SPI (Standard Precipitation Index) (McKee et al., 1993) as a tool to investigate dry and wet conditions in southern Togo but did not discuss the dependence of these conditions on SST variability.

1.2. Research Questions

Focusing on Togo, and aiming to contribute to advance current knowledge about the occurrence of wet and dry conditions across its territories, below are listed the main questions that summarize the driver motivations of the present study goals:

- Is the IMERG rainfall product able to reproduce the spatial and temporal distributions of rainfall across Togo administrative regions? Answer this question would be important to evaluate IMERG rainfall product ability to support the monitoring of dry and wet periods in Togo.
- Did regions in Togo experience very dry, extreme dry and very wet, extreme wet events during the last two decades? Was IMERG rainfall product able to capture these events?
 - Is it possible to identify associations between dry and wet events in Togo during the last two decades and ENSO and SAOD ocean-atmosphere climate variability modes events?

1.3. Relevance and importance of this research

With the results of the present research, we expect to contribute to improving the current knowledge on the recent variability of precipitation across Togo and its relationship with Tropical Pacific and South Atlantic Ocean SST conditions. We also see this work as an opportunity to evaluate the application of the new high spatial resolution spaceborne rainfall products and of the SPI as a relevant tool to monitor dry and wet events across Togo on an operational basis as a support to the national rain gauge network, for both scientific and public policies purposes. Therefore, based on the results of this work, a practical tool that help to monitor dry and wet conditions over Togo considering as input both rain gauge rainfall and the IMERG rainfall product could be developed.

1.4. Objectives of the work

The main goal of the present work, is to assess wet and dry events of precipitation in Togo during the last two decades (2001-2019), applying the Standard Precipitation Index (SPI). Subsequently, it was analysed the relationship between these wet and dry events with the El Niño–Southern Oscillation (ENSO) and South Atlantic Ocean Dipole (SAOD). To achieve this main goal, the following specific objectives are to:

- Characterize the spatial and temporal variability of the monthly precipitation over Togo during the last two decades (2001-2019) by comparing rain gauge measurements with the IMERG rainfall product.
- Evaluate the historical evolution and intensity of wet and dry events across Togo at different scales: meteorological, agricultural and hydrological, using SPI.
- Access the role of Tropical Pacific and South Atlantic oceans SST variability on the dry and wet events in Togo, with a particular emphasis on extreme events focusing on ENSO and SOAD climate variability mode.

1.5. Structure of the work

This thesis is organized as follows: The introduction is presented in section one; the conceptual framework and literature review in section two; study area, data, and methodology used are presented in section three; the results and discussion are described in section four. The conclusion and future work recommendations are shown in section five.

2. CONCEPTUAL FRAMEWORK AND LITERATURE REVIEW

2.1. Conceptual framework

2.1.1. Sea Surface Temperature (SST) and rainfall variability

The variability of global SST patterns is important for the modulation of extreme temperature and precipitation globally (Alexander et al., 2009). It is evident that the Earth's climate system will be seriously impacted by the increase that has been observed in the ocean's temperature (IPCC, 2014).

Rainfall in West Africa during the boreal summer is known to exhibit two distinct anomaly patterns (Motha et al., 1980). The first one shows opposite signs in rainfall anomalies in the Sahel and in the wetter region further south, closer to the Gulf of Guinea. This pattern suggests that the latitude of the ITCZ (Inter-Tropical Convergence Zone) regulates the region of maximum precipitation during the rainy season. The second pattern, characterized by a widespread reduction or increase in rainfall throughout the entire West Africa region, is possibly associated with large-scale tropical circulation features. Fontaine and Janicot (1996) showed that the rainfall anomaly patterns documented by Motha et al. (1980) could be associated with different SST anomalies located over the Atlantic and the Eastern Pacific oceans.

In addition, Nmanchi et al. (2011) indicated that the summer precipitation variability over the Gulf of Guinea is influenced by the Sea Surface Temperature Anomalies (SSTA) in the South Atlantic Ocean. A strong relationship between the South Atlantic Ocean Dipole and Guinea Coast rainfall anomalies during the monsoon season was found by Nmanchi et al. (2011). Their study indicated that the SAOD positive phase, characterized by the warming of SST in the Atlantic Niño sector, which coincide with North East Pole of SAOD, and the cooling of SST in the South West Pole of SAOD, leads to an important convergence and upward motion in the Atlantic Niño sector. This atmospheric process (convergence and upward motion) contributes to enhancing the flux of moisture from the Gulf of Guinea and the equatorial Atlantic Ocean into the Guinea Coast, thereby leading to rainfall enhancement.

The interannual and intra-seasonal rainfall variability in Togo and most of the West African countries have been documented by several researchers in numerous publications. A strong link between interannual rainfall variability in West Africa and patterns of sea surface temperature anomalies in the tropical Atlantic, Pacific, and Indian Oceans has been suggested

(Nicholson & Grist, 2001). Compositing five Sahelian wet and dry years, Rowell et al. (1992) found that SST forcing from these three major ocean basins may contribute to seasonal Sahelian rainfall variability.

The El Niño-Southern Oscillation (ENSO) that occurs in the tropical Pacific Ocean (Sharon E. Nicholson & Kim, 1997; S. E. Nicholson & Selato, 2000; Hulme et al., 2001), has been pointed as one of the most important factors influencing rainfall variability for some regions in Africa. Hulme et al. (2001), in their detailed analysis of African climate change, observed a relationship between rainfall and ENSO in equatorial east Africa (high rainfall during ENSO warm event) and southern Africa (low rainfall during ENSO warm event), consistent with earlier studies. Elsewhere in Africa, West Africa in particular, there has been controversy on the influence of ENSO on precipitation. While there is a general consensus among researchers on the ENSO's influence in some regions, for instance, the Guinea coast, where it tends to increase rainfall during the La Niña phase (Nicholson & Selato, 2000), there is also controversy over its influence in the Sahel region. Nicholson & Grist (2001) found a weak correlation between ENSO and Sahelian precipitation, consistent with Halpert (1987).

More recently, the causes and impacts of the 2007 flooding in most parts of sub-Saharan Africa, especially in the Sahel region, have been documented in the literature. This flooding left thousands of people homeless and impoverished. Among the potential causes of the flood is the La Niña event that occurred that year (Paeth et al., 2011). The authors observed that anomalous positive SST in the tropical Atlantic Ocean coupled with La Niña episodes favored higher precipitation than normal conditions, as occurred during the 2007 rainy season in West Africa.

2.1.2. West Africa Monsoon (WAM)

The West African Monsoon (WAM), one of the three major monsoon systems in the tropics, dominates the seasonal variability of rainfall in Togo. The WAM is a climatological feature of major social importance to local populations over West Africa (Sylla, 2013). It represents a seasonal reversal of the prevailing surface winds over most of the West African region (Figure 1), with the wintertime north-easterly Harmattan winds being replaced in the summer months by south-westerly monsoon winds (Parker and Diop-Kane, 2017). The monsoon period brings moisture from over the Atlantic Ocean into the continent and therefore helps to feed the annual rainfall, which is critical to the local population over west Africa, whose economy relies primarily on agriculture (Parker and Diop-Kane, 2017). Year to year variation

in WAM intensity and timing controls the difference between a wet and dry rainfall season in most of West Africa. WAM is a complex system where several components of the climatic system (atmosphere, ocean, land-surface) interact and generate a high temporal and spatial variability in the associated precipitation. Although it occurs during only a fraction of the annual cycle, between May and September, the WAM is a climatological feature of major social importance. It provides most of the annual rainfall for West African countries. Embedded in the radiatively forced seasonal migration of the ITCZ, it shows a strong annual cycle but also a strong variability on a wide range of timescales Figure 1. The intra-seasonal and interannual fluctuations of the WAM are relatively well documented and have been the focus of a number of researches. The monsoon precipitation also varies strongly on interannual and intra-seasonal scales (Le Barbé et al., 2002; Sultan and Janicot, 2003). This variability has been linked to different factors, like sea surface temperatures variability (Vizy and Cook, 2001), atmospheric circulation perturbations (Nicholson and Grist 2001); and land-surface feedbacks (Koster et al., 2014), in addition to possible effects of global climate change (Paeth & Hense, 2004).

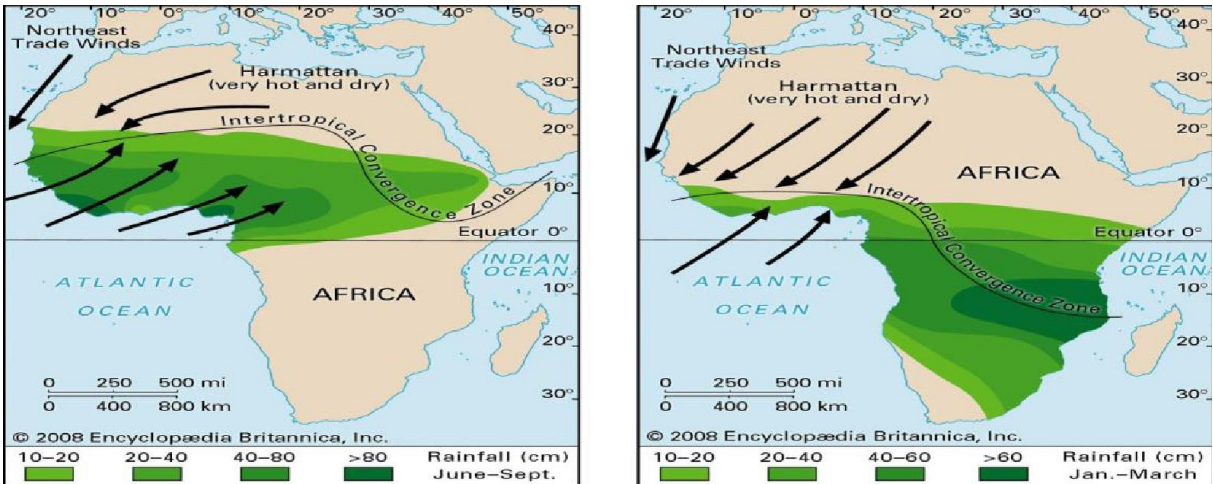


Figure 1: Surface wind patterns, ITCZ position, and precipitation features over Africa during: (left) northern hemisphere summer period (June-September), during the West Africa Monsoon; (right) northern winter period (Jan-March), when the region is not experiencing the monsoon regime. (Source: Encyclopædia Britannica, 2008).

2.1.3. Intertropical Convergence Zone (ITCZ)

The seasonal rainfall pattern in Togo is associated with the northward and southward migration of a narrow zone of reversal in the meridional wind, called the Inter-Tropical Discontinuity (ITD). It is a zone of the confluence of the winds, and an air-mass boundary,

which separates the hot, dry Saharan air from the cooler and moist monsoonal air in the spring and summer months (Parker and Diop-Kane, 2017).

Another commonly used term in the literature is the Intertropical Convergence Zone (ITCZ), associated with the zone of maximum convection. In the literature three, very different definitions are given, based respectively on wind convergence, surface air pressure, and rainfall or outgoing longwave radiation. According to Yan and Oliver (2008), ITCZ is an east-west oriented low-pressure region near the equator where surface north-easterly and south-easterly trade winds meet. Where they converge, moist air is forced upward, producing deep clouds and heavy precipitation. According to Miller and Schneider (2011), it is a region near the equator where the trade winds converge. Both the ITD and ITCZ exhibit seasonal migration following the seasonal movement of the overhead Sun.

Major intense rainfall events appear over Togo regions near the Gulf of Guinea in April and move to the latitudes of about 10°N during the boreal summer, and then retreat back to the south after mid-September–October, manifesting the seasonal march of the ITCZ (e.g., Sultan & Janicot, 2000; Le Barbé et al., 2002). Time–latitude diagrams of monthly mean rainfall indicate that this seasonal migration is characterized by an abrupt shift of the major rain zone during June - July (Sultan & Janicot, 2000; Le Barbé et al., 2002).

2.1.4. Global Warming

The extremes temperatures in the west Africa region are projected to be higher than the global mean temperature increase, with most of the intense warming observed over the Sahel. Heatwaves are expected to be more frequent and of longer duration, with serious implications for human health and agriculture (Russo et al., 2014). The global mean surface air temperature has been steadily rising since the 1950s, primarily attributed to the increase in greenhouse gases emission. Overall, the impacts of global warming are not limited to global and regional changes in temperature; it also has a significant impact on regional rainfall patterns, not only altering rainfall amounts but their distributions. Similarly, the Intergovernmental Panel on Climate Change (IPCC 2007, 2014) is continuously reporting to the United Nations that the Earth's climate system is undoubtedly getting warmer. Some global numerical experiments with General Circulation Models (GCMs) focusing on current climate change show an increase in extreme precipitation over many areas of the globe (Michael F. Wehner, 2004). According to IPCC 2021, Precipitations are projected to increase over high latitudes, the equatorial Pacific, and parts of the monsoon regions.

The details of the distribution and the magnitude of the change vary between models. Climate change has a strong influence on agricultural production, considered as the most weather-dependent of all human activities (Hansen, 2002) with socio-economic impacts whose severity varies from one region to another (Ogallo et al., 2000). There is a vital need for a trustworthy prediction of sub-Saharan West African climate; the region depends highly on agriculture and is also very prone to devastating droughts. Overall, continued global warming is projected to further intensify the global water cycle, including its variability, global monsoon precipitation, and the severity of wet and dry events (IPCC, 2021).

2.2. Literature review

Joly et al, (2014), in their study, showed that, there is a teleconnection between the West African Monsoon (WAM) and the tropical Sea Surface Temperatures (SSTs) at interannual and multi-decadal time scales. These teleconnections are indeed responsible for the main modes of rainfall variability observed over the West Africa region and represent an interesting benchmark for the models that have contributed to the fourth Assessment Report of the Intergovernmental Panel on Climate Change (IPCC4).

Kouadio et al, (2003), whose study was based on statistical correlations between SST and precipitations, analyzed the impact of the tropical Atlantic SST on the precipitation in Côte d'Ivoire. In their study, SST appeared as a key parameter for the modulation of the variability of precipitation in Cote d'Ivoire. The study focused on the statistical relationship between the latitudinal evolution of the ITCZ, the SST of certain oceanic zones of the Tropical Atlantic, and the rainfall of the three climatic regions of Côte d'Ivoire during the period from July to September (WAM season). The study shows that typically rainfall in the Ivorian coastal zone is influenced by the SST off the coast of Angola, from April to June, and by the SST off the coast of West Africa from July to September. The rainfall in the Central Zone of the country in April- May- June is influenced by the action of the ITCZ, while in July-August-September, West Africa SST plays a major role. During April - May – June, and July - August - September, Atlantic equatorial SST influences the rainfall in the North zone. In the end, the study showed that the understanding of the relationship between the tropical oceans and rainfall is fundamental for agricultural planning. Thus, the study highlights the importance of monitoring ocean conditions as a crucial step to predict rainfall and agricultural production in Côte d'Ivoire.

Dado & Takahashi (2017), used a non-hydrostatic regional climate model, the advanced Weather Research and Forecasting (WRF) Model version 3.6.1, to examine the potential impact of sea surface temperature on rainfall over the western Philippines. The results demonstrated that positive SST anomalies west of the Philippines induced positive rainfall anomalies in the north-western Philippines via an increase in latent heat flux from the sea surface, implying that summer monsoon rainfall in the north-western Philippines is modulated by interannual variations in SST west of the country. The impact of SST on the latent heat flux and rainfall was 20–40%, greatly exceeding the 7% approximation from the Clausius–Clapeyron equation, which can be explained by the enhancement of low-level winds and weak warming of surface air temperature over the ocean.

Ali et al, (2011), showed that the Gulf of Guinea Coast and Equatorial upwellings influence the precipitation along northern coasts of the Gulf of Guinea during the boreal summer period. Thus, the coastal precipitations during the July-September period are correlated with both the coastal and equatorial sea-surface temperatures. This correlation results in a decrease or a rise in rainfall when the SSTs are abnormally cold or warm, respectively. The coastal zones that are more subject to coastal and equatorial SSTs influence are located around the Cape of Three Points (Ghana), where the coastal upwelling exhibits its maximum amplitude.

Joly & Voltaire (2010), used CMIP3 coupled simulations to explore the role of the Gulf of Guinea SST and the ocean-atmosphere relationship reproduced by state-of-the-art coupled models? They pointed out that the interannual variability of SST in the Gulf of Guinea is maximum in June – July because of the Atlantic Niño (also called "zonal mode"). In the atmospheric reanalysis, a positive SST anomaly is associated with warmer and moisture air near the surface and a strong modification of the large-scale circulation in the low troposphere, which leads to a strong enhancement of the convection in the ITCZ. There is substantial interannual variability, with the strongest anomalies exceeding 0.5°C some years. The annual cycle of the standard deviations of this SST in the Gulf of Guinea reveals that SST anomalies are maximum in June–July, at the beginning of the monsoon season over the African continent. Thus, the response of the ITCZ to SST anomalies in the Gulf of Guinea is important for seasonal forecasting over West Africa.

Odekunle & Eludoyin (2008), examined Sea Surface Temperature patterns in the Gulf of Guinea (GOG) and discussed their implications for the spatial and temporal variability of precipitation in West Africa. They concluded that, although the inter-annual variability in the SST in the GOG is generally low, the SST anomalies are likely related to the precipitation over West Africa. For instance, an anomalously low SSTs condition during July–August–September

between Longitudes 8°W and 2°E, and the West African coastal border and latitude 3 °N, would lead to anomalously low rainfall during July–August–September between eastern Liberia and western Nigeria. Moreover, the pattern of the SST observed may create a north-south rainfall dichotomy; when precipitation is below normal in the Sahel, it will tend to be above normal in the Guinea Coast region. Finally, Odekunle & Eludoyin (2008) pointed out that a general increase in the SST in the GOG between the first and second half of their study period (1950–1998) may explain the increase in precipitation in West Africa. This scenario is expected to reduce the average severity of the short dry season by making the moisture-laden wind more abundant in terms of moisture and energy.

Batebana et al., (2015) examined the features of rainfall in Togo and its relationship with atmospheric circulation anomalies. According to this study, Togo experiences a unimodal rainfall pattern during the period of May to October. The years 1989, 1991, 1995, 2003, and 2007 were noted to have been wet years, while the years 1982, 1983, 1990, 1992, 2001, and 2006 were dry years. The core of the rainfall lay between 8-10°N. There was a general decrease in the mean rainfall during May-October between 1981 and 1987. After that period, the rainfall maintained an increasing trend, with a little contrast explaining the periodical increase and decrease change in climate from 1994 to 2006. According to Batebana et al. (2015), the rainfall over Togo is not significantly correlated to NAOI (North Atlantic Oscillation index) and DMI (Dipole Mode Index). Meanwhile, they found that SAOD (Southern Atlantic Ocean Dipole) has a significant positive influence on rainfall over Togo. Wet years were associated with an anomalous low-pressure area over Togo and the Saharan heat low in the north of the country as opposed to the dry years, which exhibited an anomalous high-pressure area over Togo at low levels. Vertical velocity analysis revealed that the region experiences rising motion during wet years, which is associated with convergence at low level and divergence at the upper level. During dry years, sinking motion is dominant over Togo, leading to anomalous moisture divergence in the same region.

Based on the SPI, Wu & Kinter (2009) studied droughts at different time scales and reported that the relationship between SST, soil moisture, and U.S. droughts during boreal summer differs significantly between short-term and long-term droughts. The result indicated that the short-term droughts are more influenced by simultaneous remote SST forcing. For The medium-term and long-term droughts, they are influenced by both preceding and simultaneous remote SST forcing. The anomalous soil moisture can favor the persistence of droughts through a positive soil moisture - precipitation feedback. According to Wu & Kinter (2009), the most important remote forcing for U.S. summer droughts is the tropical Pacific SST variability.

Tropical Indian Ocean SST forcing also contributes to the occurrence of medium-term and long-term droughts. Additional impacts for short-term and medium-term droughts are related to the North Atlantic SST forcing. Medium-term and long-term droughts in the southwest of the U.S. are more impacted by the tropical Pacific SST forcing, with extensions into the Great Plains. The SST forcing affects the summer droughts through soil moisture and evaporation changes. The pathway for processes described may be as follows, SST forcing induces atmospheric circulation and precipitation anomalies, the precipitation changes affect winter-spring soil moisture and the spring-summer surface evaporation, the induced soil moisture and surface evaporation anomalies then contribute to summer droughts in the U.S.

3. STUDY AREA, MATERIALS, AND METHODS

3.1. Study area

Togo is located between 6° and 11° North latitude and 0° and 1°40 East longitude. With an area of 56,600 km² and a population estimated to be 6,191,155 inhabitants in 2010 (4th RGPH, 2010), the Togo domain consists of a corridor that stretches over 650 km long, between Burkina-Faso to the north and the Atlantic Ocean to the south, over a maximum width of 150 km, between Benin to the East and Ghana to the West. This configuration helps to explain the great climatic, biological, economic, and human diversity that characterizes Togo. The country has a sandy coastline of around 60 km, which has suffered from severe marine erosion and experience a tropical climate influenced by trade winds: The Harmattan (boreal trade wind), hot and dry wind blowing from the Northeast to the Southwest; and the Monsoon (southern trade wind), a hot and humid wind blowing from the Southwest to the Northeast. The agricultural sector occupies a preponderant place in the Togolese economy since it represented 35.1% of the GDP in 2000 and 38% on average during these last years and provided more than 20% of export earnings. Togo is subdivided into 5 economic regions, which correspond to the 5 ecological zones (Pessiezoum Adjoussi, 2000), present in the country (see Figure 2):

➤ **Savanes region**

Savanes region is bordering the country to the north. It is characterized by one rainy season and one dry season. The rainy season starts effectively in May. It is brief for five months on average. This description conceals serious disparities. In fact, not only is the average monthly rainfall much lower and more irregular than in the northern regions, which receive more rain with the same unimodal regime, but it is concentrated in three months: July, August and September. The dry season begins in October with the early onset of the very virulent harmattan, given the sub-desert situation of the region. The dry season here is longer and very harsh. It lasts on average 7 months. Four ecologically dry months (January, February, November and December) and three ecologically sub-dry months (October, March, April.). The seasonal behavior of rainfall in the savannah region shows that the rainy season begins moderately and ends quickly and abruptly.

➤ **Kara region**

This region is an important agricultural center where yam, millet, peanuts, mangoes, and other fruits are produced. Rainfall in this region, like that of the central region, is mainly governed by the ITD; however, at this latitude, the effect of continental climate is already

beginning to be felt. The seasonal evolution of precipitation shows two very contrasting seasons (dry season and wet season). The rainy season is relatively short compared to the central region. In the central region, it lasts on average 7 months. It starts in April and ends in October. The rainiest months are July, August and September. The dry season is longer than in the central region with an average duration of five months, from November to March. From November, and because of the location relatively close to the centers of high desert pressure, the region is subject to an early phenomenon, the harmattan, which reinforces the drought by its very dry character.

In short, the Kara region enjoys a rainfall regime that is suitable for agriculture, especially for the diversity of crops. However, the harsh and relatively long dry season, due to the effects of continental climate, breaks this harmony and imposes a very harsh rhythm of life on living beings.

➤ **Centrale region**

The Centrale region has a tropical climate. The rainfall pattern is characterized by a rainy season and a dry season. The rainy season lasts on average 7 to 8 months from March to October, i.e. more than 93%. However, this is only a normal duration, which varies from year to year and seriously affects agricultural calendars, especially at the beginning of the season. The end of the season is generally abrupt, marked by short-lived thunderstorms and showers of short duration. Rainfall during the rainy season is generally well distributed throughout the season, which allows the region to be very agriculturally productive. The dry season covers 4 to 5 months, from November to February/March. It is a period of very little rainfall. The harmattan (a hot, dry, often dusty wind from the Sahara that blows over West Africa, particularly Togo, from November to February) reinforces the drought in the region in December and January. All in all, the central region has a rainfall pattern that is conducive to agricultural production.

➤ **Plateaux region**

Plateaux region is the largest region of Togo. It produces almost all of the coffee and cocoa exported. It is a region that stretches from the latitude of Gamé to the latitude of Blitta. In terms of food products, it provides more than 35% of the overall tonnage of the main foodstuffs and is one of the most visited tourist regions in the country. It is one of the rainiest regions in the country, with a normal rainfall of 1,500 mm, despite its relatively advanced location inland. The rainfall regime is marked by two seasons that are not very distinct from each other, given the amount of monthly rainfall throughout the year. The rainy season begins in February and ends in November/December, it lasts on average 10 months with a slight

depression in August. The monthly rainfall varies from month to month. As one moves inland, the small dry season of the Guinean climate regimes diminishes in importance, sometimes becoming non-existent, which gives the region the characteristic of a climatic transition towards a unimodal regime with two clear seasons. The dry season is very short and covers two to three months of relatively good rainfall, December, January and February.

➤ **Maritime region**

The Maritime region is located in the south of Togo on the edge of the Atlantic Ocean. The rainfall regime is bimodal, with two extremes, the first in June and the second in September-October. There are two rainy seasons: a short one and a long one. The long rainy season lasts five months on average. It starts in March, the monthly water level increases progressively and regularly until May/June when it reaches its maximum, then it starts to decrease in July and ends in August. The second rainy season, which is short, covers three months, from September to November. Its maximum is reached in September. The rainfall of this season is less important than the first one. The dry season is also characterized by two seasons: The long dry season, which is longer, has more of the characteristics of a dry season in a tropical Sudanese climate. Rainfall is generally low, with relatively high average temperatures making the period very harsh. It begins in November and ends in February/March with the beginning of the main rainy season, and lasts on average four months. The month of January is the least rainy month and therefore drier, it is the month of the Harmattan. The very low amount of rainfall recorded during this month, places it in the category of ecologically very dry months, the short dry season is centered on August. It's The dryness of the season is accentuated by the cold Benguela current that settles on the Togolese coast during this month. Unlike the long dry season, which is less rainy and warmer, the short season is cool with frequent gales.

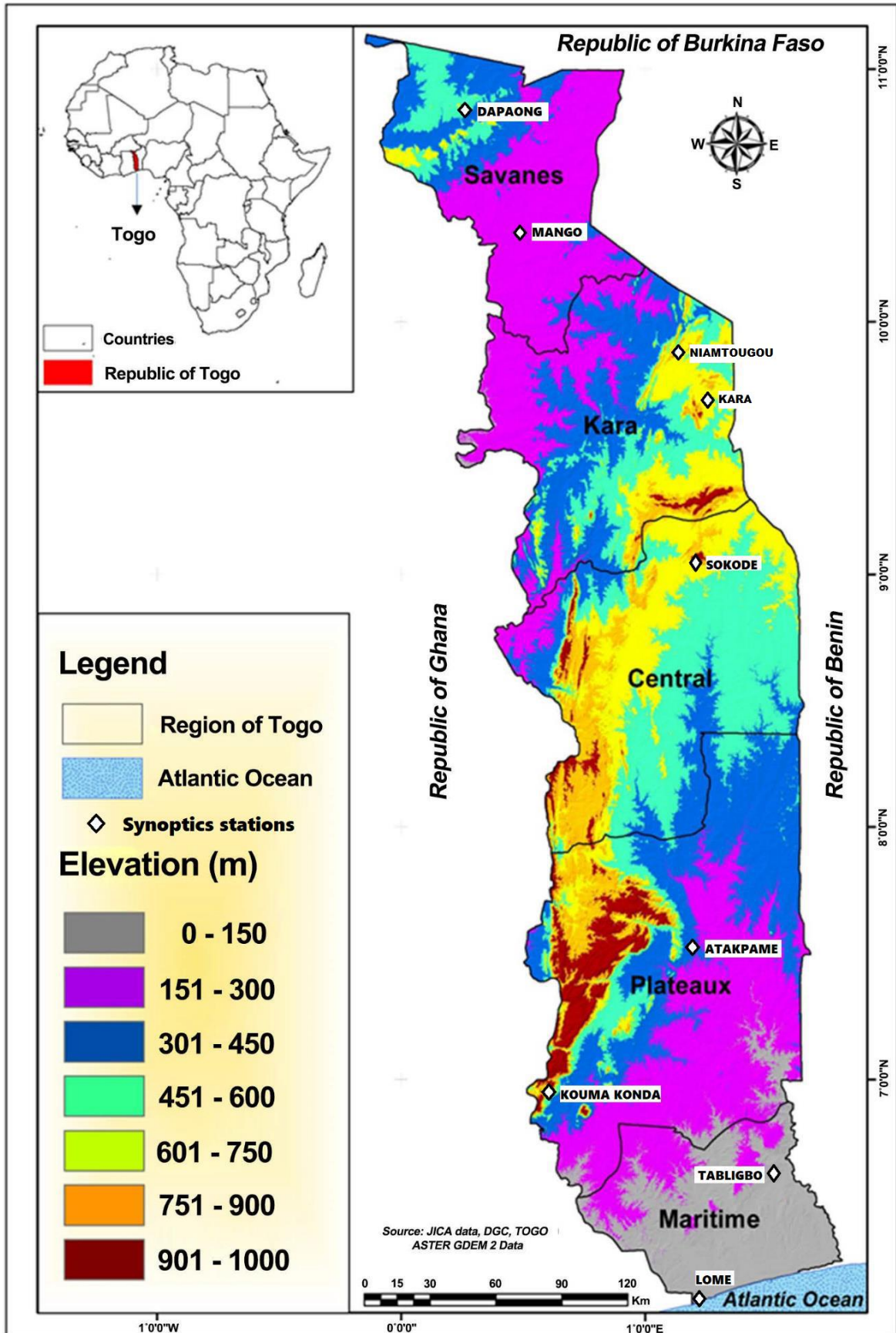


Figure 2: Study area with the 5 administrative regions and the locations of the synoptic weather stations used in this study (Source: JICA data, DGC, TOGO ASTER GDEM 2 Data).

3.2. Rainfall dataset

The primary data used in this study is monthly accumulated rainfall. For this, two datasets of rainfall were selected, rain gauge rainfall data from Togo synoptic weather stations network, which can be referred to as ground truth, and the monthly rainfall product derived from the Integrated Multi-Satellite Retrievals for GPM (IMERG) algorithm, which combines information from the Global Precipitation Measurement (GPM) mission satellite constellation to estimate precipitation at a global scale. While rainfall data from in situ weather stations are expected to present higher accuracy than satellite estimates, their spatial representativeness is limited (Orlowsky & Seneviratne, 2014). Therefore, the integration of the IMERG rainfall product in the current analysis aims to better constrain the spatial distribution of dry and wet events across Togo. Detailed information on these datasets is provided.

3.2.1. Togo synoptic weather stations network rainfall data

Monthly rainfall time series from January 2001 to December 2019 of nine synoptic weather stations (Lomé, Tabligbo, Kouma Konda, Atakpamé, Sokodé, Kara, Niamtougou, Mango, and Dapaong) over Togo were obtained from Togo Meteorological Services without any missing value and quality assured. The dataset period covers 19 years, therefore almost spanning the last two decades. Geographical distribution and additional details on the stations are presented in Figure 2 and Table 1. The stations' spatial distribution includes all the five administrative regions of Togo, from north to south, Savanes, Kara, Centrale, Plateaux, and Maritime.

The stations' data are used firstly to characterize time (interannual and seasonal) and spatial variability of precipitation in Togo and, subsequently, to evaluate IMERG rainfall product in order to analyze if the satellite estimate capture adequately the seasonal and interannual variability of precipitation over the country's five administrative regions. Finally, from the stations' rainfall data, SPI time series were calculated for each site to characterize the dry and wet events and their respective intensity and scale.

Table 1: Togo weather stations used in the present study and their location details.

Weather Station Site	Admin. Region	Elevation (m)*	Latitude (°N)	Longitude (°E)
Lomé	Maritime	20	6,17455	1,25315
Tabligbo	Maritime	44	6,60475	1,50789
Atakpamé	Plateaux	250	7,538338	1,12143
Kouma Konda	Plateaux	643	6,95617	0,572
Sokodé	Centrale	340	8,99517	1,15176
Kara	Kara	341	9,62788	1,20357
Niamtougou	Kara	278	9,8	1,083333
Mango	Savanes	145	10,36191	0,46916
Dapaong	Savanes	330	10,836	0,22809

*MASL: Meters Above Sea Level

3.2.2. IMERG rainfall data

The IMERG rainfall data is available globally at a spatial resolution of $0.1^{\circ} \times 0.1^{\circ}$, which is considered as a high-resolution product. The products are available with various latency periods, the early-run (IMERG-E) and late-run (IMERG-L) products, which are released 4 hours and 12 hours after a real-time, respectively; and the final run (IMERG-F), which is post-real-time and calibrated with the GPCP data and released after about two months. For the present study, we selected the final run (IMERG-F) and at monthly temporal resolution also for a period spanning from January 2001 to December 2019. The IMERG rainfall dataset was obtained from NASA's website¹. The performance of IMERG precipitation products has been evaluated worldwide under distinct topographical features and also used to characterize rainfall variability in different climate regimes (arid and wet) across the world. Sun et al. (2018) found IMERG rainfall final-run product IMERG-F at a monthly timescale to have good detection ability and, therefore, able to provide data support for long-time series analyses in the Northeast of China. Mohammed et al., (2020), evaluating IMERG rainfall for arid climate, found high detection accuracy over moderate elevation areas (inland regions), whereas it had poor performance over flat plains (coastal regions) and high altitudes (foothills and mountainous regions). In addition, their results also showed that IMERG rainfall had high performance in capturing the various rainfall intensities, with light rain having the highest accuracy, while higher rainfall intensity experienced lower accuracy. However, focusing their evaluation on Africa, Dezfuli et al.(2017) found that IMERG precipitation presented a better agreement with gauge data in East Africa and humid West Africa than in the southern Sahel. These results reveal that IMERG rainfall product performance varies by season and region.

¹ <https://pmm.nasa.gov/data-access/downloads/gpm>.

Therefore, validation of IMERG monthly precipitation over Togo, focusing on interannual and seasonal variability and in the context of the present study, is performed via comparison with the observed precipitation at each of the synoptic stations (Lomé, Tabligbo, Kouma Konda, Atakpamé, Sokodé, Kara, Niamtougou, Mango and Dapaong). Once validated, IMERG rainfall gridded data are used to map Togo dry and wet events and their respective intensity and timescale (meteorological, agricultural and hydrological) using SPI.

3.3. Ocean-Atmosphere climate modes variability

Among the several ocean-atmosphere climate variability modes reported in the literature, to relate to the variability of rainfall (dry and wet events) over Togo, two were selected for this study: a) El Niño/Southern Oscillation (ENSO), the main worldwide predictor for climate variability; b) the South Atlantic Ocean Dipole (SAOD). Additional information on these climate modes, the indices selected to represent their occurrence and intensity, and the links from where their time series were obtained are described below.

3.3.1. Niño3.4 index

For the ENSO climate variability mode, the Niño3.4 Index is used. This index is largely used for seasonal rainfall forecasts over West African countries and is NOAA's main indicator for monitoring El Niño and La Niña events, which are positive and negative phases of ENSO, respectively. The Niño 3.4 index typically uses a 5-month running mean, and El Niño or La Niña events are defined when the Niño 3.4 SST anomalies exceed ± 0.5 °C for a period of six months or more. According to the National Oceanic and Atmospheric Administration (NOAA), if El Niño3.4 Index is $+0.5$ or higher, it means that there is El Niño condition indicating that the east-central tropical Pacific surface water is significantly warmer than usual. For La Niña conditions, this index should be -0.5 or lower, which indicates that the region is cooler than usual.

To compute the Niño3.4 Index, NOAA's Climate Prediction Centre calculates the average sea surface temperature in the Niño 3.4 region in the east-central tropical Pacific between 5N-5S,170W-120W (see figure 3) for each month, and then they average it with values from the previous and following months. This running 5-month average is compared to a 30-year average. Niño3.4 Index time series used in the present study were obtained from NOAA/PSL website².

² <http://www.cpc.ncep.noaa.gov/data/indices>

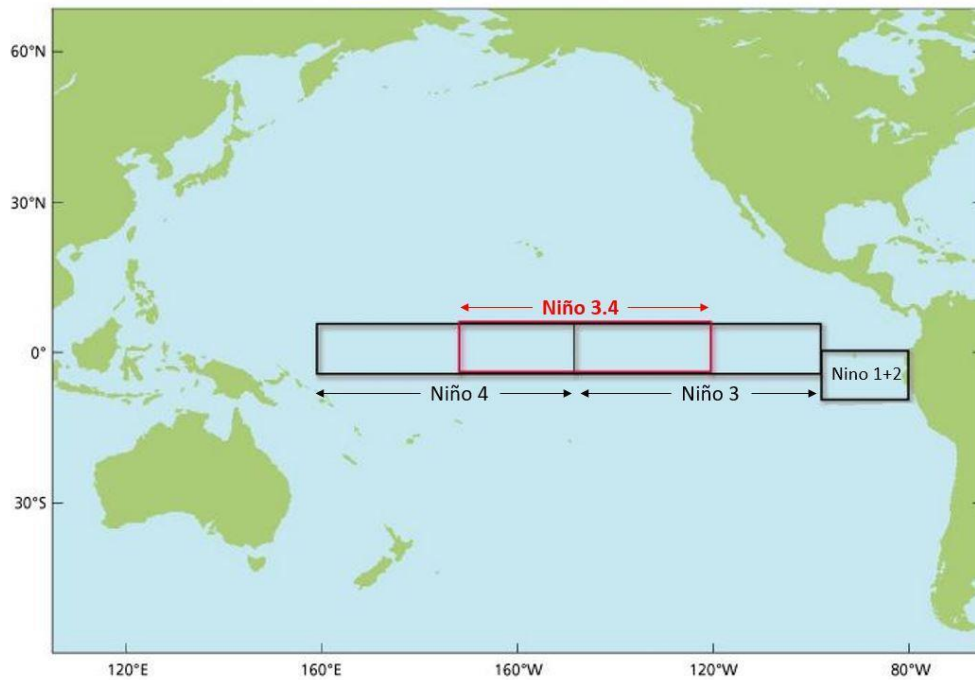


Figure 3: Geographical location of Niño 3.4 region (Source: NOAA, 2015)

3.3.2. South Atlantic Ocean Dipole Index (SAODI)

The South Atlantic Ocean Dipole (SAOD), as the name indicates, occurs in the Atlantic, when the sea surface waters are warmer than normal off the coast of West and Central Equatorial Africa region and at the same time is observed cooling of surface waters with the similar amplitude off the coast of Argentina-Uruguay-Brazil (Nnamchi & Li, 2011). These sea surface temperature (SST) patterns are coupled to the atmospheric circulation field and regional climates.

A typical SAOD episode has a life cycle of about eight months, although the peak intensity in which the SST anomalies are evidently coupled to atmospheric circulation and precipitation anomaly fields lasts for four months (May-August), during the austral winter (Nnamchi et al., 2011). A simple measure of the dipole, the SAOD Index (SAODI), is defined by differencing the domain-averaged normalized SST anomaly (SSTA) of the two mentioned centers of intense warming and cooling associated with the SAOD (see figure 4).

$$\text{SAODI} = [\text{SSTA}]_{\text{NEP}} - [\text{SSTA}]_{\text{SWP}}$$

Where the square brackets indicate the domain averages, the subscripts show the two regions over which the SSTA averages are calculated. These domains are described by their locations in the South Atlantic Ocean as the North East Pole (NEP: 10°E–20°W, 0°–15°S) and

the South-West Pole (SWP: 10°–40°W, 25°S – 40°S). The SAODI was obtained from the UNIFEI website³

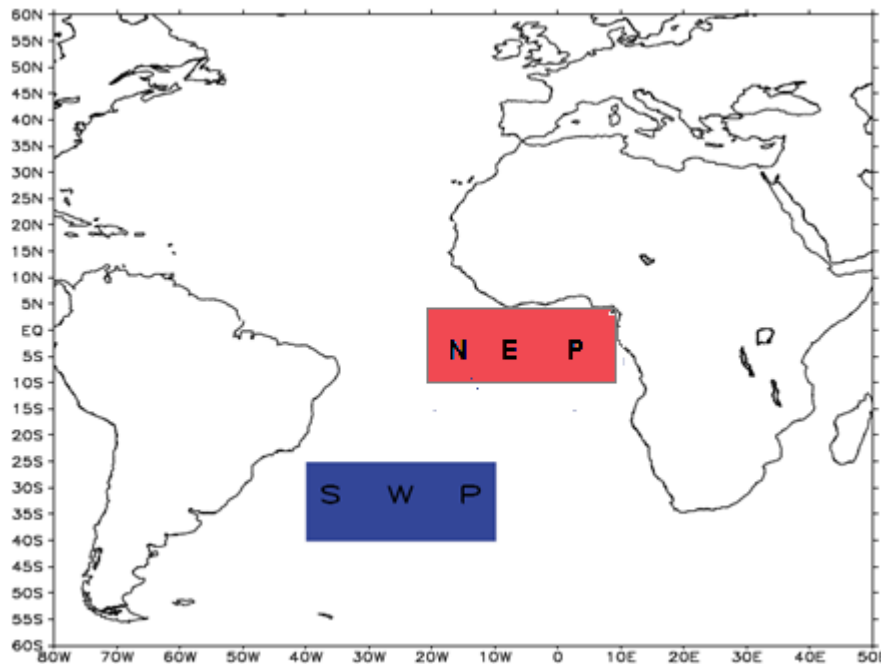


Figure 4: Geographic location of the North East Pole (NEP, 10°E–20°W, 0°S–15°S) and South-West Pole (SWP, 10°W–40°W, 25°S–40°S) used to calculate the SAODI. (Source: Nnamchi et al., 2011)

3.3.3. Extended Reconstructed Sea Surface Temperature (ERSST) dataset

The Extended Reconstructed Sea Surface Temperature (ERSST) dataset is derived from the International Comprehensive Ocean-Atmosphere Dataset (ICOADS) (Huang et al.; 2017), and it has a resolution of $2^\circ \times 2^\circ$ grid with spatial completeness enhanced using statistical methods. In the present study, was used the Extended Reconstructed Sea Surface Temperature, version 5 (ERSST V5) for the South Atlantic Ocean region from 2001 to 2019. The dataset was obtained from the NOAA website⁴.

According to Huang et al. 2017, the ERSST newest version (V5) has been revised and updated from version 4. This update incorporates a new release 23 of ICOADS R3.0, a decade of near-surface data from Argo floats, and a new estimate of 24 centennial sea-ice from HadISST2 (Hadley Center Ice-SST version 2).

³ <https://meteorologia.unifei.edu.br/teleconexoes/indice?id=saodi>

⁴ <https://www.ncdc.noaa.gov/data-access/marineocean-data/extended-reconstructed-sea-surface-temperature-ersst-v5>.

3.4. Methods

3.4.1. Inter-comparison between rain gauge data and IMERG rainfall product

The satellite monthly rainfall estimates intercomparison with rain gauge was based on point-to-pixel validation. Essentially, each rain gauge is compared with the closest IMERG pixel. It is worth mention that IMERG rainfall information consists of area-averaged within its 0.1° grid (Huffman et al., 2019). However, one would expect that the effect of this discrepancy in spatial representativeness for the IMERG-F monthly product used in this study would be generally lower.

This intercomparison process goal was to evaluate the ability of IMERG to reproduce monthly, seasonal and interannual variability of precipitation across Togo.

The statistical metric used to carry out the intercomparison are described below.

These are commonly used to describe the level of agreement between the IMERG products and gauge observations (Tang et al., 2020). Thus, the statistical indicators used are: **(1)** the Mean Absolute Error (MAE) is commonly used to measure the average magnitude error between two samples (Eq.1); **(2)** the Bias reflects the degree to which the estimated precipitation (rainfall from IMERG) value is over or underestimated (Duan & Liu, 2012) (Eq.2); **(3)** the root mean square error (RMSE) is a frequently used as a measure of the differences between two variables. It also, like MAE, measure the average magnitude error (Eq.3). The smaller the numerical value of RMSE is, the closer the observed values are to the precipitation estimations (F. Chen & Li, 2016). In addition to the 3 previous statistics metrics, R^2 was also computed to show how well the station's observation rainfall data are fitted with IMERG estimation data. R^2 (coefficient of determination) is the square of correlation coefficient (r), which is used to analyse how one variable can be explained by a second variable, and its range is 0 to 1.

$$MAE = \frac{1}{n} \sum_{i=1}^n |S_i - G_i| \quad (\text{Eq.1})$$

$$Bias = \frac{\sum(S_i - G_i)}{n} \quad (\text{Eq.2})$$

$$RMSE = \sqrt{\frac{1}{n} \sum_{i=1}^n (S_i - G_i)^2} \quad (\text{Eq.3})$$

Where:

G_i = gauge rainfall measurement (mm);

S_i = satellite rainfall estimate (mm)

n = is the sample total number

Targeting regional dry and wet events analysis, IMERG rainfall estimate was averaged across the domain of each five administrative regions of Togo.

3.4.2. Dry and Wet events characterization: Standard Precipitation Index (SPI)

There are several indices to evaluate precipitation anomalies in the literature, Palmer Drought Severity Index (PDSI, (Wayne Palmer, 1965), Deciles Method (DM, (Gibbs and Maher, 1967), the Standardized Precipitation Index (SPI, (McKee) and Standardized Precipitation Evapotranspiration Index (SPEI, (Stagge et al., 2015)). Their importance as tools to support public policies, agricultural systems monitoring, and study climate variability and trends has been largely recognized (Nandintsetseg & Shinoda, 2013; Parry et al., 2016). For the present study, SPI was selected; it is a simple measure of drought and wet periods and considers only precipitation data as input, which is a differential in relation to the other indices. SPI quantifies the deficit or excess rainfall at different time scales, allowing the monitoring of short and long-term droughts (McKee et al., 1993). Usually calculated for periods of 1 to 48 months, along with the timescale nature, it also provides the evaluation of the dry and wet periods intensity.

The SPI calculation used in the current study is based on the density and probability function Gamma (Eq. 4), where, $F(x)$ is the general formula for the probability density function of the exponential distribution, $\alpha > 0$ and $\beta > 0$ are, respectively, the form and scale parameters, $\Gamma(\alpha)$ is the gamma function, and x is the rainfall amount, with x varying according to α and β . Apart from being the most used distribution function in SPI studies, (Guenang and Kamga, 2014) found that gamma and the Weibull are the functions that best fit precipitation in Cameroon, which is dominated by a climate regime similar to Togo, tropical and strongly influenced by the West African Monsoon.

$$F(x) = \int_0^x f(x)dx = \frac{1}{\Gamma(\alpha)\beta^\alpha} \int_0^x x^{\alpha-1} e^{-x/\beta} dx \quad (\text{Eq.4})$$

The SPI values represent the number of standard deviations from the mean at which an event occurs. Thus, for instance, the 3-months SPI value compares accumulated rainfall over that specific 3-months period with the mean accumulated rainfall for the same period calculated over the full study period (Guenang and Kamga, 2014). This applies to any n-month SPI value, where n, the number of months of accumulation, is the time scale. High SPI positive values indicate wet conditions, and high negative values correspond to drought scenarios. According

to (Guttman, 1998), time scales on the order of 3 months may be important to evaluate drought scenarios (negative SPI) for agricultural applications, while for water-supply management, longer time scales, up to years, are of more interest (Guttman, 1998). Although it is possible to determine specific thresholds (Guenang and Kamga, 2014), SPI scales and categories of dryness and wetness events that are followed in this study are those based on McKee et al.,(1993) and presented in Table 2.

Table 2: Categories and scale of SPI index adapted from (McKee et al.,1993)

SPI values	Categories
≥ 2	Extremely humid
1.50 to 1.99	Very humid
1.00 to 1.49	Moderately humid
0.99 to -0.99	Close to normal
-1.50 to -1.49	Moderately dry
-1.50 to -1.99	Very dry
≤ -2	Extremely dry

Also, dry(wet) evaluation parameters were accessed at different time scales as described below:

- **Peak Intensity (PI):** indicates the lesser SPI value (Dry) or the higher SPI value (Wet) reached in a dry and wet event, respectively.
- **Duration:** the number of months between the beginning of a dry event (or a wet event) and its end.
- **Drought Magnitude (DM):** corresponds to the cumulative water deficit over a drought or dry period. Thus, DM is the sum of all SPI values during a drought event.

To compute SPI at different time scales (1, 3, 6, 12 months) from rainfall at each Togo synoptic weather station and from IMERG-GPM, SPI function developed for MATLAB software (Taesam Lee, 2021), which use the gamma function distribution was used.

3.4.3. Correlation analysis between regional SPI and Nino 3.4 index, SAODI, and South Atlantic SST anomaly.

The relationship between SST variability and the occurrence of dry and wet events in the five administrative regions of Togo is investigated based on the interaction matrix analysis. The SPI 1 month (short-term) for each Togo region is correlated with SSTs indices (Nino 3.4 index and SAODI) and South Atlantic SST anomaly. These correlation analyses aim to identify

the potential variabilities or teleconnections between Pacific, Atlantic, and Gulf of Guinea SST and the occurrence of wet and dry conditions over Togo.

The correlation analyses were based on the Pearson coefficient (r), while the P. value, or the calculated probability, was adopted to evaluate the statistical significance of the obtained correlations.

Pearson correlation coefficient, r , measures the degree of a linear relationship between two quantitative variables, and it is given by Eq. (5). It is a dimensionless index with values between $-1 \leq r \leq 1$, which represents the intensity of a linear relationship between two sets of data, being +1 a perfect positive correlation and -1 a perfectly negative correlation, while values near zero indicated the absence of a linear relationship link (Alhamsry et al., 2020).

$$r = \frac{\sum_{i=1}^n (x_i - \bar{x})(y_i - \bar{y})}{\sqrt{\sum_{i=1}^n (x_i - \bar{x})^2 \sum_{i=1}^n (y_i - \bar{y})^2}} \quad (\text{Eq.5})$$

where $x_1, x_2, x_3 \dots x_n$ and $y_1, y_2, y_3 \dots y_n$ are measured values of both variables, and \bar{x} and \bar{y} are arithmetic means of both variables. Pearson coefficient has been applied in previous studies to evaluate the relationship between rainfall and SST at different significance levels (ex. Alhamsry et al., 2020). The P.value test was used to evaluate the following scenarios: **i)** Accept null hypothesis (H_0): There is no correlation between SPI- n and Nino 3.4 index, SAODI and SST anomaly, where n is the SPI time scales (e.g., 1, 3, 6, 12, months) and **ii)** alternative (H_1 : There is correlation between SPI- n and Nino 3.4 index, SAODI and SST anomaly). The choice of significance level at which H_0 is rejected is arbitrary. However, in this study, it considered as reference the 5% level, which has been commonly used. Therefore, if $P < 0.05$, then the null hypothesis is rejected, and it is accepted that the samples give reasonable evidence to support the alternative hypothesis (Wilks, 2011).

4. RESULTS AND DISCUSSION

4.1. Spatial and temporal variability of monthly precipitation over Togo: Comparison of gauge measurements with Integrated Multi-Satellite Retrievals for GPM (IMERG) estimates.

In this section, the spatial and temporal variability of monthly rainfall over Togo, from 2001 to 2019, are analyzed focusing on two datasets, rain gauge measurements from nine (9) Togo Meteorological Service stations and the rainfall estimates of the Integrated Multi-satellite Retrievals for Global Precipitation Measurement mission (IMERG). The analysis and results obtained are based on comparisons of both datasets to describe Togo mean precipitation and its interannual variability across the country subdivisions at monthly, seasonal and annual time scales for the period from January 2001 to December 2019 when IMERG estimates are available.

4.1.1. Spatial and mean precipitation variability based on IMERG

From 2001 to 2019, the analysis based on IMERG monthly rainfall estimation shows that, Plateaux region was the wettest during the analyzed period, with a mean precipitation of $105 \text{ mm month}^{-1}$; followed by the Centrale region ($104 \text{ mm month}^{-1}$), Kara ($104 \text{ mm month}^{-1}$), and Maritime (90 mm month^{-1}). Savanes with only 88 mm month^{-1} was the region that received the lowest amount of precipitation according to IMERG estimates. It is important to highlight that, Maritime region, which is considered the driest region across Togo (Djaman et al., 2017; Pessiezoum Adjoussi, 2000), received more rainfall during our study period than the Savanes region, making it the driest region.

Maritime, the southernmost region, and Savanes, the northernmost region, registered their highest amount of rainfall in 2019, while Plateaux, Centrale, and Kara had their wettest year, respectively, in 2008, 2003, 2009. The lowest amount of precipitation estimates by IMERG across the country regions, except for Savanes (2001), occurred in 2015, which is the country's driest year for the present study time period. Savanes driest years occurred in 2001. Figure 5 presents monthly mean precipitation maps for Togo considering this study period (2001 - 2019). In the Maritime region (southern Togo), the precipitation began in March and progressed gradually from South to North. September, with an average rainfall of 200 mm, was the rainiest and wettest month across the country. Centrale and the northern regions of Kara and Savanes registered their highest monthly precipitation in July, August, September, according to IMERG estimates, with mean monthly precipitation of 208 mm, 207.5 mm, and

162.5 mm, respectively. During the months of July and August, the southern part of Togo (Maritime and Plateaux regions) experiences a short dry season. Thereafter, precipitation in the Maritime and Plateaux regions start to increase again from September to October, which comprised the second rainy season in southern Togo. In November, Savanes regions received less than 5 mm of precipitation, while the northern part of Central and Kara regions received between 10 to 15 mm. The southern part of Centrale received around 25 mm of rainfall. These patterns found in monthly rainfall mean variability across Togo in the present analysis, in general, are similar to those described by Djaman et al., (2017) using interpolated data from surface stations.

IMERG maximum precipitation over Togo occurred from June to September, during the West African Monsoon period, consistently with previous climatology (Nimon et al., 2020). The South-North migration of the ITCZ is also consistently captured, as described by two rainy seasons regimes seen in the Southernmost region, near the Gulf of Guinea (April to October), and a single rainy season regime in the North (June to September). These results are consistent with Le Barbé et al., (2002) and Djaman et al., (2017) description of the two rain seasons regime near the Gulf of Guinea and one single rainy season in the North of West Africa in their studies.

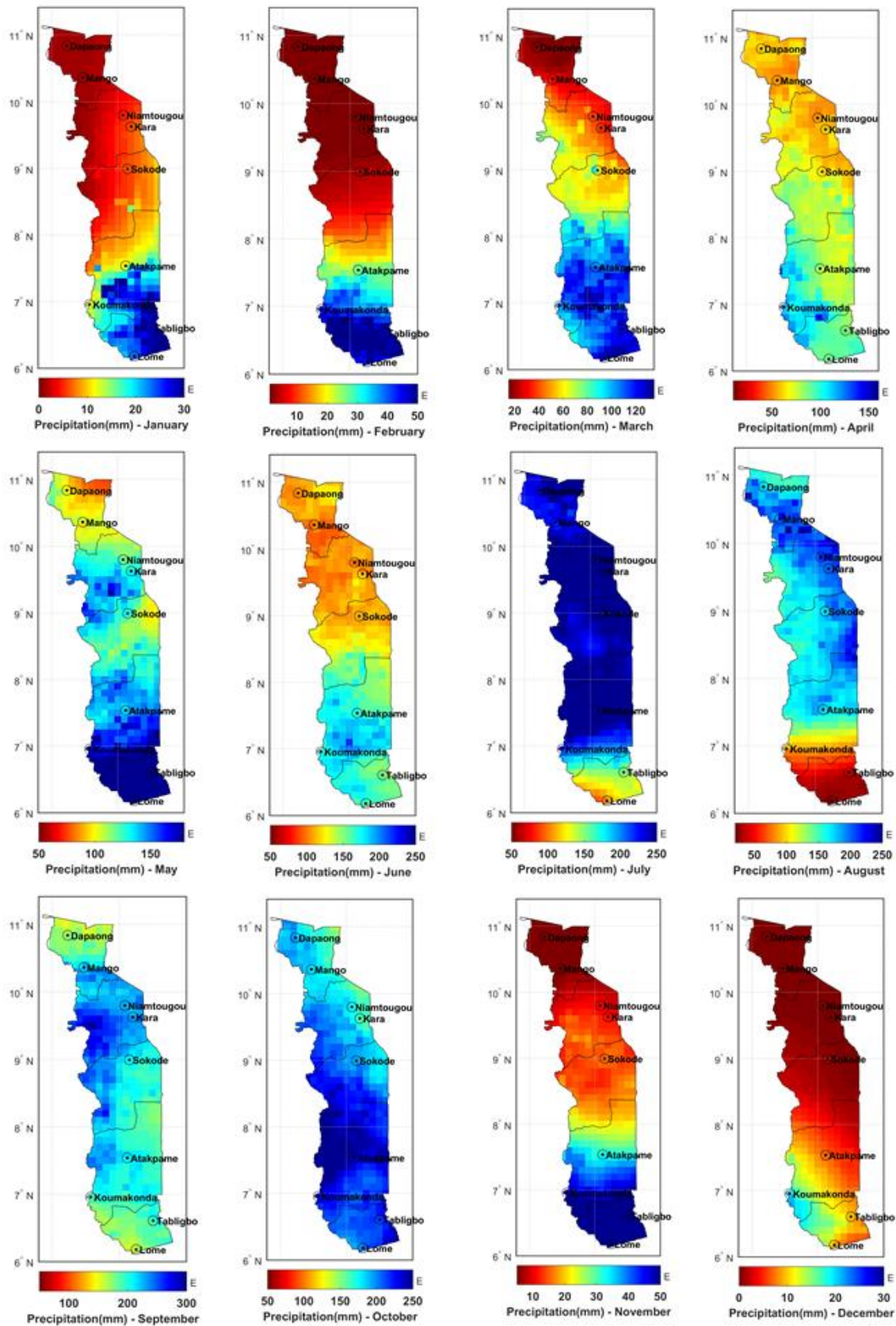


Figure 5: Spatial distribution of monthly mean precipitation across Togo from 2001 to 2019. The named sites correspond to the location of the rain gauge stations used in this study, and the division of the country to the sub-regions, from north to south, Savanes, Kara, Centrale, Plateaux, Maritime.

4.1.2. Comparative evaluation at seasonal scale between rain gauge and IMERG rainfall

In this section, it is conducted an evaluation of IMERG mean seasonal rainfall estimation against rain gauge measurement based on point-to-pixel validation. The focus is to evaluate the IMERG rainfall product's ability to reproduce the mean seasonal variation of precipitation during the period analysis (2001-2019) when compared with the selected meteorological stations.

Figure 6 presents the mean seasonal variability of rainfall based on rain gauges measurements and IMERG estimates at the nine meteorological stations for the study period. During the rainy season in the northern regions of the country, June – July – August – September – October, which coincide with the WAM, both datasets present consistent seasonal variation. In most of the country, the precipitation volume increases from June on, the beginning of the season, peaking in July-August-September, and decreases toward October, which marks the end of the rainy season. IMERG rainfall estimate can consistently depict the seasonal rainfall variation in the northern stations (Dapaong; Mango; Kara; Niamtougou and Sokoké) (Dapaong; Mango; Kara; Niamtougou and Sokoké). However, there are slight differences in the mean amount of the precipitation; in general, IMERG underestimates rainfall during the peak of the rainy season and tends to overestimate during the dry season.

At Kouma Konda, in the mountain area of Plateaux region, IMERG rainfall product captured the seasonal cycle; however, systematically, it underestimates the precipitation amount. At Atakpamé, also in the Plateaux region, a close similarity between IMERG and rain gauge is observed during the dry season. That was not the case for the peak of the first (AMJ) and second (JAS) wet seasons, when IMERG overestimated and underestimated the rainfall volume compared with the gauge data, respectively.

At the stations in the southern part of Togo (Tabligbo and Lomé), seasonal cycle and rainfall amount show high similarity between IMERG and rain-gauge data. IMERG rainfall product demonstrated the ability to capture the precipitation variation for the two rainy seasons that occur in the southern part of the country (April to June and September to October).

In summary, it was observed that, in general, the IMERG dataset is able to reproduce gauge measurement major feature regarding the mean seasonal cycle of precipitation over Togo regions. Nevertheless, notable differences were found at a particular time of the year between the two sets of data. Systematically, IMERG tends to underestimate the precipitation for Kouma Konda (more pronounced) and Atakpamé. This underestimation can be related to

altitude. Indeed, Kouma Konda (641 m altitude) and Atakpamé (400 m altitude) are located in the Atakora mountain chain, which has a higher elevation and more rugged terrain than the other Togo regions. Previous studies reported that complex topography might significantly influence the quality of satellite precipitation estimation (S. Chen et al., 2013; Zhao & Yatagai, 2014).

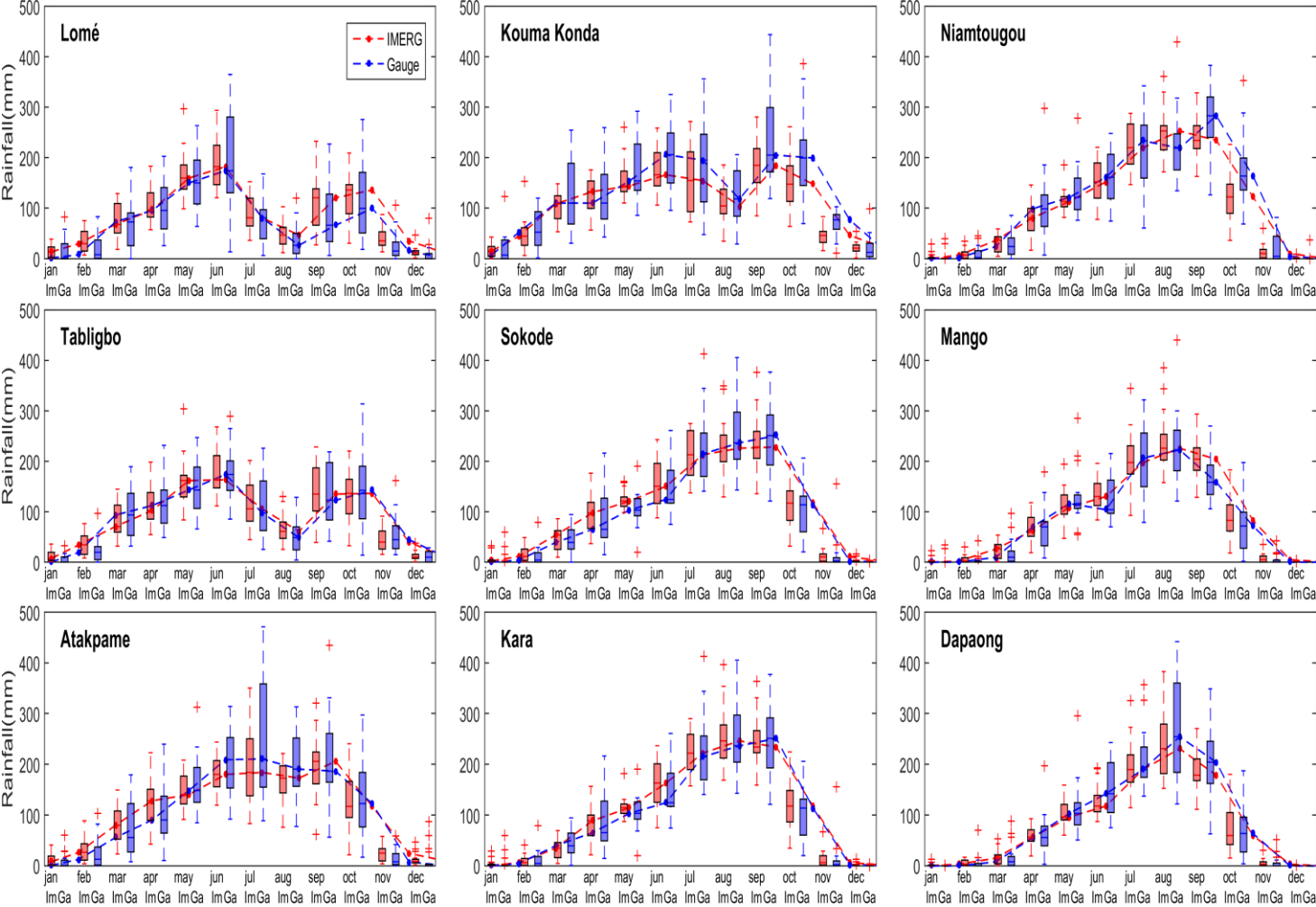


Figure 6: Mean seasonal variability of rainfall (2001-2019) at Togo meteorological stations location as estimate by IMERG rainfall product and obtained from the rain gauge: IMERG (red), Rain gauge (blue).

4.1.3. Interannual rainfall variability over Togo meteorological stations: IMERG versus Rain Gauge

Once evaluated IMERG rainfall product's ability to reproduce the mean seasonality and spatial distribution of precipitation over Togo, this topic's main focus is on evaluating IMERG rainfall products to represent the interannual variability of rainfall across the country. The monthly

accumulated rainfall data were further accumulated to annual precipitation for both rain-gauge data and IMERG data at the station's location for the study period.

Figure 7 presents the interannual variability of the year total precipitation and precipitation anomaly from rain-gauge data, and IMERG rainfall estimates data for Dapaong and Mango meteorological stations in the Savanes region. At Dapaong station, IMERG overestimation occurred from 2002 to 2012; however, the anomaly of precipitation was fairly represented. From 2013 on, underestimation (2013) was alternated with a period of a good match (2014-2016) and overestimation (2017-2019), which led to a significant mismatch of anomaly signal when compared with rain gauge for the year of 2013. At Mango station, also in the northern region of Savanes, a similar IMERG overestimation behavior was found for the first period (2002 – 2012). From the two times periods, IMERG estimated rainfall and rain gauge dataset; it was possible to identify negative anomaly dominant during the year of 2005, as observed for the southern stations, which indicates a lack of rainfall across the country in 2005. Also, according to the IMERG anomaly time series at Dapaong and Mango (see figure 7), a relatively long period, from 2013 to 2016, characterized with negative anomalies found for the southern stations also appeared in the north portion of the country. These features in IMERG are fully consistent with Mango rain gauge anomalies and partially consistent with the Dapaong rain gauge, which only presents a negative anomaly for the year 2015 during the mentioned period. The 2015 anomalies were consistently negative across the country analyzed sites for both dataset IMERG estimate and rain gauge.

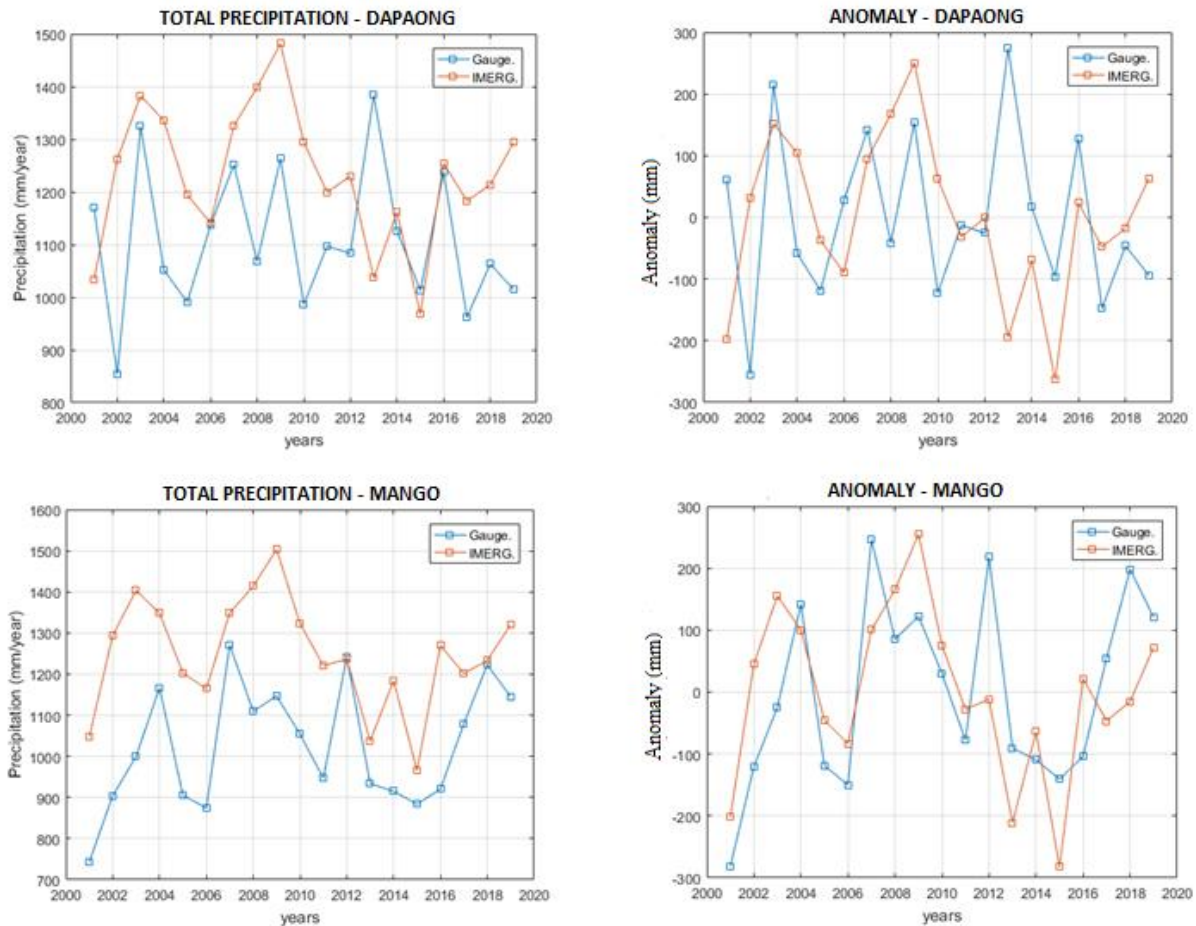


Figure 7: Interannual variability of the total precipitation (right) and precipitation anomaly (left) from rain-gauge data and IMERG rainfall estimates data for Dapaong and Mango meteorological stations

At Kara station, in the north, as shown in figure 8, IMERG underestimates precipitation in 2003, 2010, 2012, and 2016 and this situation matched with the anomalies for the same period. Nevertheless, 2012 and 2016 anomalies were not well captured (IMERG shows positive anomaly while rain gauge shows a negative anomaly). For the remaining years, IMERG presented an anomaly pattern consistent with the rain gauge, except for the years 2018 and 2019, when overestimation occurred. Analyzing Niamtougou station (figure 8, in the same region with Kara station, in general, the anomalies presented by IMERG are consistent with those presented by rain gauge, revealing the satellite-based product to capture the interannual variability. Nevertheless, IMERG underestimation was observed for 2009 and 2012, although the anomaly signal for the two years was similar to that of the rain gauge data. The two stations, Kara and Niamtougou, was also observed a strong negative anomaly in 2015, indicating that this year was characterize by a generalized rainfall deficit, as shown in the Savanes region.

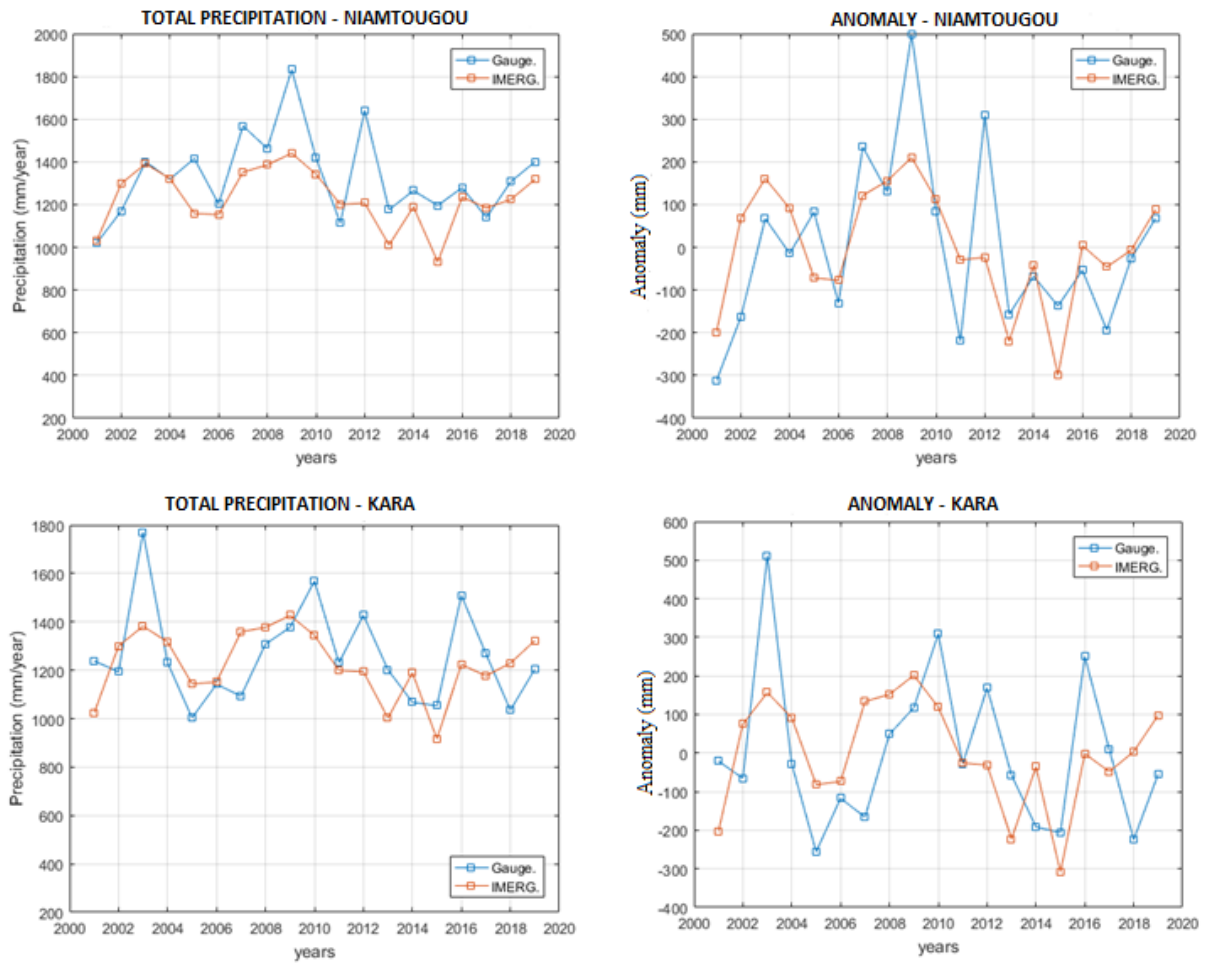


Figure 8: Interannual variability of the total precipitation (right) and precipitation anomaly (left) from rain-gauge data and IMERG rainfall estimates data for Kara and Niamtougou meteorological stations.

Figure 9 shows that at Sakodé in the Centrale region, where only one station was available, the two datasets, IMERG and rain gauge, exhibited strong similarities (2001- 2002) at the beginning of the time series, the anomaly of precipitation was also very well represented for this short period. However, from 2003 to 2005, the IMERG underestimation feature was observed, followed by a slight overestimation for 2006 – 2007 – 2008. From 2009 to the end of the time series, excepted 2019 when a clear overestimation was shown by IMERG, a good consistency was found between the two datasets (IMERG and rain gauge). Moreover, IMERG was able to reproduce the negative anomaly trend of 2015, however more pronounced than rain gauge.

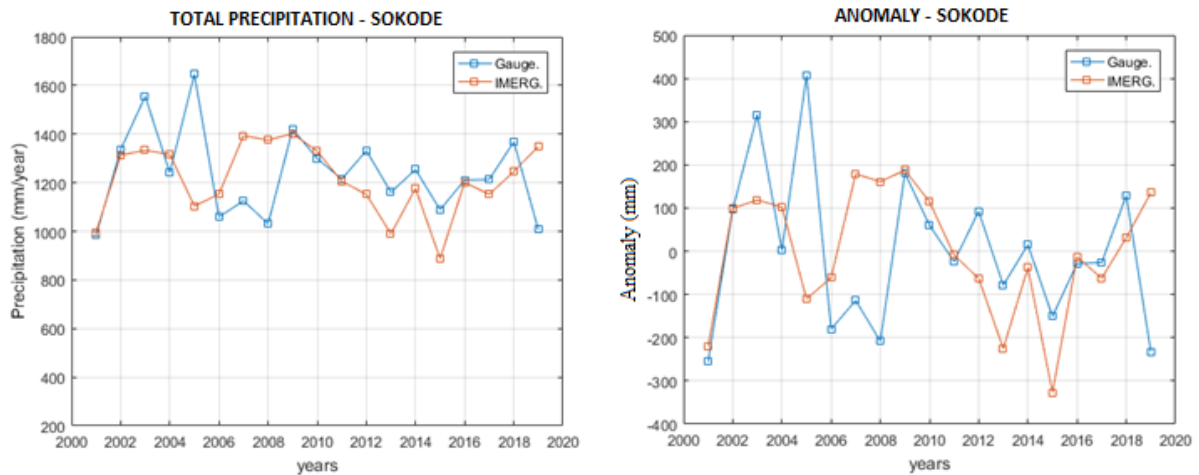


Figure 9: Interannual variability of the total precipitation (right) and precipitation anomaly (left) from rain-gauge data and IMERG rainfall estimates data for Sokodé meteorological station.

In the Plateaux region (see figure 10), in general, IMERG exhibited an underestimation of precipitation for the entire study period at Kouma Konda station. Nevertheless, regarding precipitation anomaly variability, IMERG performs better when compared to the rain gauge. However, it is worth to mention the substantial disagreements between IMERG and rain gauge anomalies for several years (e.g., 2001, 2005, 2010, 2011, 2016, etc.) at Kouma Konda. For Atakpamé, a station located within the same region as Kouma Konda, IMERG also presented an underestimation behavior for the entire time series. Considering the anomaly pattern, a consistent behavior with rain gauge anomaly was observed, although slight underestimations were observed in 2004, 2007, 2008, 2009, and 2019. In general, it is clear that the anomalies variability presented by IMERG is more consistent with rain gauge than the accumulated annual precipitation variability.

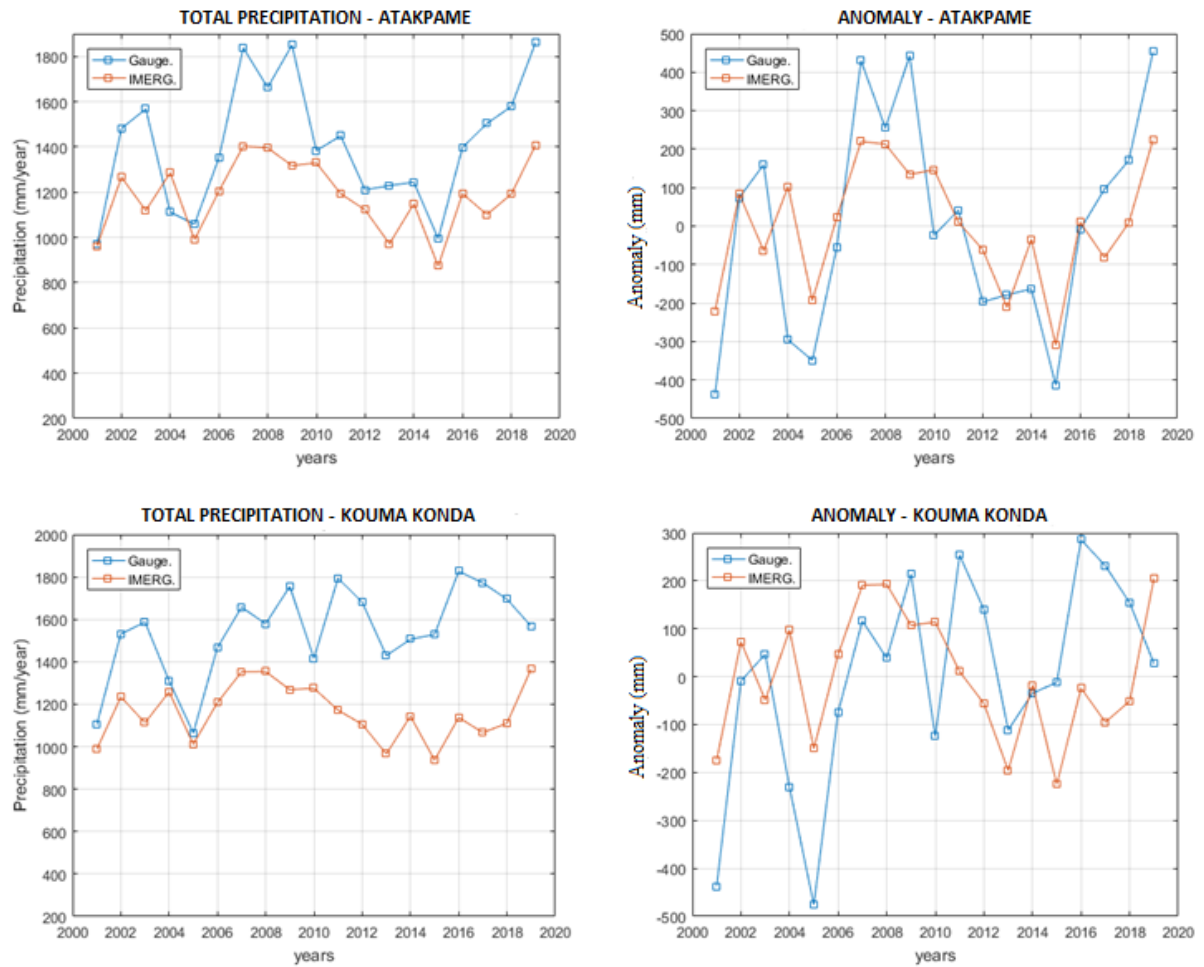


Figure 10: Interannual variability of the total precipitation (right) and precipitation anomaly (left) from rain-gauge data and IMERG rainfall estimates data for Atakpamé and Kouma Konda meteorological stations.

Figure 11 presents the interannual variability of annual precipitation and its anomaly at Lomé and Tabligbo meteorological stations, both located in the Maritime region. However, as can be seen in the comparison, except for the years 2010 and 2019, the satellite-based product was able to capture the interannual variability of rainfall anomalies over Lomé and Tabligbo, consistently. It is possible to identify periods dominated by a negative anomaly, lack of rainfall, in both datasets and the two stations. For instance, a lack of precipitation in the year 2005 was also identified by IMERG over Lomé and Tabligbo. A relatively long period, between 2013 and 2016, marked by a significant decrease in precipitation, is also captured consistently by the IMERG product over both stations. IMERG presents its best performance over Tabligbo.



Figure 11: Interannual variability of the total precipitation (right) and precipitation anomaly (left) from rain-gauge data and IMERG rainfall estimates data for Lomé and Tabligbo meteorological stations.

Despite the IMERG’s tendency to overestimate and underestimate annual precipitation at some stations, in general, it presented a good performance to capture the interannual variability of rainfall anomalies over Togo, an important aspect for its application in the context of precipitation monitoring. Periods of major negative (2005 and 2015) and positive (2008) anomalies in precipitation across the country were consistently represented. The rainfall products struggle to fully captured the rainfall patterns over stations characterized by strong local effects, for instance, Kouma Konda, a mountain area. These results of the intercomparison between IMERG and rain gauge measurements across Togo stations corroborate F. Chen & Li, (2016) conclusion about the relationships between the local climate and the accuracy of precipitation estimation amount from satellites. While these local features are a challenge for satellite products, they also reveal that rain gauge spatial representativity can be limited.

Therefore, satellites estimates may provide complimentary precipitation variability information overall Togo regions.

4.1.4. Statistical comparison between rain gauge rainfall and IMERG rainfall at monthly scale

IMERG monthly precipitation extracted at the closest pixel to the rain gauge stations coordinates were compared to the monthly precipitation of the rain gauge. Figure 12 shows scatter plots of IMERG monthly accumulated rainfall from 2001 to 2019 against accumulated rainfall data from each synoptic ground station.

In general, the scatter plots suggest a consistent correlation between IMERG and rain gauge data, except for Lomé. It is worth mention that the Tabligbo rain gauge, which seems to be better correlated with the IMERG estimate, is located in the same region that Lomé, Maritime. As pointed out previously, this suggests that IMERG's limitation to capture monthly precipitation at Lomé may be related to local issues. Another aspect that can be pointed out from a qualitative assessment of the scatter plot is that IMERG tends to overestimate months with a high amount of precipitation in most of the stations. For months with a low amount, its values tend to be lower than the rain gauge. This feature is less perceptible for the Tabligbo station.

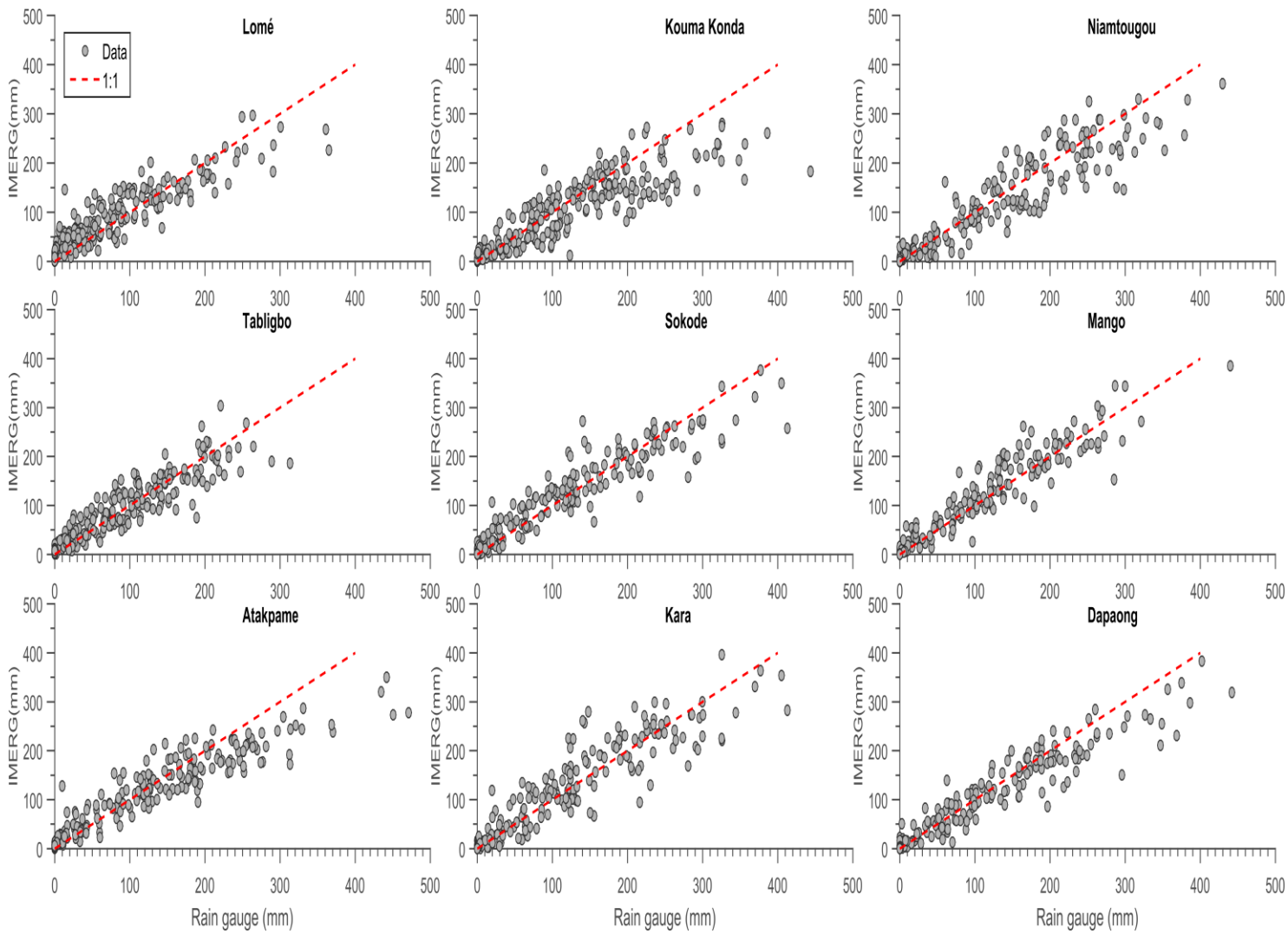


Figure 12: Scatter plots of monthly accumulated rainfall from rain-gauge stations versus IMERG rainfall estimate at rain gauge coordinates considering all months of the year.

A summary of the statistical indicators (RMSE, MAE, Bias, and R^2) used to compare IMERG quantitatively against rain gauge is presented in Table 3.

These parameters are commonly used to evaluate or quantify the differences between the satellite product's precipitation estimation against precipitation measurement provided by rain gauges (F. Chen & Li, 2016; Dembélé & Zwart, 2016).

Table 3: Statistics indicators obtained from the intercomparison between IMERG monthly rainfall estimate and rain gauge measurements considering the entire year.

STATIONS	MAE	RMSE	Bias	R²
ATAKPME	41.68	61.66	-18.76	0.80
DAPAONG	39.51	56.86	10.14	0.70
KARA	33.70	49.18	-1.17	0.79
KOUMAKONDA	45.34	63.96	-32.10	0.87
LOME	25.6	33.68	8.98	0.80
MANGO	35.42	47.92	18.65	0.71
NIAMTOUGOU	36.28	51.77	-9.89	0.76
SOKODE	38.37	55.27	-2.06	0.77
TABLIBO	22.15	30.01	1.66	0.87

As suggested by the scatter plot analysis (figure 12), the best MAE score is obtained for Tabligbo station (22.15), where the IMERG product presented a better performance in representing local precipitation, and the higher MAE is observed for Kouma Konda (45.34), a station where IMERG rainfall estimate needs improvement. These results are also confirmed by RMSE; at Tabligbo, IMERG presented the lowest RMSE (30,01 mm), whereas, for Kouma Konda, it presented the highest RMSE with 63.96 mm. The results suggest that there can be local characteristics that may influence the performance of IMERG in these two localities, given that they are in the same region and distanced just about 50 km. This also shows that spatial precipitation representativity may be restricted for some stations, which can be a challenge for precipitation maps based on ground station interpolation.

At Tabligbo it was obtained the smallest Bias, which is positive (1.66), meaning that on average, IMERG slightly overestimated precipitation, and the highest Bias (-32.1) was found for Kouma Konda, where IMERG underestimated local rainfall. The particular characteristic of Kouma Konda is that it is in a mountain region, and as has been shown in some previous studies (Chen et al., 2013; Zhao & Yatagai, 2014), IMERG struggle to reproduce precipitation in high elevated and rugged regions.

For Atakpamé (in Plateaux region), Kara, Niamtougou (in Kara region), and Sokodé (in Centrale region), IMERG rainfall product presented a negative Bias in comparison with rain gauge, which indicated that IMERG tends to underestimate rainfall at these stations. And for the stations in the Maritime region, Lomé and Tabligbo, and those in the northern region of Savannes, Mango, and Dapaong, positives Bias was found, which indicates that on average, there is an overestimation of rainfall by IMERG over these regions.

The evaluation of the performance of IMERG during the WAM season (June -July-August-September) and during the months out of WAM season was also conducted. The statistical analysis for these two periods, which are shown in tables 4 and 5, demonstrates that during WAM season compared to the period out of the WAM season, IMERG tends to underestimate the precipitation amounts, as we can see with the negative Bias for most of the stations except for Lomé (Bias = 32.92), Tabligbo (Bias = 7.59) and Mango (Bias =12.36) where the satellite estimate presented overestimation of rainfall.

In addition, in general, the performance of IMERG regarding the statistic metric indicators (tables 4 and 5) is better out of the WAM season, when the country receives less precipitation than during WAM season when it receives most of its annual precipitation. It is worth mentioning the significant improvement in IMERG rainfall estimate at Sakodé, and Dapaong during the period out of the WAM.

Table 4: Statistics indicators obtained from intercomparison between IMERG monthly rainfall estimate and rain gauge measurements during the period out of West Africa Monsoon season (June, July, August and September)

STATIONS	MAE	RMSE	Bias	R²
ATAKPME	25.16	35.67	4.26	0.75
DAPAONG	29.30	40.52	22	0.58
KARA	22.34	32.12	12.89	0.71
KOUMAKONDA	36.90	54.39	-23.50	0.84
LOME	21.93	27.98	7.92	0.76
MANGO	28.63	39.27	21	0.58
NIAMTOUGOU	27.35	40	0.33	0.66
SOKODE	25.34	35.48	15.57	0.70
TABLIGBO	19.54	27.85	-1.30	0.84

Table 5: Statistics indicators obtained from intercomparison between IMERG monthly rainfall estimate and rain gauge measurements for the meteorological stations during the West Africa Monsoon season

STATIONS	MAE	RMSE	Bias	R²
ATAKPME	74.71	94.13	-64.68	0.71
DAPAONG	59.90	80.10	-15.35	0.31
KARA	56.39	72.07	-29.33	0.52
KOUMAKONDA	62.23	79.71	-49.29	0.79
LOME	32.92	42.86	11.1	0.87
MANGO	48.97	61.69	12.36	0.51
NIAMTOUGOU	54.13	68.84	-30.36	0.52
SOKODE	64.41	81	-37.33	0.38
TABLIGBO	27.36	33.92	7.59	0.88

Overall, the IMERG product, in general, shows the ability to represent the main temporal and spatial features of rainfall over Togo. Over specific locations, mainly mountain (Kouma Konda), the product presented important limitations that need to be further explored aiming improvement of IMERG over these particular regions.

In general, IMERG overestimates precipitation during the scenario of large precipitation volume (ex. Monsoon period) and underestimates precipitation during low rainfall amount scenario (dry season).

IMERG has shown significant improvement, when compared with other satellites product, in describing annual and monthly precipitation (Salles et al. 2019).

The annual rainfall spatial distribution from rain gauges much very well with the regional distribution of rainfall obtained from IMERG. This showed that IMERG precipitation estimation over Togo Regions has an excellent accuracy at an annual scale.

Although our results did not give the perfect scores of statistics indicators (1 for the Bias and 0 for MAE and RMSE), we can conclude that IMERG can give a good estimation of the precipitation over Togo regions. This is confirmed by the studies of F. Chen & Li (2016) who's also founded a good performance between IMERG products and rain-gauge data over China.

In summary, despite the observed and discussed disagreements, IMERG rainfall estimate inter-comparison with rain gauge demonstrated that the satellite-based product could reproduce the main features of temporal and spatial variation of precipitation across Togo. Based on monthly mean rainfall distribution across all Togo subdivisions, the results showed that the IMERG rainfall product reflected well the seasonal precipitation distribution (e.g. at the station of Atakpamé in 2008, although IMERG estimation of total precipitation was lower

than rain gauge measurement, the anomaly which is the deviation from the mean was consistent with rain gauge. The major deviations from rain gauge features, were the underestimation in the high elevation region of Kouma Konda (Plateaux region).

Certainly, continuous evaluation of the accuracy and reliability of the IMERG monthly products is highly recommended in order to improve its performance over Togo and West Africa countries as a whole. Satellite-based high-quality precipitation data with high spatiotemporal resolution is fundamental to optimize rainfall monitoring coverage in areas with limited rain gauge networks and, therefore, to improve the accuracy of climate extremes (e.g. Drought) early system warning.

An important aspect observed in the intercomparison between rain gauge and IMERG rainfall is the ability of the latter to reproduce the interannual anomalies of precipitation, even for Lomé and Kouma Konda, where large deviations from accumulated precipitation were observed. This result suggests that IMERG rainfall product could be used to monitor interannual variability climate extreme events occurrences, namely those related to drought and wet period in Togo.

4.2. Characterization of dry and wet events in Togo using SPI at a different time and spatial scales

In this section, SPI results are applied to characterize dry and wet climate events in Togo. The results are analyzed considering the different time (3-months; 6-months, and 12-months) and on spatial (local and regional) scales. Gauge precipitation measurement and IMERG rainfall estimate at pixels closer to rain gauge stations coordinates were used to obtain SPI at the local scale, while IMERG rainfall averaged across each Togo administrative region domain was taken as representative of regional scale.

3-months SPI reflects short- and medium-term moisture conditions and provides a seasonal estimation of precipitation (National Drought Mitigation Center, 2021). In agriculture areas like Togo, this time step SPI is very important because it highlights moisture conditions availability at different stages for different crops, for example, maize which is the most cultivated crop in all regions in Togo.

6-months SPI indicates the medium-term trend in precipitation. It also gives information about anomalous stream flows and reservoirs levels. 6-month SPI can be very effective in showing the precipitation over distinct seasons (National Drought Mitigation Center, 2021), for example, during the monsoon season.

12-months SPI gives information's on long-term precipitation patterns and is associated with streamflow, reservoir levels, and as well as to groundwater levels for a longer time scale. The following SPI analysis focus on very wet events (SPI values between 1.5 to 1.99); extremely wet event (SPI values higher than +2.0); very dry events (SPI values between -1.5 to -1.99); and extremely dry events (SPI values lower than -2), these are the events expected to have the largest social, economic and environmental negative consequences.

4.2.1. SPI analysis at the local scale: Rain gauges measurements against IMERG's precipitation estimations at rain gauges coordinates

The aim of this section is to analyze SPI features at a local scale based on rain gauges measurements and to evaluate IMERG's precipitation estimation's ability to capture the occurrence of wet and dry events at a local scale.

4.2.1.1. SPI from rain gauge and IMERG at Dapaong and Mango (Savanes region)

Figure 13 shows the different categories of wet and dry periods from 2001 to 2019, respectively, using the IMERG dataset and rain gauge dataset at Dapaong and Mango, both located in the Savanes region.

SPI 3-months (SPI-3) obtained based on rain gauge at Dapaong (figure 13) indicates 8 dry events occurrences; 2 lasted 7 months and were the longest periods in terms of duration. The first one started in June 2002 and ended in December 2002, with a peak intensity (PI) of -1.62, reached in October 2002. This event was critical since it occurred during the monsoon period (June to September). It had a Magnitude (DM) of 7.43. The second one started in March 2015 and ended in September 2015, with a PI of -2.73 (August 2015), during the monsoon season and had a DM of 9.82. Concerning wet periods scenarios, 7 cases were identified using rain gauge data; the longest lasted 8 months, from July 2009 to February 2010, with a PI of 1.54 peaked in January 2010.

Results of SPI 6-months (SPI-6) highlighted 6 cases of dry periods. The longest duration was 13 months, and this dry event started in March 2002 and ended in March 2003, with a PI of -2.27 in November 2002 and a DM of 17.62. The highest PI (-3.03 extremely dry) occurred between April – November 2015 within the monsoon period, and the related dry event lasted 9 months, with a DM of 11.90. Regarding wet periods and considering only the very and

extremely wet events, 5 cases were found, and the longest one begun in February 2013 and ended up in March 2014, with 14 months duration and PI of 2.12 (very wet) in December 2013.

Accordingly, to the SPI 12-months (SPI-12) analysis, within the entire study period, a total of 3 long-term dry events were identified within the category of very and extremely dry. The longest duration was 25 months and was related to a dry event that started in October 2004 and ended in October 2006. However, this event was lesser intense (-1.53) than the one that started in September 2017 and that ended in September 2019. This later event was shorter (13 months) but presented a higher PI -2.22 (extremely dry). The DM of this dry period was 14.40. For the same time scale (SPI-12), 5 cases of wet periods occurred at Dapaong accordingly to the rain gauge measurements. The event that started in July 2013 to August 2014 (within the monsoon period), lasting 15 months, was extremely wet, with a PI of 2.14 reached in April 2014.

Based on IMERG's rainfall estimation, the SPI-3 reveals 9 dry events for the study period, and 3 were within the extremely dry category at their peak. The most extremely dry lasted 8 months, with a PI of -3.01 reached in July 2015 a DM of 13.99. On the other hand, there were 11 wet periods. The longest lasted 14 months (from February 2009 to March 2010) and with a PI of 2.35 (within the category of extremely wet).

The analysis of SPI-6 shows that 7 major dry periods occurred. The most intense reached its PI, about -2.92 (extremely dry), in July 2015 with a DM of 21.39, and it lasted 11 months (from May 2015 to March 2016). For the same time scale, 5 wet periods were identified. The longest lasted 25 months; it begun in June 2008 and ended in May 2010, and was extremely wet with a PI of 2.13.

SPI-12 shows 3 long-term dry periods and 2 long-term wets periods. The longest dry event lasted 39 months with a PI of -2.44 and the longest wet period lasted 37 months (from August 2007 to August 2010) with a PI of 2.05.

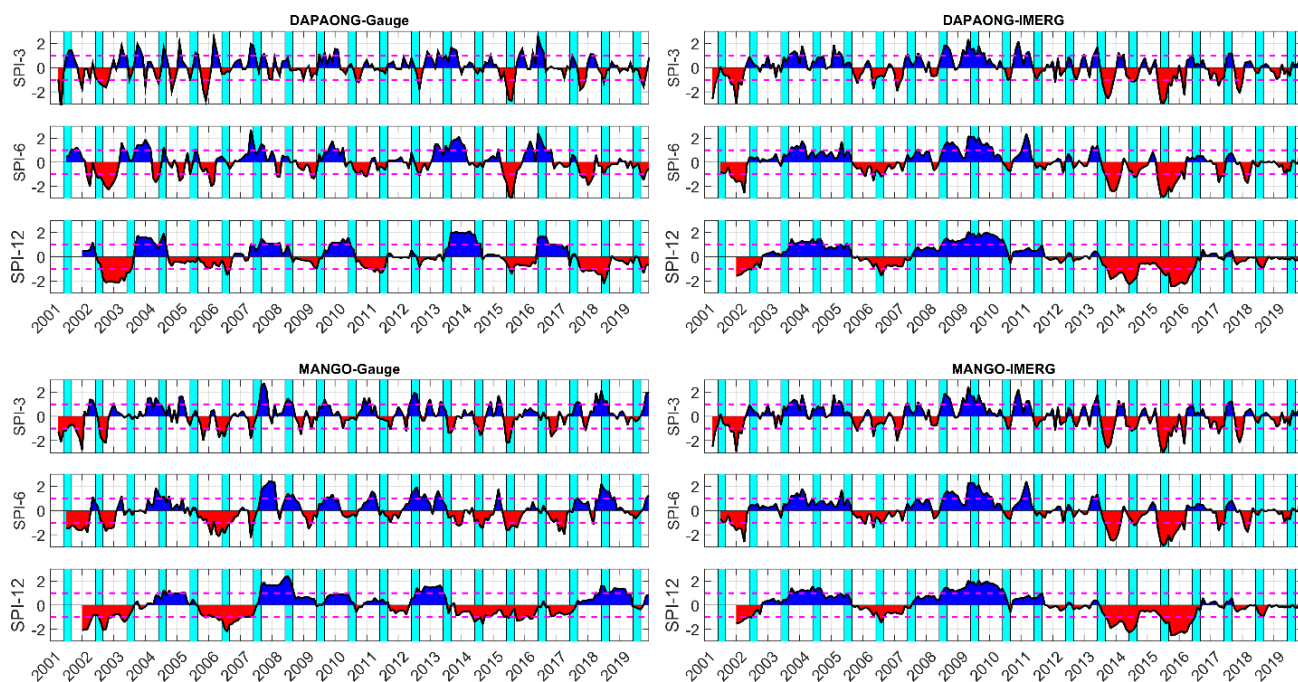


Figure 13: Standard Precipitation Index calculated for Dapaong (top figures) and for Mango (down figures) sites using IMERG rainfall dataset (right figure) and rain gauge rainfall dataset (left figure). The vertical cyan colors indicate the monsoon season period, and the horizontal dot pink line indicates the separation of the near and normal conditions (values between -1 and 1) from the very, moderately, and extremely scenarios (≤ -1 and $\geq +1$)

As also shown in figure 13, SPI-3 analysis for Mango site using rain gauge rainfall measurement, also in the Savanes region, revealed that, from 2001 to 2019, there were a total of 6 cases among very and extremely dry events at this station, 3 cases were classified as very dry, and 3 were extremely dry. The longest, extremely dry one lasted 10 months (April 2001 to January 2002). This event lasted all the monsoon season and reached a PI of -2.78 in January 2002 with 13.76 as DM. The 3 subsequent dry events of 2013, 2014, and 2015 occurred within the monsoon period and were a direct consequence of the decrease of rainfall during this period, which contributed to the build-up of a long-term dry event (SPI-12) that lasted from 2014 to 2016. It is important to highlight that a dry event during the monsoon period is more critical than a dry period that occurred out of the monsoon season. Five wet periods were observed at Mango using the gauge dataset, with 2 extremely wet cases and 3 severely wet. The wet event of August 2007 to December 2007 was short in duration, but it was the most extreme wet, with a PI of 2.75 reached in October. We also observed that the wet events of 2007, 2008, and 2009 occurred within the monsoon period, and that helped to build up a long-term wet period between 2007 and 2012 for the SPI-12-time scale.

SPI-6 analyses show that 5 dry medium-term periods occurred, out of which 1 was extremely dry and 4 very dry. The extremely dry period lasted 16 months, from September

2005 to December 2006, reached a PI of -2.13. On the other hand, there were a total of 5 wet periods at Mango. The longest one lasted 14 months (February 2004 to March 2005), therefore including the 2004 monsoon periods, it reached a PI of 1.85. From these 5 wet periods, 2 were extremely wet and 3 very wet. The 3 very wet events reached their PI respectively in May 2004 (1.85), in March 2011 (1.57), and in August 2012 (1.95). Regarding the 2 extremely wet events, their PI occurred respectively in December 2007 (2.41) and in June 2018 (2.19).

The results of SPI-12 indicated that 1 dry event reached a category of very dry (-1.58 as PI) in September 2014, and 2 events reached a category of extremely dry. Among the 2 extremely dry events, that of September 2005 to July 2007 was the most intense, with a PI of -2.19 reached in August 2006 and a DM of 24.76. The second extremely dry event (from January 2002 to August 2003) reached a PI of -2.10 in January 2002 out of the Monsoon period.

The event of November 2013 to July 2016 was only very dry (-1.58 as PI); however, it lasted 32 months, and its DM was 35.23. As pointed out, this long-term dry period was a result of 3 subsequent monsoons periods (2013, 2014, and 2015) with a rainfall deficit. From SPI-12 results, 3 wet periods were also identified, out of which 2 were very wet and 1 extremely wet. With a PI of 1.62 reached in May 2013, the first very wet event lasted 15 months (from June 2012 to July 2013). The second lasted 21 months (from September 2017 to May 2019). The extremely wet event started in August 2007 to May 2009, was the longest (22 months), and it reached a PI of 2.42 in July 2008. This event was a result of 3 consecutive wet Monsoon periods (2007, 2008, and 2009).

SPI-3 plot using IMERG rainfall for Mango presented in figure 13 shows that 8 cases of dry periods occurred, 3 were extremely dry, and 5 were very dry. The dry period of April 2001 to April 2002 was the longest one and lasted 13 months, with a PI of -2.89 and a DM of 14.63.

From 2013 to the beginning of 2016, three important dry events occurred with PI of -2.60 (October 2013), -1.19 (July 2014), and -2.98 (July 2015), respectively. The event of 2013 lasted 6 months (from August 2013 to January 2014), and the 2015 event lasted 8 months (from May 2015 to January 2016). These two events were extremely dry. IMERG captured these subsequent dry events, which occurred within the monsoon period consistently with the rain gauge, and they were the base of the most important long-term dry event when considering SPI-12. For the same SPI time scale (SPI-3), there were 8 wet events, with 6 very wet and 2 extremely wet. The most extremely wet period lasted 15 months (from February 2009 to March 2010), and it occurred mainly in the 2009 monsoon period and reached a PI of 2.43. The events of 2003, 2005, 2007, 2008 also occurred within the monsoon period. The subsequent medium-

term (SPI-6) and long-term (SPI-12) wet events were a consequence of the very wet event of 2008, which reached a PI of 1.89 (August 2008), and that occurred in 2009.

Looking at the medium-term scale (SPI-6), 6 dry periods were identified at the Mango site, 3 extremely dry and 3 severely dry. The most important events were those that occurred in 2013 and 2015. They were extremely dry and reached, respectively, PI of -2.49 (in December 2013) and -2.91 (in July 2015). These two critical dry events occurred within the monsoon period. Thus, IMERG was consistent with the rain gauge at this station, although the PI for SPI-6 produced using rain gauge is much higher compared to IMERG.

Concerning wet periods, 5 events were identified, 2 extremely wet and 3 very wet. The period from August 2007 to March 2008, lasting 8 months, appeared to be the wettest among the extremely wet, with a PI of 2.41.

SPI-12 results for Mango revealed 1 extremely dry period and 1 very dry event. The dry event, which started in July 2013 and ended in September 2016, lasted 39 months with a DM of 52.58, was the longest and more intense. It reached its first PI in June 2014 with -2.28 at the beginning of monsoon season and the second PI in November 2015 at the end of monsoon season, suggesting that the 2015 dry event was associated with further monsoon period, which can be seen in SPI-3 and SPI-6. The 2 others dry events lasted, respectively, 10 months (January 2002 to 2002) and 23 months (September 2005 to July 2007). Regarding wet periods, there were 1 extremely wet and 1 very wet. The very wet event lasted 37 months (from November 2002 to August 2005) and reached a PI of 1.57 in June 2004, while the extremely wet event lasted 37 months (August 2007 to August 2010) with a PI of 2.04 reached in September 2009. This extremely wet event was associated with the subsequent very wet monsoons periods of 2008 and 2009, as can be seen in SPI-3 and SPI-6.

4.2.1.2. SPI characterization from rain gauge and IMERG at Niamtougou and Kara (Kara region)

Figure 14 shows the different categories of wet and dry periods from 2001 to 2019, respectively, using the IMERG dataset and rain gauge dataset at Niamtougou and Kara stations. At Niamtougou station (Cf. figure 14), located in the western portion of the Kara region, SPI-3 analysis from rain gauge shows that there were 3 extremely dry and 4 very dry periods. The most extremely dry period lasted 5 months (from October 2017 to February 2018) and reached a PI of -2.67 in December 2017. This event started at the end of the monsoon season when a deficit of rainfall was observed, and it had a DM of 8.57.

The longest dry event occurred at the beginning of the study period and lasted 21 months (April 2001 to December 2002), and reached a PI of -2.11 in January 2001 and a DM of 18,82. In addition, 3 important dry events occurred in 2003, 2014, and 2015 within the monsoon period. The 2015 event was extremely dry, with a PI of -2.38 reached in June 2015.

On the other hand, 6 wet periods occurred, 3 were very wet, and 3 were extremely wet. The longest wet period lasted 14 months; it started in March 2007 and ended in May 2008, with a PI of 1.61 in February 2008. This event happened during and at the end of the monsoon period, indicating that the 2007 monsoon period was very wet.

SPI-6 time series show 6 dry periods at Niamtougou; the longest one lasted 21 months, from July 2001 to March 2003, and had a PI of about -2.16 and a DM of about 22.12. The events that occurred in 2013, 2014, and 2015 were important in the sense that they were related to the subsequent monsoon period of these years. Regarding wet periods, it was possible to identify a total of 4 events, 2 very wet and 2 extremely wet, and all of them occurred within the Monsoon period. The longest event lasted 13 months (from June 2012 to July 2013), and its PI was 2.26 in April 2013. With a PI of 2.82, reached in October 2009, the event started in May 2009 and ended in March 2010 (12 months) was the most intense.

SPI-12 analyses revealed 4 dry periods at Niamtougou, 3 very dry and 1 extremely dry, which lasted 23 months (from October 2017 to August 2019) and reached a PI of -2.12 and with a DM of 20.85. The event that begun in November 2013 and ended in July 2016 was the longest and lasted 33 months. This event lasted all the monsoon season of 2014 and 2015, and its PI was observed in September 2014 (-1.58). SPI-12 analysis also pointed out 3 wet periods 2 very wet and 1 extremely wet. The extremely wet event lasted 39 months (from August 2007 to August 2010) and was also the longest one, and its PI was 2.35 in October 2009. The 2 very wet events reached their PI respectively in May 2015, with 1.70, and in October 2016, with 1.67.

Based on the IMERG rainfall dataset, figure 14 shows wet and dry periods events identified at Niamtougou. The 3 months SPI revealed 7 dry periods, 5 extremely dry and 2 very dry. The most extremely dry period started in May 2015 and lasted 11 months, with a PI of -2.90 during the 2015 monsoon period and a DM of 17.34. The second extremely dry event lasted 9 months (from August 2001 to April 2002) with a PI of -2.32, reached in January 2002. The event of 2013 was also important, and it occurred within the monsoon period, with a PI of -2.51 and a duration of 9 months (July 2013 to January 2014). For wet periods, there were a total of 8 wet events, 5 extremely wet and 3 very wet. The event of 2009 was the most important

one in terms of duration (10 months) and in PI (2.38 reached in May 2009). Also, this extremely wet period occurred within the monsoon season as the very wet events of 2003, 2007, and 2008.

The results of SPI-6 show 5 dry periods, 3 extremely dry and 2 very dry. The most extremely dry event, with a PI of -2.93 and a DM of 22.55, lasted 11 months (May 2015 to March 2016). The extremely dry event of 2013 lasted 9 months (from August 2013 to March 2014) and reached a PI of -2.42 in November 2013. Regarding extremely dry events that occurred from July 2001 to May 2002 (11 months), it reached a PI of -2.51. For the wet periods, 2 extremely wet and 1 very wet were identified considering SPI-6. Figure 14 also shows 2 wet periods that sustained for a period at Niamtougou, according to the IMERG dataset. The first lasted 26 months (from July 2003 to August 2005) with a PI of 1.89 reached in February 2004. The second one, with a PI of 2.38 reached in July 2009, lasted 20 months (from July 2008 to February 2010). Both events occurred during the monsoon season.

The SPI-12 shows a sustained and long dry period and a short dry period. The longest period lasted 39 months with a PI of -2.61 and a DM of 52.02. It started in July 2013, reached an intensity of -2.20 before weakened in 2015, and went up again to reach its highest PI in November 2015 (-2.61). The 2014 monsoon season rainfall was not enough to recover the moisture conditions, and the 2015 monsoon season presented a strong rainfall deficit.

On the other hand, two wet periods were identified. The longest one started in July 2007 and lasted 36 months. It was extremely wet and reached a PI of 2.11 in October 2010. The second wet period was very wet and reached a PI of 1.85 in June 2004, and it lasted 34 months (from November 2002 to August 2005).

Figure 14 also shows the different categories of wet and dry periods obtained at Kara station, also located in the west portion of the Kara region. Analyzing SPI 3-months' time scale based on rain gauge dataset, there were in total 3 dry periods, 2 were very dry and 1 extremely dry. The extremely dry period lasted 10 months (February 2019 to November 2019) and reached a PI of -2.13, with a DM of 8.95. The Very dry event occurred in 2006; it reached a PI of -1.98 in July 2006 and lasted 6 months (from May 2006 to October 2006). For wet periods, as can be seen in figure 12, 3 wet events were identified, 2 extremely wet and one very wet. The longest wet period lasted 9 months (July 2003 to March 2004), and at certain times it was extremely wet, mainly at the end of the 2003 monsoon season. The 2005 extremely wet period occurred during the monsoon period; it lasted 8 months (from April 2005 to November 2005) and reached a PI of 2.45 in August 2005.

SPI-6 analysis shows that for the Kara site, there were 5 dry periods, 3 extremely dry and 2 very dry. The most extremely dry period lasted only 9 months (May 2006 to January

2007) and reached a PI of -2.12 in July 2006, with a DM of 5.13. On the other hand, there were 3 wet periods at the Kara site, one very wet and 2 extremely wet.

The results of SPI-12 indicated 3 long-term dry periods at Kara, all of them severely dry. The longest one lasted 37 months (from August 2006 to August 2009) and had the highest PI (-1.89), with a DM of 36.75. Regarding the wet events, there were only 2, and both were extremely wet. The longest one started in October 2002 to September 2004 (24 months) and reached a PI of 2.42 in June 2004. With a PI of 2.63, the extremely wet event of April 2005 to July 2006 (16 months) was the most intense.

The SPI-3 (see figure 14) obtained using IMERG rainfall estimate revealed 6 dry periods at the Kara site, all of them were in the category of extremely dry. The 2015 dry period was the most extremely dry, with a PI of -2.87 and a lasting time of 8 months. Its DM was 14.37. Regarding wet periods, 5 were identified, 3 were very wet, and 2 extremely wet. The first extremely wet event lasted 9 months (July 2003 to March 2004) and reached a PI of 1.84 in February 2004. The second one lasted 10 months (February 2009 to November 2009); it was the longest and intense at a certain time (2.39 as PI).

IMERG 6-months SPI shows 5 dry periods, 2 severely dry and 3 extremely dry. The year 2015 registered the most extremely dry event, which lasted 11 months and reached a PI of -2.92 in July 2015 and a DM of 22.78. On the other hand, there were 3 wet periods, 2 extremely wet and one very wet. The longest extremely wet event lasted 36 months (August 2007 to July 2010), and it was also the most intense one with 2.12 as PI, reached in September 2009. The second extremely wet period lasted 34 months and reached a PI of 1.83.

The results of SPI-12 pointed out a severely dry period (from January 2002 to October 2002) and an extremely dry period (July 2013 to September 2016) which had a PI of -2.65 and a DM of -52.04. Also, 2 wet periods occurred within the SPI-12-time scale, one severely wet (November 2002 to August 2005) and one extremely wet (August 2007 to July 2010).

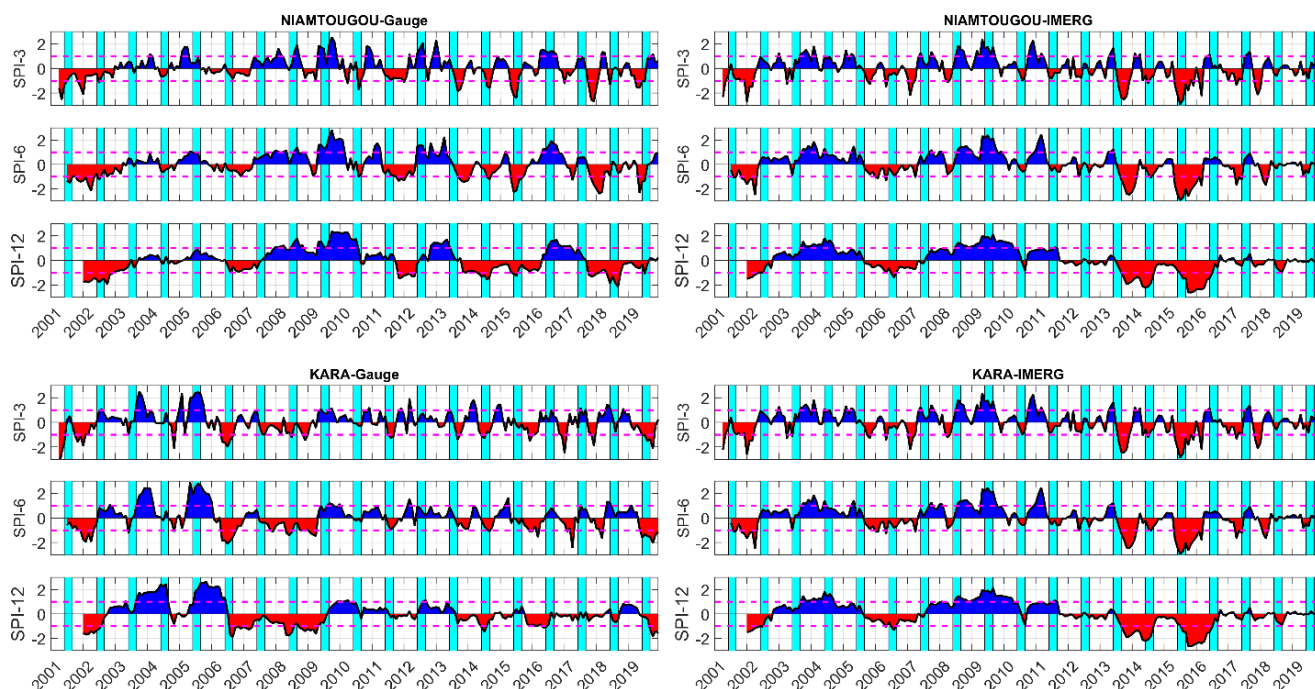


Figure 14: Standard Precipitation Index calculated for Niamtougou (top figures) and for Kara (down figures) sites using IMERG rainfall dataset (right figure) and rain gauge rainfall dataset (left figure). The vertical cyan colors indicate the monsoon season period, and the horizontal dot pink line indicates the separation of the near and normal conditions (values between -1 and 1) from the very, moderately, and extremely scenarios (≤ -1 and $\geq +1$).

4.2.1.3. SPI Characterization from rain gauge and IMERG at Sokodé (Centrale region)

Figure 15 shows the SPI time series at 3, 6, and 12-months scales obtained using rain gauge at Sokodé station (located in the northwest portion of Centrale region) for the entire period of this study. The SPI-3 time series show that there were 5 dry periods, 3 were very dry, and 2 were extremely dry. The most extremely dry period lasted 4 months, from November 2016 to February 2017, with a peak Intensity of -2.5, a DM of 5. The very dry event of 2006 (PI = -1.98) and the two moderates' consecutive dry events of 2007, 2008 were particularly important because they occurred during the monsoon periods and led to medium (SPI-6) and long-term (SPI-12) dry events. This suggests that consecutive dry periods during consecutive monsoon seasons will have a higher impact on the economy than an extremely or very dry event that occurred out of the monsoon season. In addition, the moderate dry event of 2014 and very dry event of 2015 with respectively a PI of -1.46 and -1.52 occurred during the monsoon period, and they were observed throughout all the stations and across all the country.

The wet periods at Sokodé were in total of 6 cases, 4 very wet and 2 extremely wet. The most extremely wet (PI of 2.51) started in July 2003 and ended in March 2004 (9 months), which suggests a wet monsoon season in 2003. The event of 2005, which was related to an

extremely wet monsoon, lasted 8 months (from April 2005 to November 2005) and had a PI of 2.45 reached in August 2005.

For the SPI-6-time scale, the results showed 5 dry periods at Sokodé, two very dry and 3 extremely dry. The longest, very dry period lasted 1 year (from July 2001 to June 2002) and reached a PI of -1.94, and with a DM of 12.65. However, the dry events that occurred in 2006 (from May 2006 to January 2007), with a PI of -2.12 in July 2006, and that from July 2007 to April 2009 (-1.48 as PI) were the most important due to the fact that they occurred within monsoon season. They were at the basis of the longest long-term dry period observed in SPI-12. On the other hand, for SPI-6, there were 3 wet periods at Sokodé, one very wet and 2 extremely wet. The most extremely wet event lasted 10 months (April 2005 to January 2006) and reached a PI of 2.90 in the middle of the monsoon period. The second extremely wet period lasted 10 months (from August 2003 to June 2004) and reached a PI of 2.43 in December 2003.

The SPI 12-months' time scale results revealed 3 events that reached the very dry category at Sokodé. No one event was within the extremely dry category. The longest very event lasted 37 months (from August 2006 to August 2009), with a PI of -1.89 and a DM of 36.75. Although not as severe, another period characterized by a long-term rainfall deficit at Sokodé was the period from 2013 to 2016. For wet periods, 2 extremely wet events were identified, and the longest lasted 23 months, from October 2002 to September 2004, and reached a PI of 2.45 during the 2004 monsoon season. With a PI of 2.63 reached in November 2005, the second extremely wet event was the most intense and lasted 16 months (from April 2005 to July 2006); it resulted from an extremely wet monsoon in 2005.

SPI time series based on IMERG precipitation was also computed for the Sokodé site (see figure 13). The analysis of SPI-3 shows that 7 dry periods occurred, and all of them reached the extremely dry category. The most extremely dry period that peaked in the monsoon season (-2.74 as PI) lasted from May 2015 to December 2015, a total of 8 months. IMERG data also indicates an important deficit of precipitation during the 2013 monsoon, which contributed to the dry event that followed the rainfall season of that year and peaked at its end. The wet periods were in total of 6; 4 very wet and 2 extremely wet. The most extremely wet event lasted 9 months (From February 2009 to October 2009) and had a PI of 2.45 at the beginning of the monsoon season.

The results of SPI 6-months pointed out a very dry period and 3 extremely dry periods at Sokodé. The most extremely dry, which reached a PI of -2.78, lasted 11 months, from May 2015 to March 2016, with a DM of 22.82. On the other hand, based on IMERG rainfall, there were 3 cases of wet periods at Sokodé, one that reached the very wet category and two

extremely wet. The most extreme wet event lasted 19 months; it started in July 2008 and ended in January 2010, with a PI of 2.66, during the 2009 monsoon period. The second extremely wet peak occurred in the earlier months of 2011 and lasted until the period before the monsoon season.

IMERG SPI-12 time series shows 2 major dry periods within the study period, one very dry and an extremely dry event with a PI of -2.83 and that lasted 39 months (from July 2013 to September 2016), its DM was 52.22. For the wet periods, 2 cases were identified, a very wet event and one that reached the extremely wet category, which lasted 36 months, from August 2007 to July 2010 and reached a PI of 2.08 during the 2009 monsoon season. The very wet period reached a PI of 1.65 in June 2004 at the beginning of monsoon season, and it lasted 34 months (from November 2002 to September 2005).

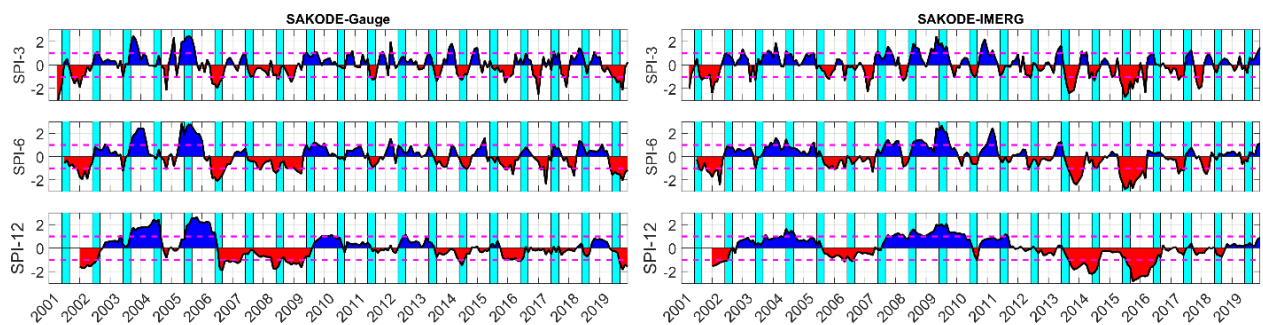


Figure 15: Standard Precipitation Index calculated for Sokodé sites using IMERG rainfall dataset (right figure) and rain gauge rainfall dataset (left figure). The vertical cyan colors indicate the monsoon season period, and the horizontal dot pink line indicates the separation of the near and normal conditions (values between -1 and 1) from the very, moderately, and extremely scenarios (≤ -1 and $\geq +1$).

4.2.1.4. SPI Characterization from rain gauge and IMERG at Atakpamé and Kouma Konda (Plateaux region)

Figure 16 shows the SPI time series at 3, 6, and 12-months scales obtained using rain gauge and IMERG rainfalls at Atakpamé and Kouma Konda stations for the entire period of this study. Based on rain gauge measurement, the results of SPI-3 show 4 dry periods that surpass the moderately dry category at certain a point at Atakpamé; 3 very dry and one extremely dry which lasted 9 months, from July 2014 to March 2015, and was also the most intense, with a PI of -2.40. The very dry event occurred from May 2015 to December 2015 (8 months), had its PI (1.75) during the monsoon season, and as a consequence of rainfall deficit during this important rainy season over all the country. For the wet periods, there were also identified 4 cases, a very wet and 3 extremely wet. The most extremely wet event lasted 18 months (July 2008 to November 2009) with a PI of 2.26. This event was preceded by another

important wet event that lasted 11 months and had a PI of 1.89 in October 2007. The combination of these two events marked a long-term wet period at Atakpamé.

The results of the SPI 6-months' time scale show 4 dry periods at Atakpamé, 2 very dry and 2 extremely dry. The longest and most intense period lasted 21 months (from July 2014 to March 2016) and had a PI of -2.12 in October 2015 and a DM of 19.96.

The second extremely dry event lasted 11 months (July 2001 to May 2002) and reached a PI of -2.03 in August 2001. Five wet periods were identified at Atakpamé using gauge datasets, 2 very wet and 3 extremely wet. The most extremely wet event begun in August 2008 and lasted 19 months, to end in February 2010, and it reached a PI of 2.79 at the beginning of the 2009 monsoon season.

Regarding SPI-12 time series, it revealed 3 dry periods, 2 very dry and one extremely dry with the later one had a PI of -2.44, a DM of 36.53, and lasted 39 months (from July 2013 to September 2016), it was also the longest among the analyzed dry periods at Atkpmé.

Gauge measurements revealed 2 wet periods, a very wet and one extremely wet event, which lasted 37 months (from August 2007 to June 2010) with had a PI of 2.52.

The results of the SPI 3-months' time scale using IMERG rainfall data shows 6 dry periods, one very dry and 5 that reached the extremely dry category. The longest extremely dry event occurred between August 2001 and April 2002 (9 months) and reached a PI of -2.10 and a DM of 10.67. The 2013 event lasted 8 months (from July 2013 to January 2014), with a PI of -2.22 reached at the end of the year. Regarding the 2015 event, it was also extremely dry and peaked in July 2015 (PI=-2.5), and it lasted 8 months (May 2015 to July 2015). The 3 extreme events occurred during the monsoon season, and as a result, they led to a lack of precipitation during these 3 monsoon periods. On the other hand, there were 6 wet events at Atakpamé according to IMERG rainfall, 3 very wet and 3 extremely wet. The most extremely wet period, which reached a PI of 2.45 at the beginning of the monsoon season, started in February 2009 and lasted 9 months, ending in October 2009. This event was preceded by another important wet event that peaked at the end of the 2008 monsoon season.

For the SPI 6-months' time scale, 5 dry events were observed, 2 very dry and 3 extremely dry. The most extremely dry period started in March 2015 and ended in March 2016, lasting 1 year and reaching a PI of -2.76 during the monsoon season of 2015. Its DM was 21.54. For wet periods, 5 events were identified, 3 very wet and 2 extremely wet. The longest period lasted 18 months (from July 2008 to December 2009) and reached the most intense peak (2.68).

SPI-12 results revealed 1 very dry period and one extremely dry period, which lasted 39 months (from July 2013 to September 2016) and reached a PI of -2.99 in October 2015 with a

DM of 47.67. On the other hand, there was only one extremely wet period identified using IMERG data at Atakpamé, and this event lasted 35 months (August 2007 to June 2010) and reached a PI of 2.42. There was no severely wet period at the SPI-12 scale for Atakpamé.

Based on rain gauge measurement at Kouma Konda, the results of SPI 3-months' time scale indicated 4 dry periods, one very dry and 3 extremely dry. The longest extremely dry period lasted 11 months (March 2005 to February 2006), reached a PI of -2.43 during the 2005 monsoon season, and had a DM of 12.80. The very dry period occurred in 2004, lasted 7 months (from March to September), and reached a PI of -1.55 in May. This period was the basis of the long-term dry event observed in SPI-12. The identified wet periods were in a total number of 6, with 5 very wet and one extremely wet, which lasted 13 months (from July 2012 to July 2013) and reached a PI of 2.48 at the beginning of the 2013 monsoon season. Between 2016 and 2017, two important very wet events also occurred during the monsoon season and led to producing the most long-term wet event in SPI-12. The first one lasted 8 months (from June 2016 to February 2017) with a PI of 1.83 in August 2016, and the second one lasted 7 months (from April 2017 to October 2017), with a PI of 1.81 reached in August 2017.

The SPI-6 for Kouma Konda shows 5 cases of dry periods, 2 very dry and 3 extremely dry. The extremely dry period, which started in March 2005 and ended in June 2006, was the most intense, with a PI of -2.37, and lasted 16 months. Its DM was 21.78.

Regarding wet events, 5 occurred at this time scale, 3 very wet and 2 extremely wet. The most intense extremely wet period lasted 16 months (June 2012 to September 2013) and reached a PI of 2.41. Although the event which occurred from July 2007 to March 2008 (9 months) was moderately wet (1.01 as PI), it had a significant impact because of its association with a monsoon season characterized by abundant rainfall.

The analysis of SPI-12 showed a very dry period and 2 extremely dry periods. The most intense and longest extreme period lasted 30 months (May 2004 to October 2006); its PI was -2.88 and DM 42.40. On the other hand, there was a very and an extremely wet period. The extremely wet lasted 2 years (from August 2016 to June 2018) and reached a PI of 2.05.

Figure 16 also shows the SPI time series for 3, 6- and 12-months' time scales obtained based on IMERG precipitation estimate for the Kouma Konda site. The SPI-3 time series presented 9 cases of the dry period, 4 very dry and 5 extremely dry. The longest extremely dry event lasted 8 months (May 2015 to December 2015) and reached a PI of -2.11 during the monsoon period and a DM of 10.30. On the other hand, there were 8 wet periods, 5 very wet and 3 extremely wet. The most extremely wet period lasted 7 months (from March 2009 to September 2009) and reached a PI of 2.25 during the monsoon season.

The results for SPI-6 revealed a very dry period and 4 extremely dry periods. The longest extremely dry event, which started in April 2015 and ended in March 2016, was the most intense, with a PI of -2.59 and a DM of 16.94. It lasted approximately one year. In terms of wet periods, there were a total of 4 events, one was very wet, and 3 were extremely wet. The longest extremely wet period lasted 18 months (August 2008 to December 2009) with a PI of 2.5, which occurred during the monsoon season.

SPI-12 calculations identified a very dry event and an extremely dry event, which lasted 22 months (December 2014 to September 2016) and reached a PI of -2.65 and a DM of 25.02. Only one case of the extremely wet period occurred at the SPI-12 scale, it started in August 2007 and ended in June 2010 (35 months), and it reached a PI of 2.25. There was no very wet period for this time scale.

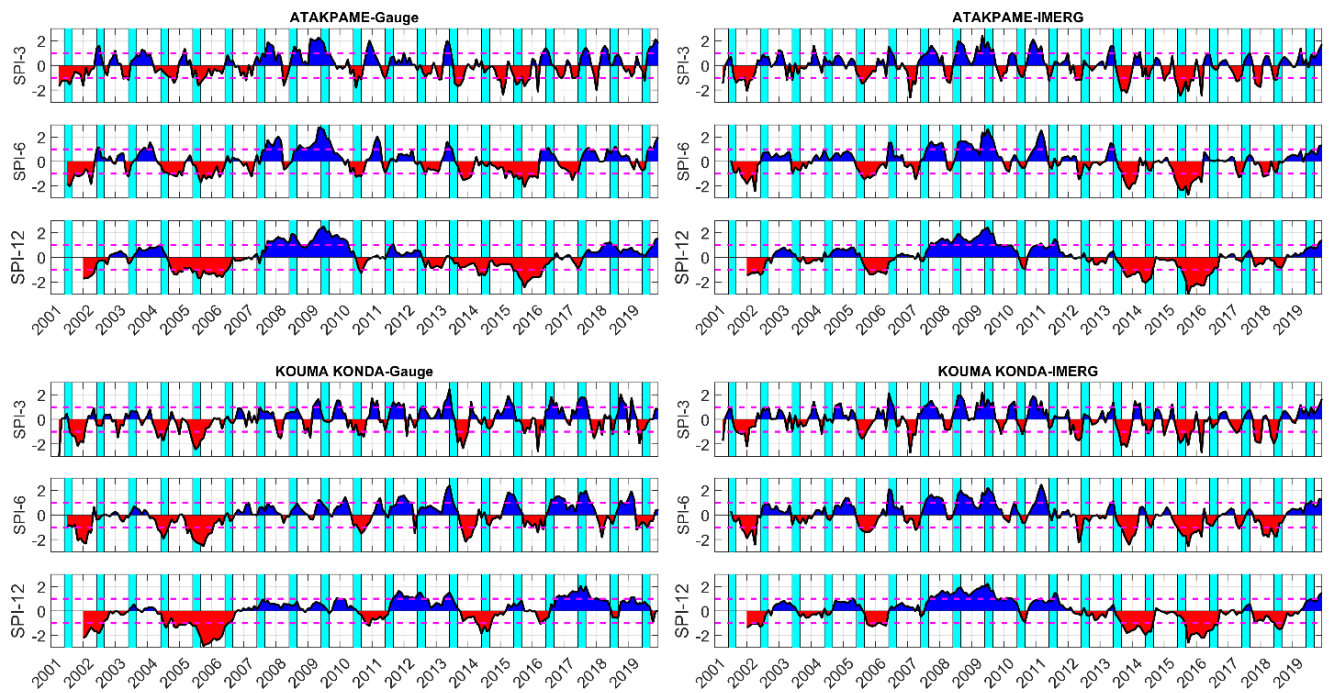


Figure 16: Standard Precipitation Index calculated for Atakpamé (top figures) and for Kouma Konda (down figures) sites using IMERG rainfall dataset (right figure) and rain gauge rainfall dataset (left figure). The vertical cyan colors indicate the monsoon season period, and the horizontal dot pink line indicates the separation of the near and normal conditions (values between -1 and 1) from the very, moderately, and extremely scenarios (≤ -1 and $\geq +1$)

4.2.1.5. SPI Characterization from rain gauge and IMERG at Tabligbo and Lomé (Maritime region)

Figure 17 shows the SPI time series at 3, 6- and 12-months scales obtained using rain gauge and IMERG rainfalls at Tabligbo and Lomé stations for the entire period of this study.

The SPI-3 using rain gauge shows that there was a very dry period and an extremely dry period at Tabligbo; the latter lasted 15 months (from January 2005 to March 2006) and was the longest. Its PI reached the value of -2.05 with a DM of 14.09. However, the most intense, extremely dry event lasted 6 months (from February 2012 to August 2012), and it reached a PI of -2.35 in May 2012 and a DM of 6.19. Regarding the very dry event, it lasted 7 months (from June 2015 to December 2015) with a PI of -1.52 in July 2015. On the other hand, there were 6 cases of wet periods, 2 very wet and 4 extremely wet. The most extremely wet period lasted 5 months (from March 2010 to July 2010) and reached a PI of 2.34 before the Monsoon season.

For the SPI-6, there was a total of cases of 5 dry periods, 2 very dry and 4 extremely dry. With a PI of -2.24, the dry period, which began in June 2015 and ended in March 2016, was the most extreme period. It lasted 10 months with a DM of 10.52. For the same time scale, five wet periods were identified, 3 very wet and 2 extremely wet. The longest event lasted 17 months (from December 2010 to April 2012) and reached a PI of 2.16 before the 2011 monsoon season.

The results of SPI-12 showed a total of 2 dry periods, and the two were very dry. The longest periods lasted 16 months (June 2005 to September 2006) with a PI of -2.13 and a DM of 17.63. On the other hand, there were 4 cases of wet periods, and all of them were very wet. The most severely wet lasted 21 months (October 2016 to June 2018) and reached a PI of 1.97 during the 2017 monsoon season.

The results of a 3-months SPI using IMERG rainfall estimate show that, at Tabligbo station, there were a total of 8 dry periods, 5 very dry and 3 extremely dry. The most extremely dry period lasted 7 months (from December 2006 to June 2007) and reached a PI of -2.43 and a DM of 7.38. Regarding wet periods, there were 8 at Tabligbo accordingly to IMERG precipitation, 7 very wet and one extremely wet, which reached a PI of 2.0 and lasted 3 months, from June 2006 to August 2006.

For SPI-6, the results show 7 dry periods, 3 very dry and 4 extremely dry. The longest and most intense extreme period lasted 10 months (from June 2015 to March 2016) and reached a PI of -2.75, with a DM of 14.49. On the other hand, 6 wet periods were recorded, two very wet and 4 extremely wet. The longest extremely wet event lasted 13 months (from May 2010 to May 2011) with a PI of 2.44.

The SPI-12 revealed 5 cases of long-term dry periods, 3 very dry and 2 extremely dry. The longest and most intense, extremely dry episode lasted 16 months and reached a PI of -2.65; it started in June 2015 and ended in September 2016. Its DM was 23.41. In terms of wet

periods, 3 cases of very wet periods were detected. The very wet event that begun in August 2007 and ended in June 2010 was the longest one (35 months) and reached a PI of 1.68.

For rain gauge measurements, the SPI-3 analysis at Lomé indicated a very dry period and a case of an extremely dry period. The latter lasted 13 months (from July 2016 to July 2017) and presented a high PI of -3.46 during the 2016 Monsoon season and a DM of 17.93. The wet periods were in total of 2 cases, one very wet and one extremely wet, which reached a PI of 2.08 and lasted 1 year (from March 2010 to February 2011).

The results of SPI-6 revealed 4 dry periods, 2 very dry and 2 extremely dry. The most extremely dry period lasted 17 months (July 2016 to November 2017), reaching a PI of -2.68 during the 2016 monsoon season and a DM of 24.93. On the other hand, there were 2 cases of severely wet periods and only one case of the extremely wet period at Lomé, which lasted 1 year (from June 2010 to June 2011) and reached a PI of 2.32.

The SPI-12 highlighted 2 cases of a very long-term dry period and 1 extremely dry period. The extremely event lasted 22 months (from June 2016 to March 2018) and reached a PI of -2.98, with a DM of 34.28 and. For wet events, 3 were identified, 2 very wet and 1 extremely wet. The extremely wet period lasted 16 months (July 2010 to November 2011), with a PI of 2.83.

Based on IMERG rainfall estimation, the SPI-3 time series show 9 dry periods at Lomé station, 3 very dry and 6 extremely dry. The most extremely dry event lasted 9 months (from May 2015 to December 2015) and reached a PI of -2.86 during the Monsoon season. Its DM was 14.28. Regarding wet events, there were 5 cases, 3 very wet and 2 extremely wet. The longest extremely wet period lasted 10 months (from February 2009 to November 2009) with a PI of 2.44 just before the monsoon period.

The results of SPI-6 showed 2 very dry periods and 3 extremely dry periods at Lomé. The most intense extreme period started in May 2015 and ended in March 2016 (lasting 11 months) and reached a PI of -2.94 with a DM of 22.54. For wet periods, there were one very wet period and 2 extremely wet periods. The longest extremely wet event lasted 20 months (from July 2008 to February 2010) and reached a PI of 2.56 during the monsoon season of 2009.

For SPI-12, at Lomé, there was only 1 and long extremely dry period, according to IMERG rainfall. It lasted 39 months (from July 2013 to September 2016) with a PI of -2.64 and a DM of 52.40. For the same time scale, IMERG rainfall showed 1 case of the very wet period and 1 case of the extremely wet period. The latter lasted 37 months (from August 2007 to July 2010) and reached a PI of 2.1 during the 2009 monsoon season.

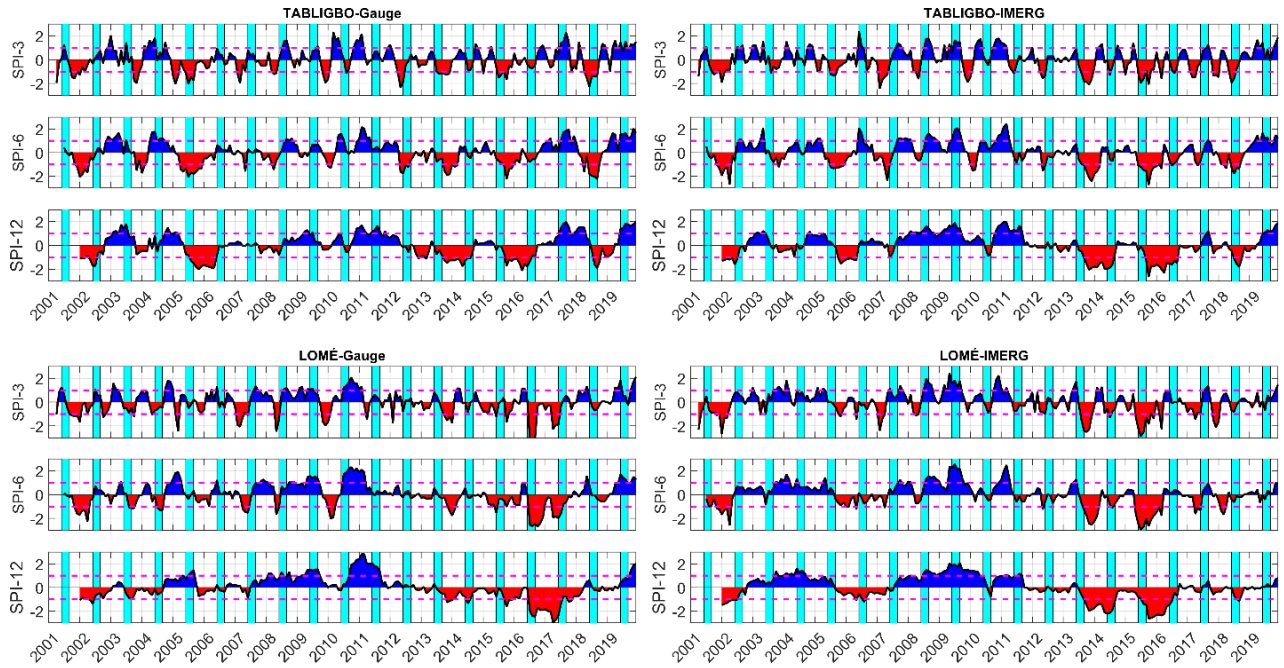


Figure 17: Standard Precipitation Index calculated for Tabligbo (top figures) and for Lomé (down figures) sites using IMERG rainfall dataset (right figure) and rain gauge rainfall dataset (left figure). The vertical cyan colors indicate the monsoon season period, and the horizontal dot pink line indicates the separation of the near and normal conditions (values between -1 and 1) from the very, moderately, and extremely scenarios (≤ -1 and $\geq +1$).

Despite differences in the duration, intensity, and magnitude (for dry events), the SPIs time series obtained from the IMERG rainfall estimation are capable of capturing the major occurrence of wet and dry periods over the 9 meteorological stations. Therefore, we evaluated that IMERG rainfall data can be used in addition to rain gauge measurements to improve the monitoring coverage of dry and wet events across Togo.

Accessing SPI at the meteorological station provides accurate information about the occurrence of dry and wet events at a local level, which is crucial for the local stakeholder to better plan mitigation efforts to protect local communities' activities in the context of climate extreme events. However, it is also very important to look at a regional level to understand and have a large overview of these events across the entire country, and this can be done with an SPI map in addition to SPI time series considering only satellite rainfall data (e.g., IMERG). Due to its spatial coverage limitation, the rain gauge network cannot be able to capture all the diversity that can occur in a specific year throughout the country.

Figure 18 shows a 12-months SPI map based on IMERG rainfall at the end of December for all the years and over the 5 regions within our study period. During The years 2001, 2013, and 2015, all the regions (the entire country) experienced a dry event. For 2015, 85% of the country was extremely dry, and in 2001 Togo scenario was very dry, excepted for the Centrale region and western part of the Savanes region, which were extremely dry. The drought event

of 2015 was observed across the Gulf of Guinea countries because of a deficit of seasonal rainfall in those areas, which was associated with the 2015 El Nino event (Anyamba et al., 2019; Owusu et al., 2019). In 2002, except in the north part of the Savanes region, which was very dry, the remainder of the country experienced in general near-normal conditions. During 2003, very to extremely wet periods (exceptionally in the western part of Centrale region) occurred in the Northern regions, while in the southern regions normal condition was observed. The year 2013 was extremely dry in the Maritime region and in the Southeast of Plateaux. The remaining country was very dry, except in the northern part of the Savanes region, which was under normal conditions.

In 2006, the northern region (Savanes, Kara, Sokoké) experienced moderated to very dry periods while the southern regions (Plateaux and Maritime) were under normal conditions. The situation was reversed in 2005, where the regions in the south undergone moderately dry periods, and those in the north experienced normal conditions to moderately wet periods. During the years 2007, 2008, and 2009, most of the country experienced very wet and extremely wet events. Nevertheless, the Kara region and the north part of the Centrale region presented normal conditions. Similar results were obtained by (Koudahe et al., 2017) for southern Togo, where 12-Months SPI showed significant wet events in 2007 and 2008, which caused sporadic flooding events in south Togo. The flooding events destroyed 11,688 hectares of cultivated land, resulting in an important loss of income for farmers and creating a spike in food shortages across the region (World Bank, 2011).

The Maritime region was moderate to very wet in 2007-2008, a near-normal condition in 2009 and wet in the west portion, and extremely wet in the east during 2010. This situation may have had positive impacts on agriculture, underground reservoir levels, and water supply. During the same year, the southeast of the Kara region and the eastern part of the Centrale region was also very wet, while the remainder of the country presented a situation near to normal conditions. For the years 2011, 2012, 2014, 2016, 2017, and 2018, the situation in most of the regions was close to normal, although with a slight tendency to dry conditions in some regions.

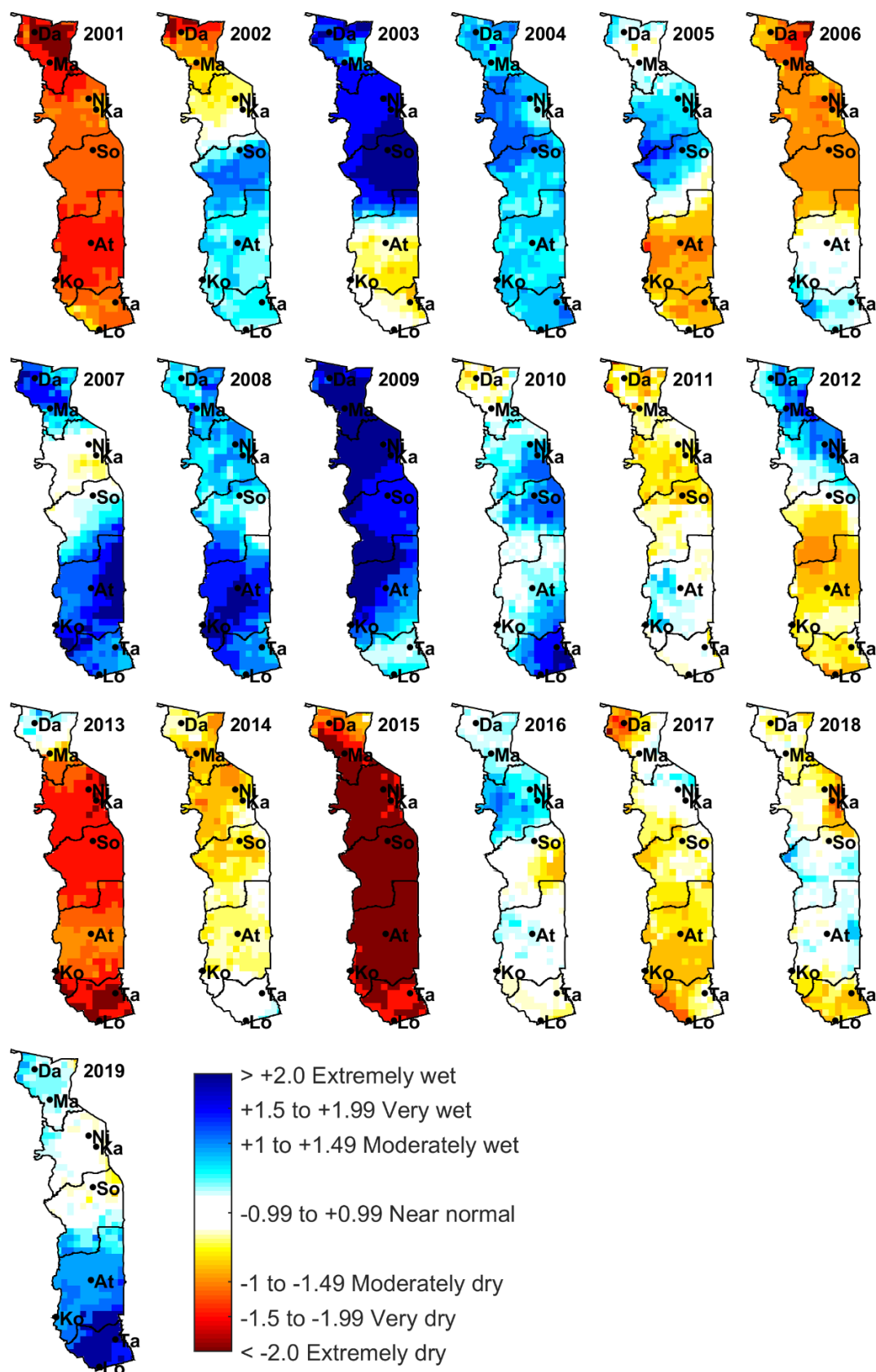


Figure 18: 12-months SPI at the end of each year for the entire study period over Togo. From north to south, the five administrative divisions are displayed: Savanes, Kara, Centrale, Plateaux, and Maritimes. The black dots represent the rain gauge stations used in the present study: Dapaong (Da), Mango (Ma), Niamtougou (Ni), Kara (Ka), Sokodé (So), Atakpamé (At), Kouma-Konda (Ko), Tabligbo (Ta) and Lomé (Lo).

While IMERG comparison with rain gauge showed that the satellite-based product is not always able to capture the local signature of precipitation, rain gauge, in general, gives information at a local scale and, as seen in this study, therefore spatially limited. The significant differences between scenarios (dry/wet) observed by rain gauge stations relatively close for the same period revealed the need to add satellite products to the climate warning system since a full spatial monitoring coverage based on rain gauge is a challenge. Thus, satellites rainfall estimation appeared to be the suitable option to access the occurrence of extreme events at a regional level and in areas not covered by in situ measurements.

In the next section IMERG dataset was used to categorize wet and dry (very and extremely severe) periods across each Togo administrative region, an attempt to contextualize temporal evaluation of regional dry and wet events.

4.2.2. Medium and long term dry and wet events across Togo administrative regions

The purpose of this section is to characterize and analyze the dry and wet events (very and extremely severe) at a regional level, considering the 5 administrative regions of Togo using SPI calculated using IMERG rainfall. IMERG product offers broad spatial coverage, which favors regional SPI computing. Figure 19 shows the medium (SPI-6) and long-term (SPI-12) for each region. In general, there is a sequence of dry and wet scenarios during the last 19 years, with the long-term wet and dry events from 2008 to 2010 and from 2014 to 2016, respectively, affecting the entire country, as it was observed at a local scale.

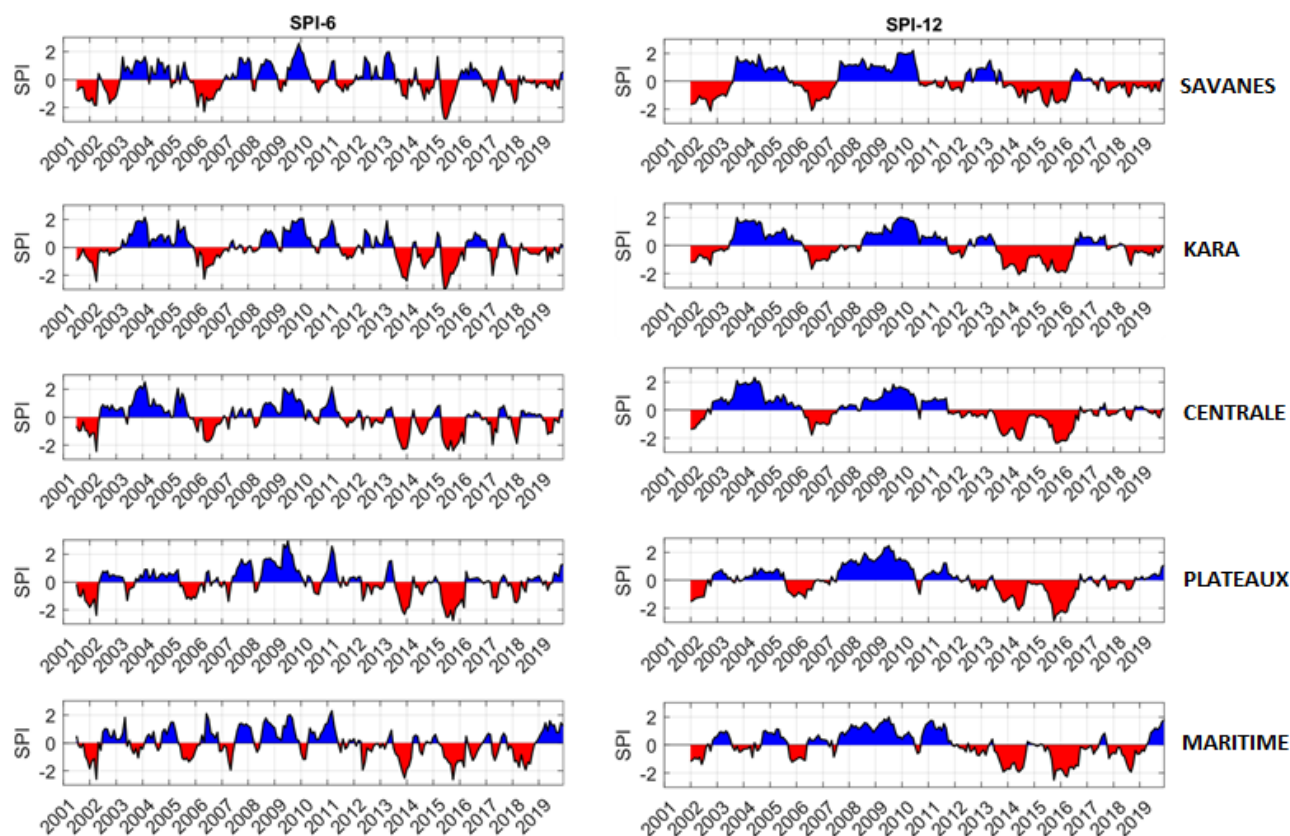


Figure 19: SPI-6 (left figures) and SPI-12 (right figures) time series for each Togo administrative region.

Table 6 and Table 7 show the number of different categories of dry and wet periods observed over each region for the entire study period based on 6-months and 12-months' time scale SPI. SPI-6 time series for the Savanes region shows that the longest dry events lasted 15 months (from November 2005 to January 2007) with a PI of -2.28 reached in May 2006 and DM of 15.99. For the wet event, the longest and most intense one started in November 2012 and ended in August 2013 (10 months), and it reached a PI of 2.21 in May 2013.

For SPI-12, at the same region, the most intense dry event lasted 20 months (from January 2002 to August 2003) and reached a PI of -2,13 with a DM of 23,79. On the other hand, the wet event of August 2007 to July 2010 (37 months) was the most intense and longest, with a PI of 2.21.

At Kara region, the longest and intense dry event considering SPI-6 lasted 21 months (from July 2001 to March 2003). It reached in April 2002 a PI of -2.44 with a DM of 13.01. For the wet period, the longest one lasted 33 months (from April 2003 to December 2005) with a PI of 2.15 reached in February 2004. The SPI-12 showed that, for the same region, the most important dry event lasted 36 months (August 2013 to July 2016) with a PI of -2.07 in June 2014 and a DM of 47.35. The wet event that occurred from July 2008 to September 2011 (39 months) was the most important, with a PI of 2.02 reached in January 2010.

At Centrale region, and looking at SPI-6, the most intense dry event reached a PI of -2.39 in October 2015, and lasted 11 months (May 2015 to March 2016), and had a DM of 20.48. On the other hand, the most important wet event lasted 19 months (July 2003 to January 2005) with a PI of 2.51 in February 2004. For the same region, SPI-12 showed one longest and most intense dry event, which lasted 41 months (June 2013 to September 2016), with a PI of 2.37 and a DM of 51.17. For the wet event, there was one important, which also lasted 41 months (November 2002 to March 2006) and reached a PI of 2.33 in June 2004.

At the Plateaux region, the SPI-6 revealed one intense and longest dry event, which lasted 12 months (April 2015 to March 2016), with a PI of -2.75 in October 2015 and a DM of 21.65. Regarding the wet event that occurred from July 2008 to February 2010 (20 months), it was the most intense, with a PI of 2.94 peaked in July 2009.

For the SPI-12, the dry event which, started in July 2013 to September 2016 (40 months), was the longest and intense. It reached a PI of -2.90 in October 2015 and a DM of 48.3. The most important wet event for the same time scale lasted 36 months (August 2007 to July 2010), with a PI of 2.48 peaked in July 2009.

Finally, in the Maritime region, the most important dry event obtained from SPI-6 lasted 1 year (April 2015 to March 2016), and it reached a PI of -2.62 in October 2015 and a DM of 15.25. For the same time scale, the most important wet event lasted 14 months (April 2010 to May 2011), with a PI of 2.31 reached in March 2011. On the other hand, SPI-12 showed one intense and longest dry event from June 2015 to June 2017 (25 months). It reached a PI of -2.49 in October 2015 with a DM of 26.21. For the wet events, the one that occurred from August 2007 to June 2010 (35 months) was the most important in duration and intensity; its PI was 2.0 reached in July 2009.

Table 6: Number of dry events per category in different regions for medium (SPI-6) and long-term (SPI-12).

Number of cases per region										
Category	SAVANES		KARA		CENTRALE		PLATEAUX		MARITIME	
	Extremely dry	very dry	Extremely dry	very dry	Extremely dry	very dry	Extremely dry	very dry	Extremely dry	very dry
SPI-6	2	3	4	2	3	2	3	0	3	1
SPI-12	2	1	1	1	4	2	1	1	1	2

Table 7: Number of wet events per category in different regions for medium (SPI-6) and long-term (SPI-12).

Number of cases per region										
Category	SAVANES		KARA		CENTRALE		PLATEAUX		MARITIME	
	Extremely wet	Very wet	Extremely wet	Very wet	Extremely wet	Very wet	Extremely wet	Very wet	Extremely wet	Very wet
SPI-6	0	3	2	2	4	0	2	1	3	4
SPI-12	1	2	2	0	1	1	2	1	1	2

The results obtained in this section show that; for the stations located in the Savanes region (Mango and Dapaong), it is possible to evaluate that IMERG results, from the point of view of SPI-12 dry and wet periods, are consistent with the results from rain gauge measurements at Mango. Although the intensity, duration, and magnitude presented some differences, the sequence of dry and wet conditions throughout the time is consistent with the Mango rain gauge dataset. The long-term dry (wet) period between 2014 and 2016 (2008 – 2010) at Mango is captured by both IMERG and rain Gauge. However, for Dapaong, IMERG presented significant divergences with the rain gauge, and it is important to emphasize that. Although located in the same region and relatively close, Dapaong and Mango rain gauge datasets resulted in significant differences in long-term climate scenarios from the point of view of dry and wet. Another aspect related to IMERG results, they produce dry (wet) events with a longer duration than those generated from the rain gauge. Also, the events obtained with IMERG were lesser in number compared to those obtained with the rain gauge.

At Niamtougou station, important agreements are found between rain gauge and IMERG for SPI-12 (ex. 2008-2010 wet period, 2014-2015 dry trend) but also some differences (2013 and 2016-2017 wet period in gauge data are not present in IMERG). Also, there are some

differences regarding the intensity and duration of the events. However, important long-term wet and dry events are captured by IMERG.

For Kara station, located in the same region as Niamtougou, IMERG was able to capture the main long-term wet period (2003 – 2005), which occurred at the beginning of the study period. However, there were some differences in the intensity and duration. The remain of SPI-12 time series exhibited important differences between the two datasets. For example, when the rain gauge is presenting an important dry event between 2006 – 2009, IMERG is showing an important wet scenario that extended to 2010.

Comparing the two stations, Niamtougou and Kara, and considering SPI-12, we observed important differences, although they are so close. For example, Kara station experienced a long dry scenario between 2007 – 2008, while Niamtougou station experienced a dry scenario during 2007 and a wet scenario in 2008.

At Sokodé station, in the Centrale region, IMERG showed the ability to capture the long-term wet (dry) trend of 2003 – 2006 (2014 – 2016) but fails to reproduce the intensity and duration accurately.

At the Kouma Konda station, the two datasets had some similarities in describing the occurrence of dry and wet events at 3-months SPI, but also differences; both are reflected at medium and longer time scales (6 and 12 months). For instance, at SPI-12, IMERG captured the dry events of 2006 and 2014 but failed to reproduce their intensity and duration. That was also the case for the wet period between 2012 and 2013. The satellite product also revealed significant dry and wet events that are not clearly present in gauge data (the 2016 dry period and the 2007-2010 wet period). However, it is worth mention that Kouma Konda differences between IMERG and gauge datasets were somehow expected since it is well known and also shown in this study the difficulties of IMERG product to reproduce rainfall in mountain regions, which is the case of Kouma Konda. Thus, we concluded that the difficulties of IMERG to estimate the precipitation amount accurately in that locality could be the source of this under or overestimation.

Nevertheless, it's worth mentions the differences also observed between dry and wet scenarios among Kouma Konda and Atakpamé, both based on gauge datasets, despite their location in the same administrative region. For instance, an important long-term wet period occurred in Atakpamé from 2007 to 2010, and it was properly captured by IMERG but not seen in Kouma Konda station. So, it is also the case for the 2015-2016 dry event. In general, IMERG product presented better performance over Atakpamé.

Taking the SPI-12 as a reference, in general, the two datasets, IMERG and rain gauge, presented consistent patterns of a dry and wet event at Lomé station. At the beginning of the time series, there were more significant differences when IMERG presented a longer wet event (2003-2005) compared with rain gauge (2004-2005). Although also marked by differences in intensity and duration, IMERG consistently identified the long-term wet period from 2008 to 2011 and the long-term dry period from 2014 -2017. Like at Kouma Konda station, IMERG precipitation had some challenges over Lomé, showed in the first section; however, its performance to reproduce the occurrence of the dry and wet scenario for Lomé is better than for Kouma Konda.

Analyzing SPI-12 At Tabligbo station, located in the same region as Lomé (Maritime), it is observed that IMERG was able to capture the mains wet events of 2008 – 2011. The mains dry periods, one that occurred from 2014 to 2017 and that of 2002 at the beginning of the time series, were captured by IMERG. However, some significant differences were observed, for example, the wet period in 2017-2018, which is not captured by IMERG. This event seems to be very localized since it is not present in Lomé rain gauge data as well. This excellent performance of IMERG over Tabligbo station was somehow expected because it is the station that presented the best intercomparison of rainfall between IMERG and rain gauge (see results section one).

In summary, current study results demonstrate that despite differences in the duration, intensity, and magnitude, which could be related to differences in the total amount of monthly rainfall, the IMERG rainfall estimate was able to capture the major occurrence of wet and dry periods over the 9 meteorological stations. Therefore, we evaluate that IMERG's monthly rainfall product can be used in addition to rain gauge measurements to improve the monitoring coverage of dry and wet events across Togo.

In this ending section, dry and wet events over meteorological stations and over the 5 economic regions were assessed via SPI and using monthly precipitation from two types of sources (rain gauge measurement and IMERG). In the next section, the influence of near (Tropical Atlantic) and distant (Tropical Pacific Ocean) Sea Surface Temperature anomalies on these events (dry /wet) over the 5 regions will be analyzed.

4.3. Dry and wet events in Togo and their relationships with the El Niño-Southern Oscillation (ENSO) and South Atlantic Ocean Dipole

For this section, the correlation between SPI-1 time series for the 5 economic regions and El Niño-Southern Oscillation (ENSO) and South Atlantic Ocean Dipole indices are analyzed aiming to evaluate the existence of a possible link between these ocean indices and the occurrence of dry and wet events over Togo administrative regions. Pearson correlation was used for this purpose, as described in the methodology section.

4.3.1. Description of SAOD and ENSO indices features during the study period

As described in the methodology section, SAOD is defined by two poles; NEP and SWP. It's important to highlight that during a SAOD event, these two poles present SST anomalies with opposed signals (Nnamchi & Li, 2011; Nnamchi et al., 2011).

During the present study period, 3 important negative phases of SAOD occurred (see figure 20). The first one, from April 2005 to May 2006, reached a peak of -1.41°C in June 2005. The 2012 negative phase started in December 2011 and reached a peak of -1.15°C in February 2012 and ended in November 2012. The last important negative event occurred between July 2014 and March 2015. Its peak was -1.26°C in January 2015. These events were categorized as important due to the fact that they lasted longer (average duration of 10 months), and their peak intensity was above -1°C . Regarding the positive phase of the SAOD index, the most important occurred between February 2008 and August 2009. It reached a peak intensity of 1.13°C in June 2008.

From 2008 to 2011, there was a dominance of the SAODI positive phase, while from 2012 to 2015, negative events were dominant. Thus, the important dry scenario that occurred in 2015, across all the country, coincided with SAODI negative phase; meanwhile, the markedly wet years of 2007, 2008, 2009 in all the regions occurred during the positive phase of SAODI. These results corroborate with the findings of the study of Nnamchi et al., (2011), which found that the positive (negative) phase of SAOD favors the enhancement (lack) of rainfall over West Africa, especially in the Gulf of Guinea (GOG) countries. The earlier findings of Odekunle & Eludoyin (2008) also suggested that the general increase of SST in the GOG region, which is partially inside the NEP domain, may lead to an increase in precipitation in West Africa in general.

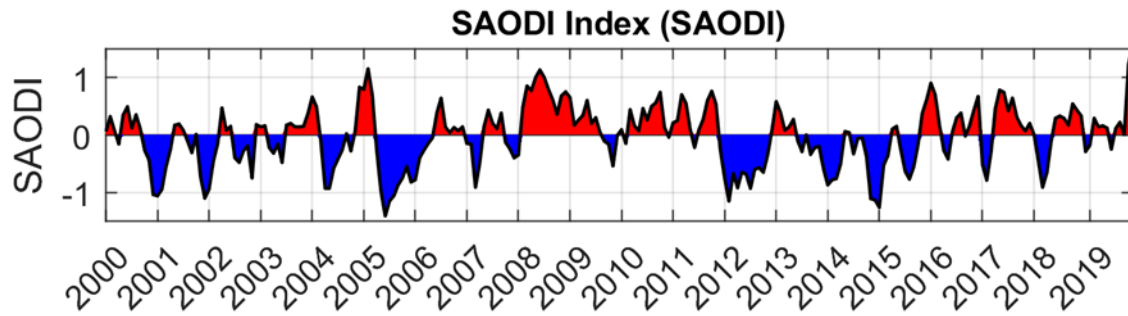


Figure 20: Time series plot of SAOD indices for the study period (2001 to 2019) based on the extended reconstruction of sea surface temperature to a base climatology from 1979 – 2020; using data from ERSST V5.

ENSO is one of the most significant phenomena in the Earth's climate system, which explains variations in tropical Pacific SST. Such variations affect tropical weather patterns but can have a global effect (Sazib et al., 2020). Among the Pacific equatorial regions used to categorize cold and the warm phases of ENSO (cf. figure 3), Niño 3.4 region has been identified as key to the ocean-atmosphere interactions (Trenberth & Hoar, 1997). Therefore, the SST anomaly at Niño 3.4 region, as an indicator of the cold and the warm phases of ENSO, is a reference to evaluate the correlation between ENSO and climate anomaly worldwide (Trenberth & Shea, 2005). The implication of ENSO, mainly the warm phase (El Niño), over West African countries during the last decades had been pointed out by some previous studies. Owusu et al., (2019) demonstrated that during the 2015 strong El Niño year, it had been observed reduction in the rainfall totals and in the number of rainy days across Ghana. Egbuawa et al., (2017) assumed the existence of an association between ENSO and rainfall in Nigeria. He found that the positive anomalies in rainfall occurred particularly near and around most of the strong ENSO years. Earlier, Bernard Fontaine and Serge Janicot, 1996 study showed that drought over West Africa is mostly characterized by the growth of positive SST anomalies in the Eastern Pacific complemented by a negative SST anomaly in the Northern Atlantic.

Figure 21 and Table 8 show the time series of the Niño 3.4 index from 2001 to 2019. 4 cases of La Niña and 6 cases of El Niño occurred within our study period. The 2015 strong El Niño event extended to 2016 and reached a peak intensity of 2.93 in November 2015. This event has been reported to cause a rainfall deficit across different West African countries (Owusu et al., 2019; Egbuawa et al., 2017; UN-WFP, 2015) and lead to a significant dry episode during that year with important consequences for the regional agriculture. The analysis of SPI in the present study shows that 2015 was characterized by dry scenarios in all Togo regions, and this situation could be linked to the strong El Niño phenomena of that year, as it was also

the case in other countries in West Africa like in Ghana (Owusu et al., 2019) and in Nigeria (Egbuawa et al., 2017).

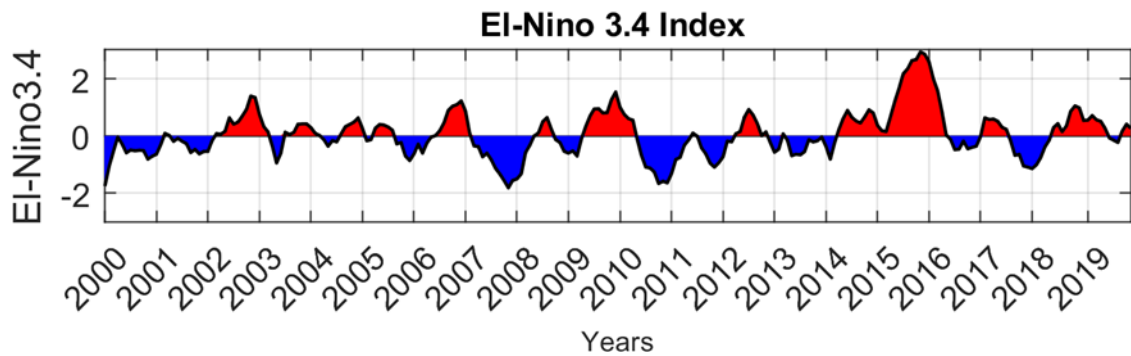


Figure 21: Time series plot of Niño 3.4 indices for the study period (2001 – 2019) based on SST data from ISST V2 to a base climatology from 1979 – 2020.

Table 8: La Niña and El Niño events occurred during this study period (2001 to 2019).

Number of events	Starting date	End date	Duration (months)
La Niña			
1	May 2007	March 2008	11
2	June 2010	March 2011	10
3	August 2011	January 2012	6
4	September 2017	March 2018	7
El Niño			
1	June 2002	January 2003	8
2	August 2006	January 2007	6
3	June 2009	April 2010	11
4	May 2014	December 2014	8
5	April 2015	April 2016	13
6	October 2018	May 2009	8

4.3.2. Relationship between ENSO and SAOD indices and SPI across Togo regions

The Pearson r correlation (r) was applied to evaluate the relationship between the SPI 1-months' time scale and SAODI and Niño 3.4 index as a way to investigate a possible relation between dry and wet events across Togo regions and the ocean-atmosphere climate variability

modes SAOD and ENSO. The analysis was done considering the entire year (all the 12 months) firstly and secondly considering exclusively West African Monsoon months (June -July - August-September). The objective for considering WAM months exclusively was to evaluate the relationship between south Atlantic and tropical Pacific Oceans conditions and the occurrence of dry and wet events in Togo during the monsoon season (WAM) when most of the precipitations occur (Nimon et al., 2020).

Table 9 presents the results of the correlation analysis between SPI-1 from each Togo region and Nino 3.4 index and their correspondent statistical significance, considering the entire year (all the 12 months) and WAM months (JJAS).

Analysis between SPI-1 and Niño 3.4 index for the entire year (table 9) showed very low and negative correlation for all regions, none of them statistically significant at 95% confidence level. Based on these results, we are not able to conclude about the role of El Niño (warm SST anomaly) and La Nina (cold SST anomaly) events in the Niño 3.4 region on the occurrence of dry and wet events in Togo.

For the correlations between SPI-1 and Niño3.4 for WAM months for all regions, we also observed a low and negative correlation and p-values higher than 0.05 (table 9). We concluded based on these results that Niño 3.4 index signal on SPI-1, therefore on dry and wet events, across Togo is not clear and not proven statistically. Therefore, for the present study period, we are not able to conclude about the influence of ENSO events on the rainfall variability across Togo during the WAM season.

It is worth mention that the relatively short temporal extension of the IMERG rainfall product may be one of the reasons for the difficulties to clarify the relationship between SPI and Nino 3.4 index and, therefore, the influence of ENSO events on Togo dry and wet scenarios. Nevertheless, two other aspects are important to be highlighted: a) only one ENSO event, the 2015/2016 El Nino, can be pointed out as a strong event, most of the remaining ENSO occurrences were relatively weak; b) In a previous study, Nnamchi et al., (2012) also found a very low correlation(-0.003) between Gulf of Guinea precipitation during boreal summer and Niño 3.0 index, and pointed out that SAOD is the dominant mechanism that modulates spatial features of summer precipitation at the Guinea coast.

Table 9: Correlation coefficient and significance level between SPI 1-month for each Togo administrative region and Niño 3.4 index considering all months of the year and for WAM season only.

Regions	SPI 1-month and Niño 3.4 index For the entire year		SPI 1-month and Niño 3.4 index for WAM season	
	r	Significance Level	r	Significance Level
MARITIME	-0.011	0.08	-0.05	0.66
PLATEAUX	-0.112	0.09	-0.05	0.66
CENTRALE	-0.09	0.167	-0.004	0.97
KARA	-0.08	0.20	-0.049	0.67
SAVANES	-0.072	0.277	-0.10	0.34

Correlations analysis between SPI-1 over each Togo region and SAODI (Table 10) was also performed considering the entire year and exclusively West Africa Monsoon months (June -July -August-September).

The results considering the entire year, in general, revealed a better correlations value than in the ENSO case, but still a low correlation between the SPI-1 and SAODI. The highest and statistically significant (at 95% confidence level) correlations, were obtained for Plateaux ($r = 0.22$, $P = 0.0005$) and Maritime ($r = 0.21$, $P = 0.001$), the two southernmost regions of Togo. The Savanes region, in the northernmost portion of Togo, presented the lowest correlation ($r = 0.09$, $P = 0.152$), which was not statistically significant. As one moves from the south toward the north, it is clear a decrease in the correlation value. These results suggest that the regions closer to the Guinea Gulf and with bimodal rainy climates (Maritime, Plateaux) are more influenced by SST variability in the South Atlantic than those further north and with only one rainy season (Sokode, Kara, Savanes). Concerning Maritime and Plateaux, correlations results presented statistical significance; although low, the positive signal is consistent with Nmanchi & Li. (2011) results. Thus, the negative and positive phases of SAODI are linked to the occurrence of dry and wet events in Maritime and Plateaux regions, respectively. These results demonstrated that negative (positive) SAODI, related to cold (warm) SST in NEP, favor dry (wet) conditions over the south of Togo.

Although correlation results in this study are not very strong, it has been recognized the presence of an ocean-atmosphere signal interaction between the South Atlantic and the precipitations in the regions close to the Gulf of Guinea.

The correlation results for SPI-1 and SAODI for WAM months only revealed substantial improvement Plateaux region had the highest correlation, with $r = 0.42$, and; at a confidence level of 95% ($P = 0.0001$), followed by Maritime region ($r = 0.31$; $P = 0.005$). Savane region presented the lowest $r = 0.09$, which was not statistically significant ($P = 0.396$). Correlation exclusively for monsoon was also positive for all the 5, decaying as one moves from south to the north of Togo. Compared to the case when all months are considered, the correlation including only WAM months, mainly for the southernmost regions (Plateaux and Maritime), is stronger and still statistically significant at 95% confidence level, indicating a potential link between the rainfall variability over these regions and the SAOD phases during WAM. It has been demonstrated that the strongest intensity of SAOD tends to occur in JJA within the WAM season (Nmanchi et al., 2011). Thus, the Nmanchi et al. (2011) study revealed that a direct connection of the SAOD phenomenon to the Guinea Coast is a key source of precipitation variability during the WAM season.

Table 10: Correlation coefficient and significance level between SPI 1-month for each Togo administrative and SAODI for all months of the year and for WAM season.

Regions	SPI 1-month and SAODI index For the entire year		SPI 1-month and SAODI index WAM	
	r	Significance Level	r	Significance Level
MARITIME	0.21	0.001	0.31	0.005
PLATEAUX	0.22	0.0005	0.42	0.0001
CENTRALE	0.13	0.044	0.17	0.122
KARA	0.10	0.101	0.09	0.395
SAVANES	0.09	0.152	0.09	0.396

Based on the Pearson r correlation analysis performed, it appeared that the South Atlantic dipole has a closer link to the occurrence of dry and wet episodes in Togo than the SST anomalies in the Pacific Ocean, corroborating Nmanchi et al., (2011) suggestion that SAOD is the dominant mechanism that modulates spatial features of precipitation at the Guinea coast. The obtained results also suggested that this link is stronger for the regions located near the Gulf of Guinea (Maritime and Plateaux) than those in the central and northern of Togo, for where we found weak and not statistically significant correlations.

Based on the present study results, it is clear that the southern regions, due to their proximity to the Gulf of Guinea, are likely to be more subject to the influence of SST conditions, which could explain the statistically significant and not negligible positive correlation between their rainfall and SAODI. Previous studies demonstrated the causal link between the air-sea phenomenon, referred to as the South Atlantic Ocean dipole (SAOD), and the interannual variability of precipitation over West Africa (Nnamchi & Li., 2011), and as well as over Togo (Batebana et al., 2015), especially during the WAM period, that support the correlation observed in the present study. Previous studies also demonstrated that the SAOD (exceptionally the NEP) mode has a significant impact on West African summer precipitation (Nnamchi & Li, 2011; Joly & Voldoire, 2010). Indeed, these studies found a positive correlation (correlations exceeding 0.6) between the NEP of SAOD and WAM rainfall over the West African Guinean coast.

Present study results have shown that drought (ex. 2015-2016) and wet events (ex. 2009 – 2010) are both likely to occur under the positive Niño 3.4 index, and this is consistent with the negative, weak correlation coefficient between the index and SPI-1 obtained for all the regions. However, the 2015 drought episode, which impacted the Gulf of Guinea countries and with a severe effect on agriculture production (Owusu et al., 2019; Egbuawa et al., 2017; UN-WFP,2015), occurred in the context of a strong El Niño event. Therefore, although our results showed a weak correlation between Niño 3.4 index and SPI-1, one should emphasize that ENSO's role in West African countries' rainfall variability has been pointed out in many studies. According to Joly & Voldoire (2010), the timing of ENSO onsets and the time lag of the atmospheric response are the two main aspects of the teleconnection between ENSO and West Africa precipitation.

4.3.3. Correlation analysis between SPI 1-month and spatial SST anomalies in the South Atlantic

To further understand the relationship between the South Atlantic Ocean SST and the occurrence of dry and wet events for each Togo region, Pearson correlation analysis was performed between spatial SST anomalies and SPI-1 time series from each Togo administrative region. Like the previous analysis, the current Pearson r correlation analysis was applied in two steps: Considering first all the months of the years and afterward only the WAM months (JJAS). To compute the correlation, the SST anomaly dataset was detrended to remove long-term tendency. Figure 22 shows the correlation between SST anomaly and SPI 1-month for each Togo region. The correlation map between SPI-1 for the southern regions (Maritime and

Plateaux) and the SST anomaly in the South Atlantic revealed a pattern consistent with the SAOD pattern. Positive correlation dominance was observed, with r value comprised between 0.1 and 0.3, across the Gulf of Guinea and Benguela current region, and dominance of negative correlation was obtained in the SWP region, off the coast of Brazil - Argentina – Uruguay, with the r values comprised between -0.05 and -0.15. It worth mention that for these correlation analyses, statistical significance at the 95% level was not observed. The northernmost regions of Togo (Kara and Savanes) presented a weaker correlation with the SST conditions in the two SAODI poles. This corroborates our previous finding that the influence of the South Atlantic SST variation in rainfall in the northern regions is not significant as it is for the southern regions of Maritime and Plateaux.

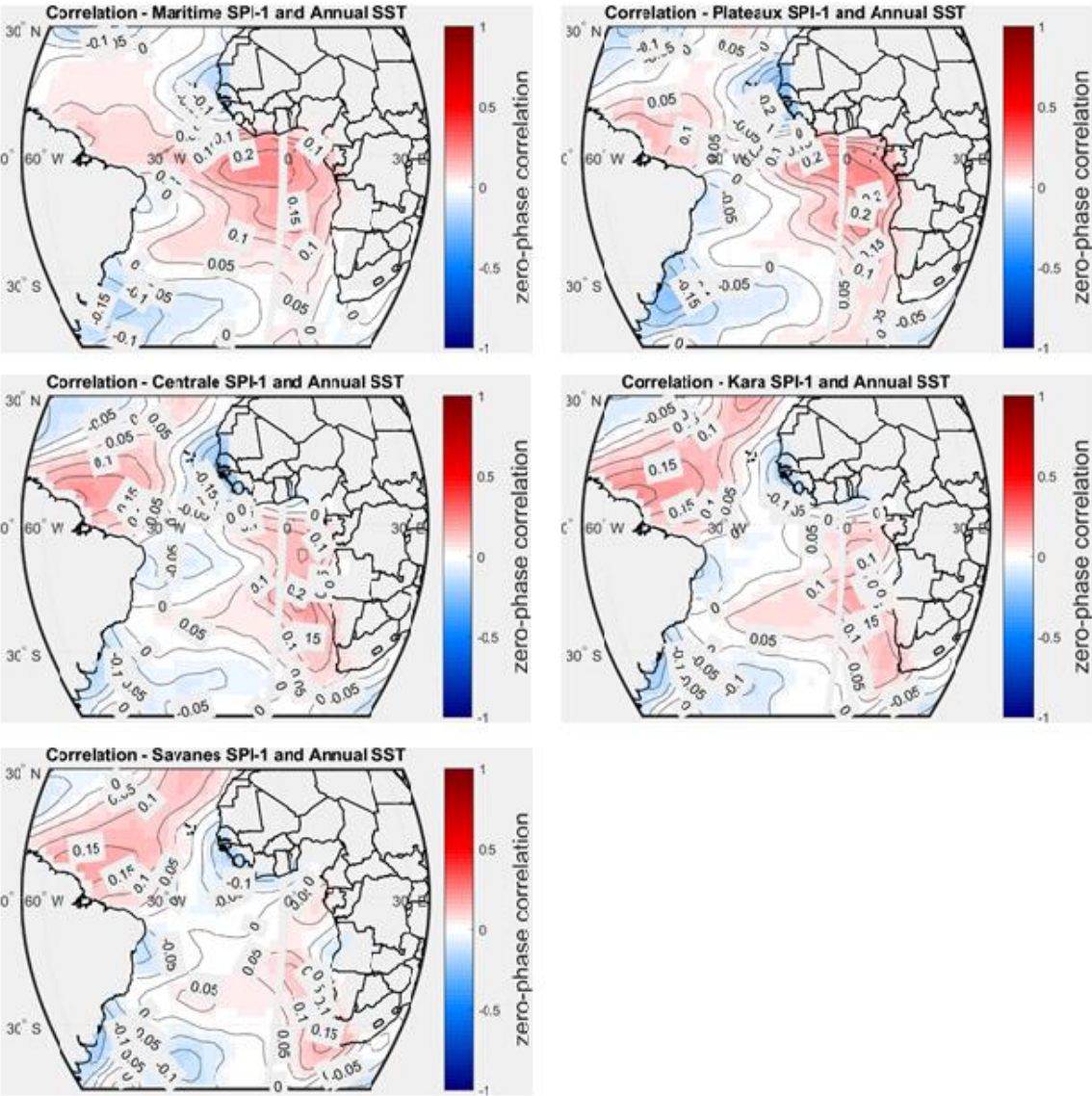


Figure 22: Correlation map between SST anomalies and SPI 1-month for in all the Togo regions considering all months.

We also conducted the Pearson correlation analysis exclusively considering WAM season to find out how SPI-1 for each Togo region responded to the South Atlantic SST anomalies (see figure 23). A positive correlation higher than when all months were considered was found between Maritime and Plateaux SPI-1 and the SST anomalies in the NEP region, which include the known Atlantic Niño region. The highest correlation was obtained for the Plateaux region ($r = 0.40$). Like for the correlation considering all months, the northern regions, which are far from the Gulf of Guinea compared to Plateaux and Maritime regions, exhibited the lowest correlation with the SST anomalies (weak positive correlation in the NEP and weak negative correlation in the SWP).

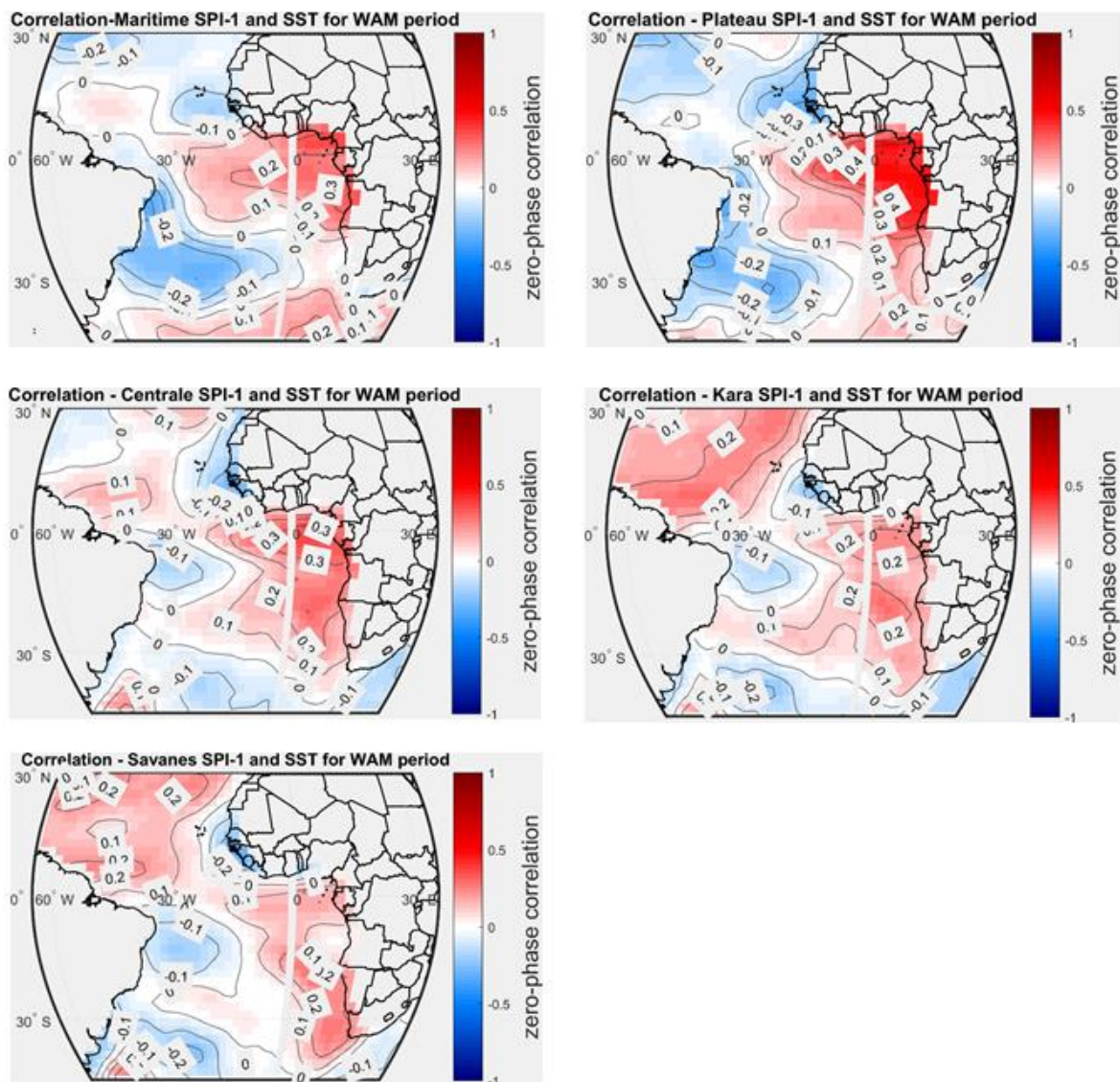


Figure 23: Correlation map between SST anomalies and SPI 1-month for each Togo region for the West Africa Monsoon months.

Based on the correlations analysis between SPI-1 and SST anomalies in the South Atlantic Ocean, the results reproduce the earlier analyses focusing on the correlation between SPI-1 and SAOD index. SST anomaly in the NEP area is positively correlated with SPI-1 in the southern regions (Maritime, Plateaux) located under 10° N while it presented a weak correlation with the northern regions beyond 10° N. Although the correlation analysis is not statically significant for all the 5 regions, it is plausible to argue that SAOD is likely an important factor to explain the occurrence of extreme events (drought, flood) over the Guinea Coast, while it has lower influence over the areas in the north, near to the Sahel. This result is basically consistent with the previous work of Nnamchi et al., (2011), who found that the precipitation variability over the Guinea Coast in West Africa is controlled not only by the Atlantic Nino but also by the combination of the two modes (NEP, SWP), which is expressed in the SAODI index. Nnamchi et al., (2011) find out that the SAODI is strongly correlated with the Guinea Coast precipitation while there is no simultaneous connection between the SAODI and Sahel precipitation, and this can explain why Maritime and Plateaux regions have a better correlation with SAOD than Centrale, Kara and Savanes regions (regions close to the Sahel).

Since the IMERG rainfall time series is not too long (19 years), this may be one of the reasons why correlations between SPI 1-month and the ocean indices here obtained were not that strong (Wu & Kinter, 2009). However, current study correlation magnitude results are consistent with those of Nnamchi et al., (2011), who found similar values (0.20 and 0.50) when they correlated SAODI and the WAM average precipitation over Gulf of Guinea countries. One should emphasize that the results of this section are mainly focused on correlation analysis; no further analysis targeting mechanism that explains the roles of Tropical Atlantic and Pacific Ocean SST variability as forcing of drought or wet episodes over Togo regions was assessed.

In summary, the results found in this section demonstrated that:

- The correlation analysis during monsoon season for the study period and using IMERG rainfall data are consistent with the results of previous studies (e.g., Nnamchi et al., 2011); which have pointed out the existence of a stronger link between rainfall variability over West Africa and the SAOD mode during WAM season.
- The correlation between ENSO and SPI 1-month was not significant, suggesting that the rainfall variability over West Africa for the current study period was weakly influenced by ENSO phenomena. Thus, the interaction between other atmospheric processes could have played an important role in the rainfall variability during this

period. It worth mention that the available time series of IMERG- rainfall also was relatively short, which may have impacted our analysis.

- The relatively stronger and positive correlation between SAODI and SPI-1 for monsoon season compared with all month's correlation corroborates that SAOD plays a major role during the rainfall season in West Africa.
- Rainfall variability in Togo and West Africa can be affected by ENSO during a strong El Nino event, which can therefore increase the intensity and extent of drought events. According to previous studies, this was the case in 2015, which in the present study was characterized by a strong rainfall deficit, also favored by a deficit observed between 2013 and 2014.
- The lack of precipitation in 2013, 2014, and 2015 and a large amount of precipitation observed in 2007, 2008, and 2009 were consistent with the signature of SAODI. During the positive SAODI scenarios, Togo experienced wet events and the most recent severe flooding events in the Savanes, Centrale, and Southern Maritime region, displacing thousands of people and causing important damages (West Africa Floods map, 2008).
- The spread of drought condition observed over West Africa in 2015 probably was not only related to the strong El Niño of that year, because as the time series of SPI had shown, Togo was already under dry condition since 2014, which was likely linked to the negative phase of SAODI. Thus, it is possible that the two ocean variability modes (ENSO and SAOD) interacted and played a combined role during this exceptional dry period.

5. CONCLUSIONS AND RECOMMENDATIONS

5.1. Conclusion

Droughts and floods are the major climate extremes events that impact the populations and economy of Togo. Their severity and frequency have been shown to increase worldwide with global warming and are expected to get worse. Thus, it is very important to adequately understand and monitor the spatial and temporal variability of precipitation across Togo in order to better assess the occurrence of these climate extremes events, so the country can be able to act preventively via mitigation and adaptation to curb their impacts.

In this study, the occurrence of dry and wet events from 2001 to 2019 at the local and regional level in Togo have been analyzed, and their relationship with indices of two major ocean-atmosphere climate variability modes, El Niño-Southern Oscillation and South Atlantic Ocean Dipole (SAOD), evaluated. The analyses of dry and wet periods were done using the Standard Precipitation Index (SPI), recommended by the World Meteorological Organization (WMO) and widely used to characterize drought on different timescales. Its dependence only on precipitation is important for regions where rainfall is the only available climate information. Based on two distinct datasets, rain gauge measurements from nine Togo Meteorological stations and rainfall from a satellite-based product, the Integrated Multi-satellitE Retrievals for GPM (IMERG); SPI were calculated, and dry and wet events across Togo regions were analyzed. IMERG global rainfall estimate is a relatively new high-resolution product, with relevant potential to be integrated into regional monitoring systems worldwide, especially in those regions that lack a dense rain gauge network, like the West African countries. Therefore, the evaluation of the IMERG rainfall performance across Togo regions was also part of the present study goals.

The intercomparison between the two datasets, IMERG rainfall estimate, and rain gauges measurements, demonstrated that IMERG is able to reproduce the main features of temporal and spatial variation of precipitation across Togo. Based on monthly mean rainfall distribution across

Togo, the results showed that in general, IMERG rainfall product reflected well the seasonal rainfall variation although important overestimations occurred at the meteorological station of Lomé in the Maritime (coastal region) and underestimations in the high elevation region of Kouma Konda (Plateaux region).

The overestimation observed at Lomé was due to the local effect, since Tabligbo, which is located in the same region (Maritime) in the northwest part, IMERG presented the best results

when compared to the rain gauge. This low performance of IMERG at Lomé occurred during the small dry period when Lomé is dominated by low clouds, which can be a challenge for satellite-based rainfall. Regarding the underestimation observed at Kouma Konda, which is also due to the local's effect, previous studies had pointed out that IMERG performance over mountain regions needed improvement. However, despite the difficulty of IMERG to capture the interannual variability of the total amount of precipitation over Lomé and Kouma Konda accurately, the product was able to present better performance for the interannual variability of annual rainfall anomaly, which from the point of view of SPI application is relevant.

SPI results obtained for distinct time scale (3-months; 6-months and 12-months) showed that, despite some differences in the duration and intensity, SPI results obtained based on IMERG rainfall were able to capture the major wet and dry periods at the local scale, consistently with the results based on rain gauge datasets. For instance, the satellite-based product captured the widespread, long-term wet period, from 2008 to 2010, and dry period, from 2013 to 2015, also seen in rain gauge data.

While rain gauge comparison with IMERG shows that SPI results based on IMERG rainfall were not able to capture local dry and wet events accurately everywhere, the significant differences observed in SPI results between rain gauge in the same region relatively close, revealed the challenge posed by a limited rain gauge network. Therefore, the need and importance of high-resolution satellite-based rainfall products development and improvement, which combined with rain gauge networks, would provide a comprehensive spatial monitoring coverage.

In addition, SPI analysis at different time scales helped to clarify the role of deficit and excess rainfall during WAM season as drivers of long-term dry and wet events. Thus, our work shows clearly that long-term dry periods, in general, were related to subsequent WAM seasons with rainfall deficit.

Results of the correlation analysis between SPI and ENSO and SAOD indices for the period analyzed were consistent with previous studies' results. For instance, a significant improvement in the correlation between SAODI and SPI 1-month was found for the WAM season compared with the entire year, corroborating previous studies that established that the coupling between the South Atlantic Ocean and Gulf of Guinea precipitation is stronger during WAM season. Moreover, the southern regions of Togo (Maritime and Plateaux) presented a stronger correlation with the SAODI than the regions in the North of the country, located further from the Gulf of Guinea (Centrale, Kara, Savanes).

In general, as previous studies suggested, in the present study, we obtain that: The positive phases of SAODI were related to an increase in precipitation in Togo, while negative phases to a lack of precipitation. This result is corroborated by the main widespread, long-term wet (2008-2010) and dry (2013-2015) events identified in this study.

The correlation analysis results also showed that, for our study period, the ENSO index, Niño 3.4, had a very weak negative correlation with SPI 1- month for both WAM season and the entire year. However, this weak correlation does not imply that there is no link or no teleconnection between ENSO phenomena and rainfall variability over Togo regions. Some likely reasons for this low correlation can be the relatively short period of the present study, the dominance of relatively weak El Niño (except 2015), and the La Niña events. Moreover, ENSO influence on West Africa rainfall involves complex interactions between the atmosphere and ocean which are not fully understood; therefore, more investigation and further studies are needed. For instance, the net effect when ENSO events occur at the same time of different SAOD phases (positive, negative) is yet to be clarified. Nevertheless, rainfall variability in Togo and in West Africa as a whole can be affected by strong El Niño events, which seems to be the case for the general rainfall deficit observed in West Africa in 2015. However, one cannot neglect the role of the SAOD negative phase that was occurring during the same time period.

Further studies are needed for the monitoring and prediction of these extreme climate events (drought and flood) over Togo regions in order to help the local communities and stakeholders in their decision-making in order to mitigate the effects of climate change. To achieve this goal, long-term, and high spatial resolution rainfall data are fundamental to establish a drought early warning system and central to advance the understanding of the influence of the atmosphere and ocean climate variability modes on rainfall distribution across the country.

5.2. Recommendations

This study has explored many important features of precipitation variability over Togo integrating satellite data and rain gauge. Additionally, dry and wet events occurred during the last two decades at the local and regional scale, and their relationship with SST variability in the Pacific and Tropical Atlantic Ocean have been discussed.

Aiming future research studies and public policies on climate, the following recommendations are made:

- ❖ Continuous evaluation of the accuracy and reliability of these high-resolution satellite-based rainfall estimates, for instance, the IMERG products, is highly recommended in order to improve the national capability to monitor climate extreme events.
- ❖ The implementation of an Early System Warning in Togo focusing on climate extremes based on multiple platforms (rain gauge, satellite) is crucial to give reliable climate information to the decision-makers and populations as a whole.
- ❖ The operational network of observation stations over Togo needs to be continuously improved in order to provide high spatial resolution observations that can be used to evaluate satellite-based and climate model rainfall information.
- ❖ Extremes weather, such as floods, directly affects the socio-economic activities of Togo. It is therefore recommended that the climate information issued by the Department of Meteorology be integrated into the management, planning, and decision-making to minimize the devastating impacts of these extreme events.

6. REFERENCES

- Adewi E., Badameli K. M. S., UK (2010). Évolution des saisons des pluies potentiellement utiles au Togo De 1950 À 2000. 7, 89–107.
- Aghakouchak A., Farahmand A., Melton F. S., Teixeira J., Anderson M. C., Wardlow B. D., & Hain, C. R. (2015). Remote sensing of drought: Progress, challenges, and opportunities. *Reviews of Geophysics*, 53, 1–29. <https://doi.org/10.1002/2014RG000456>.Received
- Alexander L. V, Uotila P., & Nicholls N. (2009). Influence of sea surface temperature variability on global temperature and precipitation extremes. 114(July). <https://doi.org/10.1029/2009JD012301>
- Alhamshry, A., Fenta, A. A., Yasuda, H., Kimura, R., & Shimizu, K. (2020). Seasonal rainfall variability in Ethiopia and its long-term link to global sea surface temperatures. *Water (Switzerland)*, 12(1). <https://doi.org/10.3390/w12010055>
- Ali, K. E., Kouadio, K. Y., Zahiri, E. P., Aman, A., Assamoi, A. P., & Bourles, B. (2011). Influence of the Gulf of Guinea coastal and equatorial upwellings on the precipitations along its northern coasts during the boreal summer period. *Asian Journal of Applied Sciences*, 4(3), 271–285. <https://doi.org/10.3923/ajaps.2011.271.285>
- Amin K. Dezfuli, Charles M. Ichoku, George J. Huffman, Karen I. Mohr, John S. Selker, Nick van de Giesen, Rebecca Hochreutener, and F. O. A. (2017). Validation of IMERG Precipitation in Africa. *Journal of Hydrometeorology*, 18(10), 2817–2825. <https://doi.org/10.1175/JHM-D-17-0139.1>
- Anyamba A., Chretien J. P., Britch, S. C., Soebiyanto, R. P., Small, J. L., Jepsen, R., Forshey, B. M., Sanchez, J. L., Smith, R. D., Harris, R., Tucker, C. J., Karesh, W. B., & Linthicum, K. J. (2019). Global Disease Outbreaks Associated with the 2015–2016 El Niño Event. *Scientific Reports*, 9(1), 1–14. <https://doi.org/10.1038/s41598-018-38034-z>
- Aondove R. Tarhule , Zakar I. Saley-Bana, (2009). A Prototype GIS for Rainfall Monitoring in West Africa. *Journal of Esthetic and Restorative Dentistry*, 1(2), A9–A9. <https://doi.org/10.1175/2009BAMS2697.1>
- Azua S. (2015) Analysis of Rainfall Variability and the Trends of Wet and Dry Periods in Makurdi and Environs Using Standardised Precipitation Index. 6th International Conference and Annual General Meeting Meeting of Nigeria Association of Hydrological Sciences (NAHS) “A.B.U 2015”, Zaria-Kaduna, Nigeria, 15-18 September 2015, 1-11.
- Badameli KSM. Analyse et prise de compte des risques climatiques en agriculture: cas de la region maritime du Togo, (1998) Travaux et recherches geographiques. *Revue Geographique de l’Universite de Lome*; p. 239–250.
- Badameli KSM (1996). La variabilité climatique et la production agricole au Togo. Université de Bordeaux III, France; p. 1–343
- Barlow M.Nigam S, BerberyEH. 2001. ENSO, Pacific decadal variability, and U.S. summertime precipitation, drought, and streamflow. *J. Climate* 14:2105–28
- Batebana K., Alex Ogwang B., Mie Mie Sein, Z., Katchele Ogou, F., Ongoma, V., & Paul Ngarukiyimana, J. (2015). Rainfall Characteristics over Togo and their related Atmospheric circulation Anomalies. *Journal of Environmental and Agricultural Sciences*,

- 5(11), 34–48. <http://www.researchgate.net/publication/282730103>
- Benjamin Sultan and Serge Janicot. (2003). The West African Monsoon Dynamics. Part II : The “ Preonset ” and “ Onset ” of the Summer Monsoon. *Journal of Climate*, 3407–3427. DOI: [https://doi.org/10.1175/1520-0442\(2003\)016<3407:TWAMDP>2.0.CO;2](https://doi.org/10.1175/1520-0442(2003)016<3407:TWAMDP>2.0.CO;2)
- Bernard Fontaine and Serge Janicot. (1996). Sea Surface Temperature Fields Associated with West African Rainfall Anomaly Types. *Journal of Climate*, 9(11), 2935–2940. [https://doi.org/10.1175/1520-0442\(1996\)009<2935:SSTFAW>2.0.CO;2](https://doi.org/10.1175/1520-0442(1996)009<2935:SSTFAW>2.0.CO;2)
- Boyin Huang; Peter Thorne ; Viva Banzon; Tim Boyer; Gennady Chepurin ; Jay Lawrimore; Matthew Menne ; Thomas Smith; Russell Vose1; Huai-Min Zhang. (2017). Extended Reconstructed Sea Surface Temperature version 5 (ERSSTv5): Upgrades, Validations, and Intercomparisons. *Journal of Climate*, 5. <https://doi.org/10.1175/JCLI-D-16-0836.1>, in press
- Brown R. W. K. and B. G. (1992). Extreme events in a changing climate: VARIABILITY IS more important than averages. 289–302. <https://doi.org/10.1007/BF00139728>
- Chen F., & Li X. (2016). Evaluation of IMERG and TRMM 3B43 Monthly Precipitation Products over Mainland China. *Remote Sens.* 2016, 8, 472, 1–18. <https://doi.org/10.3390/rs8060472>
- Chen S., Hong Y., Cao Q., Gourle J., Kirstetter, P., Yong, B., Tian, Y., Zhang, Z., Shen, Y., Hu, J., & Hardy, J. (2013). Similarity and difference of the two successive V6 and V7 TRMM multisatellite precipitation analysis performance over China. *Journal of geophysical research: atmospheres*, 118, 60–75. <https://doi.org/10.1002/2013JD019964>
- Climate Change 2014: Synthesis Report. Contribution of Working Groups I, II, and III to the Fifth Assessment Report of the Intergovernmental Panel on Climate Change / R. Pachauri and L. Meyer (editors), Geneva, Switzerland, IPCC, 151 p., ISBN: 978-92-9169-143-2.
- Dado J. M. B., & Takahashi H. G. (2017). Potential impact of sea surface temperature on rainfall over the Western Philippines. *Progress in Earth and Planetary Science*, 4(1). <https://doi.org/10.1186/s40645-017-0137-6>
- Dai A. (2013). Increasing drought under global warming in observations and models. *Nature Climate Change*, 3(1), 52–58. <https://doi.org/10.1038/nclimate1633>
- Danso D. K., Koba L. A., Anquetin, S., & Diedhiou, A. (2019). Spatio-temporal variability of cloud cover types in West Africa with satellite-based and reanalysis data. *Quarterly Journal of the Royal Meteorological Society*, August, 1–17. <https://doi.org/10.1002/qj.3651>
- Dembélé M., & Zwart S. J. (2016). Evaluation and comparison of satellite-based rainfall products in Burkina Faso, West Africa. *International Journal of Remote Sensing*, 37(17), 3995–4014. <https://doi.org/10.1080/01431161.2016.1207258>
- Deser C., Alexander M. A., Xie S., & Phillips, A. S. (2010). Sea Surface Temperature Variability : Patterns and Mechanisms. <https://doi.org/10.1146/annurev-marine-120408-151453>
- Djaman K., Sharma V., Daran R., Koudahe K., Irmak S., & Amouzou K. A. (2017). Spatial and temporal variation in precipitation in Togo. *International Journal of Hydrology*, 1(4). <https://doi.org/10.15406/ijh.2017.01.00019>

- DJ Parker, M Diop-Kane, (2017). *Meteorology of Tropical West Africa: The Forecasters' Handbook*
- Duan Z., & Liu J. (2012). Monthly and annual validation of TRMM Multisatellite Precipitation Analysis (TMPA) products in the Caspian Sea Region for the period 1999 – 2003. July. <https://doi.org/10.1109/igarss.2012.6350613>
- E. Adewi, K. M. S. B. et V. D. (2009). *Influence de la pejoration pluviometrique sur les productions agricoles au Togo*. Cluj University Press, Association Internationale de Climatologie (AIC).
- Edward K. Vizy and Kerry H. Cook. (2001). Mechanisms by Which Gulf of Guinea and Eastern North Atlantic Sea Surface Temperature Anomalies Can Influence African Rainfall. *Journal of Climate*, 1993, 795–821. <https://doi.org/10.1175/1520-04422014<0795:MBWGOG>2.0.CO;2>
- Egbuawa O. I., Anyanwu J. C., Amaku G. E., & Onuoha I. C. (2017). Assessment of the Teleconnection Between El Nino Southern Oscillation (ENSO) and West African Rainfall. *African Research Review*, 11(4), 17. <https://doi.org/10.4314/afrrrev.v11i4.3>
- FAO. (2015). *Climate change and food security: risks and responses*.
- Giannini A., & Chang P. (2005). Dynamics of the boreal summer African monsoon in the NSIPP1 atmospheric model. 1984(April 1974), 517–535. <https://doi.org/10.1007/s00382-005-0056-x>
- Guttman N. B. (1998). Comparing The Palmer Drought Index and the Standardized Precipitation Index. *Journal of the American Water Resources Association*, 33(1), 113–121. <https://doi.org/10.1111/j.1752-1688.1998.tb05964.x>
- Guy Merlin Guenang and F. Mkankam Kamga. (2014). Computation of the Standardized Precipitation Index (SPI) and Its Use to Assess Drought Occurrences in Cameroon over Recent Decades. *Journal of Applied Meteorology and Climatology*, 53(10), 2310–2324. <https://doi.org/10.1175/JAMC-D-14-0032.1>
- H. Douville S. Conil S. Tyteca A. Voldoire. (2007). Soil moisture memory and West African monsoon predictability : artefact or reality? 23–742. Doi: 10.1007/s00382-006-0207-8
- Hall N. M. J., & Peyrillé, P. (2006). Dynamics of the West African monsoon. 139, 81–99.
- Hansen J. W. (2002). Realizing the potential benefits of climate prediction to agriculture : issues approaches challenges. *Agricultural Systems*, 74, 309–330. [https://doi.org/10.1016/S0308-521X\(02\)00043-4](https://doi.org/10.1016/S0308-521X(02)00043-4)
- Hao Z., Aghakouchak A., Nakhjiri N., & Farahmand A. (2014). Global integrated drought monitoring and prediction system. *scientific data*, 1–10. <https://doi.org/10.1038/sdata.2014.1>
- Huei-Huang Lee (2020), *Programming and Engineering Computing with MATLAB*
- Hulme M., Doherty R., Ngara T., New M., & Lister D. (2001). African climate change : 1900 – 2100. *Climate Research*, 17, 145–168. [https://doi.org/Climate Research, 17, 145–168](https://doi.org/Climate%20Research,17,145-168). doi:10.3354/cr017145
- Huffman G. J., Gsfc N., Bolvin D. T., Braithwaite D., Hsu K., Joyce R., Kidd C., Nelkin, E. J., Sorooshian S., & Tan J. (2019). *NASA Global Precipitation Measurement (GPM) Integrated Multi-satellite Retrievals for GPM (IMERG). Algorithm Theoretical Basis Doc., version 06. March, 32.* https://docservet.gesdisc.eosdis.nasa.gov/public/project/GPM/IMERG_ATBD_V06.pdf.

- IPCC Panel. (2014). *Climate Change 2014: Synthesis Report*. 1–151.
- IPCC, 2021: Summary for Policymakers. In: *Climate Change 2021: The Physical Science Basis. Contribution of Working Group I to the Sixth Assessment Report of the Intergovernmental Panel on Climate Change* [Masson-Delmotte, V., P. Zhai, A. Pirani, S. L. Connors, C. Péan, S. Berger, N. Caud, Y. Chen, L. Goldfarb, M. I. Gomis, M. Huang, K. Leitzell, E. Lonnoy, J.B.R. Matthews, T. K. Maycock, T. Waterfield, O. Yelekçi, R. Yu and B. Zhou (eds.)]. Cambridge University Press. In Press.
- Jackson Tan, Walter A. Petersen, A. T. (2016). A Novel Approach to Identify Sources of Errors in IMERG for GPM Ground Validation. *Journal of Hydrometeorology*, 17, 2477–2491. <https://doi.org/10.1175/JHM-D-16-0079.1>
- John E. Oliver (2008). *Encyclopedia of World Climatology*
- Joly M., & Voltaire A. (2010). Role of the Gulf of Guinea in the inter-annual variability of the West African monsoon: What do we learn from CMIP3 coupled simulations? *International Journal of Climatology*, 30(12), 1843–1856. <https://doi.org/10.1002/joc.2026>
- Joly M., Voltaire A., Douville H., Terray, P., Joly, M., Voltaire, A., Douville, H., Terray, P., & African, J. R. (2014). African monsoon teleconnections with tropical SSTs : Validation and evolution in a set of IPCC4 simulations; HAL Id : meteo-00996738
- Kao, S. C., & Govindaraju, R. S. (2010). A copula-based joint deficit index for droughts. *Journal of Hydrology*, 380(1–2), 121–134. <https://doi.org/10.1016/j.jhydrol.2009.10.029>
- Kerry H. Cook and Edward K. Vizy. (2006). Coupled Model Simulations of the West African Monsoon System : Twentieth- and Twenty-First-Century Simulations. *Journal of Climate*, 19(15), 3681–3703.
- Komla D. K. and G. (2015). Trend analysis in reference evapotranspiration and aridity index in the context of climate change in Togo. 848–864. <https://doi.org/10.2166/wcc.2015.111>
- Koster R. D., Guo, Z., Bonan G., Chan E., & Cox P. (2014). Regions of Strong Coupling Between Soil Moisture and Precipitation. *1138(2004)*, 10–13. <https://doi.org/10.1126/science.1100217>
- Kouadio Y. K., Ochoy D. A., Servain J., & Nin E. (2003). Tropical Atlantic and rainfall variability in Côte d ' Ivoire. *30(5)*, 3–6. <https://doi.org/10.1029/2002GL015290>
- Koudahe K., Kayode A. J., Samson A. O., & Adebola A. (2017). Trend Analysis in Standardized Precipitation Index and Standardized Anomaly Index in the Context of Climate Change in Southern Togo. August. <https://doi.org/10.4236/acs.2017.74030>
- Laban O. (2009). Climate variability and change in Africa: A review of potential impacts on terrestrial water resources. *IAHS-AISH Publication*, 334(June 2008), 47–51.
- Luc Le Barbé, Thierry Lebel, and D. T. (2002). Rainfall Variability in West Africa during the Years 1950 – 90. *Journal of Climate*, 187–202. [https://doi.org/10.1175/1520-0442\(2002\)015<0187:RVIWAD>2.0.CO;2](https://doi.org/10.1175/1520-0442(2002)015<0187:RVIWAD>2.0.CO;2)
- M. B. Sylla, I. D. and J. S. P. (2013). West African Monsoon in State-of-the-Science Regional Climate Models. *INTECH*, 4–35. <https://doi.org/http://dx.doi.org/10.5772/55140>
- Maranan M., Fink A. H., Knippertz P., Amekudzi L. K., Atiah W. A., & Stengel M. (2020). A process-based validation of gpm imerg and its sources using a mesoscale rain gauge network in the West African forest zone. *Journal of Hydrometeorology*, 21(4), 729–749. <https://doi.org/10.1175/JHM-D-19-0257.1>

- M. Barlow S. Nigam and E. H. B. (2001). ENSO, Pacific Decadal Variability, and U . S .
Summertime Precipitation, Drought, and Stream Flow. 2105–2128.
- Mazzoglio P., Laio F., Balbo S., Boccardo P., & Disabato F. (2019). Improving an Extreme
Rainfall Detection System with GPM IMERG data. 1–24.
<https://doi.org/10.3390/rs11060677>
- McCabe G. J., Palecki M. A., & Betancourt J. L. (2004). Pacific and Atlantic Ocean influences
on multidecadal drought frequency in the United States. *Proceedings of the National
Academy of Sciences of the United States of America*, 101(12), 4136–4141.
<https://doi.org/10.1073/pnas.0306738101>
- Mckee T. B., Doesken N. J., & Kleist J. (1993). The relationship of drought frequency and
duration to time scales. Eighth Conference on Applied Climatology, January 17–22.
- Michael F. Wehner. (2004). NOTES AND CORRESPONDENCE Predicted Twenty-First-
Century Changes in Seasonal Extreme Precipitation Events in the Parallel Climate Model.
Journal of Climate, 17(21), 4281–4290. <https://doi.org/10.1175/JCLI3197.1>
- Mohammed S. A., Hamouda M. A., & Mahmoud M. T. (2020). Performance of GPM-IMERG
precipitation products under diverse topographical features and multiple-intensity rainfall
in an arid region. *Hydrol. Earth Syst. Sci. Discuss*, January. <https://doi.org/10.5194/hess-2019-547>
- Molua E. L. (2012). Socio-economic impacts of climate change on coastal ecosystems and
livelihoods: A case study of Southwestern Cameroon. *Conserving and Valuing Ecosystem
Services and Biodiversity: Economic, Institutional and Social Challenges*, March, 371–
392. <https://doi.org/10.4324/9781849770859>
- Mouhamed L., Traore S. B., Alhassane A., & Sarr B. (2013). Evolution of some observed
climate extremes in the West African Sahel. *Weather and Climate Extremes*, 1, 19–25.
<https://doi.org/10.1016/j.wace.2013.07.005>
- Nandintsetseg B., & Shinoda M. (2013). Assessment of drought frequency, duration, and
severity and its impact on pasture production in Mongolia. *Nat Hazards* (2013) 66:995–
1008, 995–1008. <https://doi.org/10.1007/s11069-012-0527-4>
- National Drought Mitigation Center. (2021). Map interpretation. 1–10.
- Nicholson S E, & Grist J. P. (2001). A conceptual model for understanding rainfall variability
in the west African Sahel on interannual and interdecadal timescales. 1757, 1733–1757.
- Nicholson S E, & Selato J. C. (2000). The influence of La Nina on African rainfall. *Int. J.
Climatol.*, 1776, 1761–1776.
- Nicholson Sharon E, & Kim J. (1997). The relationship of the El Nino –southern oscillation to
African rainfall. 17, 117–135.
- Nimon P., Issaou L., Konko Y., & Kokou, K. (2020). Spatio-Temporal Patterns of Rainfall
Variability for Wet Season over Togo in West Africa. *Open Access Library Journal*, 7, 1–
11. <https://doi.org/10.4236/oalib.1106044>
- Nnamchi H. C., & Li J. (2011). Influence of the South Atlantic Ocean dipole on West African
summer precipitation. *Journal of Climate*, 24(4), 1184–1197.
<https://doi.org/10.1175/2010JCLI3668.1>
- Nnamchi H. C., Li J., & Anyadike R. N. C. (2011). Does a dipole mode really exist in the South
Atlantic Ocean? *Journal of Geophysical Research-Atmospheres*, 116(15), 1–15.
<https://doi.org/10.1029/2010JD015579>

- Odekunle T. O., & Eludoyin A. O. (2008a). Sea surface temperature patterns in the Gulf of Guinea: their implications for the Spatio-temporal variability of precipitation in West Africa. September. <https://doi.org/10.1002/joc.1656>
- Odekunle T. O., & Eludoyin A. O. (2008b). Sea surface temperature patterns in the Gulf of Guinea: their implications for the Spatio-temporal variability of precipitation in West Africa. 1517(January), 1507–1517. <https://doi.org/10.1002/joc>
- OCHA, (2020). West and Central Africa flooding situation overview (January - December 2020).
- Ogallo L. A., Boulahya M. S., & Keane T. (2000). Applications of seasonal to interannual climate prediction in agricultural planning and operations. *Agricultural and Forest Meteorology*, 103(1–2), 159–166. [https://doi.org/10.1016/S0168-1923\(00\)00109-X](https://doi.org/10.1016/S0168-1923(00)00109-X)
- Orlowsky B., & Seneviratn S. I. (2014). Short Communication On the spatial representativeness of temporal dynamics at European weather stations. *Int. J. Climatol.*, 3160(February), 3154–3160. <https://doi.org/10.1002/joc.3903>
- Owusu K., Emmanuel A. K., Musah-Surugu, I. J., & Yankson, P. W. K. (2019). The effects of 2015 El Nino on smallholder maize production in the transitional ecological zone of Ghana. *International Journal of Climate Change Strategies and Management*, 11(5), 609–621. <https://doi.org/10.1108/IJCCSM-02-2018-0014>
- P Stocker T, Qin D, Plattner G, Tignor M, Allen S, Boschung J, Nauels A, Xia Y, Bex V, M. p. (2013). IPCC, 2013: Climate Change 2013: The Physical Science Basis. Contribution of Working Group I to the Fifth Assessment Report of the Intergovernmental Panel on Climate Change. IPCC Report.
- Paeth H., Fink A. H., Pohle S., Keis F., & Hermann M. (2011). Meteorological characteristics and potential causes of the 2007 flood in sub-Saharan Africa. 1926(July 2010), 1908–1926. <https://doi.org/10.1002/joc.2199>
- Paeth H., & Hense A. (2004). SST versus climate change signals in west african rainfall : 20th-century variations and future projections. *Climatic Change Volume 65*, 179–208. <https://doi.org/10.1023/B:CLIM.0000037508.88115.8a>
- Parry S., Wilby R. L., Prudhomme C., & Wood P. J. (2016). A systematic assessment of drought termination in the United Kingdom. *Hydrol. Earth Syst. Sci.*, 20, 4265–4281, 2016, 20, 4265–4281. <https://doi.org/10.5194/hess-20-4265-2016>
- Pessiezoum Adjoussi. (2000). Changement climatique global : évaluation de l' évolution des paramètres au Togo. <http://creativecommons.org/licenses/by-nc/3.0/>
- Quatrième Recensement général de la population et de l'habitat - Novembre 2010 <http://arks.princeton.edu/ark:/88435/dsp01p8418q53f>
- Raymond P. Motha, Sharon K. Leduc, Louis T. Steyaert, Clarence M. Sakamoto, and N. D. S. (1980). Precipitation Patterns in West Africa. *Monthly Weather Review*, 108(10), 1567–1578. [https://doi.org/10.1175/1520-0493\(1980\)108<1567:PPIWA>2.0.CO;2](https://doi.org/10.1175/1520-0493(1980)108<1567:PPIWA>2.0.CO;2)
- Rowell D. P., C. K. Folland, K. Maskell, J. A. Owen, and M. N. W. (1992). Modeling the influence of global sea surface temperature on the variability and predictability of seasonal Sahel rainfall. *Geophysical Research Letters*, 19(January 1992), 905–908.
- Roxy M. (2014). Sensitivity of precipitation to sea surface temperature over the tropical summer monsoon region — and its quantification. 1159–1169. <https://doi.org/10.1007/s00382-013-1881-y>

- Russo S., Dosio A., Graversen R. G., Sillmann J., Carrao H., Dunbar M. B., Singleton A., Montagna P., Barbola P., & Vogt J. V. (2014). Magnitude of extreme heatwaves in the present climate and their projection in a warming world. <https://doi.org/10.1002/2014JD022098>. Received
- Sazib N., Mladenova Iliana E., & Bolten J. D. (2020). Assessing the Impact of ENSO on Agriculture Over Africa Using Earth Observation Data. *Frontiers in Sustainable Food Systems*, 4(October), 1–11. <https://doi.org/10.3389/fsufs.2020.509914>
- Salles, L.; Satgé, F.; Roig, H.; Almeida, T.; Olivetti, D.; Ferreira, W. Seasonal Effect on Spatial and Temporal Consistency of the New GPM-Based IMERG-v5 and GSMaP-v7 Satellite Precipitation Estimates in Brazil's Central Plateau Region. *Water* 2019, 11, 668. <https://doi.org/10.3390/w11040668>
- Seager, R., Ting, M., Li, C., Naik, N., Cook, B., Nakamura, J., & Liu, H. (2013). Projections of declining surface-water availability for the southwestern United States. *Nature Climate Change*, 3(5), 482–486. <https://doi.org/10.1038/nclimate1787>
- Serge Janicot , Ali Harzallah , Bernard Fontaine, V. M. (1998). West African Monsoon Dynamics and Eastern Equatorial Atlantic and Pacific SST Anomalies (1970 – 88). *Journal of Climate*, Lmd, 1874–1882.
- Sogbedji J. M. (1999). Maize nitrogen utilization and nitrate leaching modeling in Togo and New York.
- Stagge J. H., Tallaksen L. M., Gudmundsson L., & Loon F. Van. (2015). Candidate Distributions for Climatological Drought Indices (SPI and SPEI). *Int. J. Climatol.*, 4040(February), 4027–4040. <https://doi.org/10.1002/joc.4267>
- Stephen H. Schneider (2011). *Encyclopedia of Climate and Weather, Volume 1*
- Sujitha E. and Shanmugasundaram K. (2017). Analysis of dry/wet conditions using the Standardized Precipitation Index and its potential usefulness for drought /flood
- Sultan B., & Janicot, S. (2000). Abrupt shift of the ITCZ over West Africa and intra-seasonal variability. *Geophysical Research Letters*, 27(20), 3353–3356. <http://dx.doi.org/10.1029/1999GL011285>
- Sun W., Sun Y., Li X., Wang T., Wang, Y., Qiu, Q., & Deng, Z. (2018). Evaluation and Correction of GPM IMERG Precipitation Products over the Capital Circle in Northeast China at Multiple Spatiotemporal Scales. *Hindawi*, 2018, 14. <https://doi.org/10.1155/2018/4714173>
- Ta S., Kouadio K. Y., Ali, K. E., Toualy, E., Aman, A., & Yoroba, F. (2016). West Africa Extreme Rainfall Events and Large-Scale Ocean Surface and Atmospheric Conditions in the Tropical Atlantic. *Advances in Meteorology*, 2016. <https://doi.org/10.1155/2016/1940456>
- Taesam Lee (2021). Standardized Precipitation Index (<https://www.mathworks.com/matlabcentral/fileexchange/26018-standardized-precipitation-index>), MATLAB Central File Exchange. Retrieved September 12, 2021.
- Tang S., Li R., He J., Wang H., & Fan X. (2020). Comparative Evaluation of the GPM IMERG Early, Late, and Final Hourly Precipitation Products Using the CMPA Data over Sichuan Basin of China. *Water* 2020, 12, 554; 1–20. <https://doi.org/doi:10.3390/w12020554>
- Trenberth K. E., & Hoar T. J. (1997). El Nino and climate change. *Geophysical Research*

- Letters, 24(23), 3057–3060. <http://dx.doi.org/10.1029/97GL03092>;
doi:10.1029/97GL03092
- Trenberth K. E., & Shea D. J. (2005). Relationships between precipitation and surface temperature. 32(June), 2–5. <https://doi.org/10.1029/2005GL022760>
- UN-WFP. (2020). El Niño : Implications and Scenarios for 2015. VAM-Food Security Analysis, December 12. <https://www.wfp.org/publications/seasonal-monitor>
- UN-WFP. (2015). El Niño : Implications and Scenarios for 2015. VAM-Food Security Analysis, December 12.
- Wayne C. Palmer. (1965). Meteorological Drought.
- West Africa Floods map 2008, UN Office for the Coordination of Humanitarian Affairs, [http://www.reliefweb.int/rw/fullMaps_Af.nsf/luFullMap/5598E04D6AF1AB19C12574B900467E0F/\\$File/ocha_FL_afr080902.pdf?OpenElement](http://www.reliefweb.int/rw/fullMaps_Af.nsf/luFullMap/5598E04D6AF1AB19C12574B900467E0F/$File/ocha_FL_afr080902.pdf?OpenElement).
- WBG. (2021). Climate Risk Country Profile - TOGO. www.worldbank.org
- W. J. Gibbs and J. V. Maher, (1967) “Rainfall Deciles as Drought Indicators,” Bureau of Meteorology, Melbourne.
- Winifred Ayinpogbilla Atiah ; Leonard Kofitse Amekudzi ; Jeffrey Nii Armah Aryee ; Kwasi Preko ; Sylvester Kojo Danuor. (2020). Validation of Satellite and Merged Rainfall Data over Ghana, West Africa. Atmosphere, 11. <https://doi.org/10.3390/atmos11080859>
- World Bank. (2011). Climate Risk and Adaptation Country Profile; Togo. Global Facility for Disaster Reduction and Recovery, 87–88. http://sdwebx.worldbank.org/climateportal/doc/GFDRRCountryProfiles/wb_gfdr climate_change_country_profile_for_VUT.pdf
- Wu R., & Kinter J. L. (2009). Analysis of the relationship of U.S. droughts with SST and soil moisture: Distinguishing the time scale of droughts. Journal of Climate, 22(17), 4520–4538. <https://doi.org/10.1175/2009JCLI2841.1>
- Wilks, Daniel S. (2011). Statistical Methods in the Atmospheric Sciences .3rd ed.Oxford; Waltham, MA: Academic Press.
- Xu S., Qin M., Ding S., Zhao Q., Liu H., Li C., Yang X., Li Y., Yang J., & Ji X. (2019). The impacts of climate variation and land-use changes on streamflow in the Yihe River, China. Water (Switzerland), 11(5), 1–18. <https://doi.org/10.3390/w11050887>
- Zhao T., & Yatagai A. (2014). Evaluation of TRMM 3B42 product using a new gauge-based analysis of daily precipitation over China. International Journal of Climatology, January 2018. <https://doi.org/10.1002/joc.3872>
- Zubieta R., Getirana A., Espinoza J. C., Lavado-Casimiro W., & Aragon L. (2017). Hydrological modeling of the Peruvian-Ecuadorian Amazon basin using GPM-IMERG satellite-based precipitation dataset. Hydrology and Earth System Sciences, 21(7), 1–21. <https://doi.org/10.5194/hess-2016-656>

